MTK 17.

MŰSZAKI TUDOMÁNYOS KÖZLEMÉNYEK

17.

TUDOMÁNYOS BIZOTTSÁG/LEKTOROK
SCIENTIFIC ADVISORY BOARD/PEER REVIEWERS

ISSN 2393 – 1280

Erdélyi Múzeum-Egyesület Műszaki Tudományok Szakosztálya
Transylvanian Museum Society – Department of Technical Sciences

MŰSZAKI TUDOMÁNYOS KÖZLEMÉNYEK

17.

Szerkesztette / Edited by
BITAY ENIKŐ – MÁTÉ MÁRTON

ERDÉLYI MÚZEUM-EGYESÜLET
Kolozsvár
2022

A kötet megjelenését támogatta a Magyar Tudományos Akadémia,
a Bethlen Gábor Alapkezelő Zrt., a Communitas Alapítvány,
az EME Műszaki Tudományok Szakosztálya

The publication of this volume was supported by the Hungarian Academy of Sciences,
by the Bethlen Gábor Fund, by the Communitas Foundation,
by the TMS – Department of Engineering Sciences


Kiadó/Publisher: Erdélyi Múzeum-Egyesület
Felelős kiadó/Responsible Publisher: Biró Annamária
Szerkesztette/Edited by: Bitay Enikő, Máté Márton
Olvasószerkesztő/Proofreader: András Zselyke (magyar), David Speight (English)
Műszaki szerkesztő/DTP: Szilágyi Júlia
Borítóterv/Cover: Könczey Elemér

Nyomdai munkálatok/Printing-work
F&F International Kft. Kiadó és Nyomda, Gyergyószentmiklós
Ügyvezető igazgató/Manager: Ambrus Enikő
Tel./Fax: +40-266-364171

online elérhető/online available at:
https://eme.ro/publication-hu/mtk/mtk-main.htm
DOI: 10.33895/mtk-2022.17

TARTALOM

CONTENT

sciendo

Műszaki Tudományos Közlemények vol. 17. (2022) 1–5.
DOI: Hungarian: https://doi.org/10.33895/mtk-2022.17.01
English: https://doi.org/10.33894/mtk-2022.17.01

EME MTSZ MTK

DIDACTIC AND METHODOLOGICAL ASPECTS OF TECHNICAL HIGHER EDUCATION

Enikő BITAY,[1] Gyula BAGYINSZKI[2]

[1] *Sapientia Hungarian University of Transylvania, Faculty of Technical and Human Sciences, Department of Mechanical Engineering, Târgu Mureș, Romania, ebitay@ms.sapientia.ro*

[2] *Óbuda University, Donát Bánki Faculty of Mechanical and Safety Engineering, Budapest, Hungary, bagyinszki.gyula@bgk.uni-obuda.hu*

Abstract

Technical higher education - that is engineering education, unlike the general practice of secondary vocational education - already deals with adult “students”. Although the emphasis on educational tasks in universities is less, the attitude-shaping effect and example of lecturers play a key role. With this compilation, we aim to provide clues for this.

Keywords*: education, training, didactics, methodology, curriculum.*

1. Introduction

In [1] we dealt with the teaching methods in engineering education, in [2] we drew attention to the curricular and instructional aspects of higher technical education, in [3] we reviewed the role, functions and forms of engineering education practices, while in [4] we summarised the teaching materials and didactic tools that can be used in engineering education. In [5] methodological aspects were presented, using a specific example from a specific field. In the present compilation, we focus on some of the more common didactical and methodological aspects of engineering education.

2. Principles of didactics in higher education

The subject of didactics in higher education is teaching, training and learning in higher education institutions [6]. Two thematic areas are distinguished in didactics in higher education [7]:

– the first includes the general theoretical problems of higher education and self-training which are common to all higher education institutions, and do not depend on their professional profile;
– the second thematic area is made up of questions of training theory which relate to the specialisations or subjects taught in the various courses. This includes subject didactics (e.g. in technical higher education) and subject didactics, which, although subordinate to general university didactics, applies its principles and develops them in detail.

The latter definition emphasises the developmental nature of subject-specific didactics applying general principles, which is of great importance, for example, in the planning and implementation of practical sessions in specific fields of training. The correct management of the realisation of general and specific training objectives requires that the teaching and training process is subordinated to the didactic principles. These, in turn, are derived from the general norms of didactic activity, from the analysis of the educational process and from the specific laws of the educational process, and are the conditions for achieving the objectives that determine the direction of the activity. Among the didactic principles which play a particularly important role in higher education, the following can be highlighted [7]:

2.1. The principle of the unity of science, education and the development of competences to shape attitudes

High scientific quality of curricular materials - which implies continuous updating and keeping up with the development of the discipline - should

be implemented in such a way that the student can understand, record and thus master them, while at the same time the selection of content should allow for the identification and highlighting of factors that can ensure the approach-forming, competence-developing effect in the educational and training process. An essential factor is learning by understanding as opposed to verbal learning based on memory.

2.2. The principle of conscious and active participation of students in the educational process

The didactic process must be guided in such a way that students fully understand the objectives of the training and their own responsibility in achieving them, develop positive motivation and self-monitoring, and do not become passive consumers of the knowledge they have acquired. However, in a sense they must also be active "creators" of it, e.g. by completing project tasks.

2.3. The principle of regularity

This manifests itself in two ways:

- on the part of the instructor: in well-organised, logical and clear lectures and exercises, in the whole course of the exercise which facilitates the achievement of the educational objectives and the learning objectives;
- on the part of the students: disciplined in orderly, structured and planned work, promotion and development of positive personality traits and preventing academic failure. The regularity of the students' attendance depends to a large extent on the regularity of the teacher.

2.4. Principle of coherence and consistency of the didactic system adopted

A uniform and consistent relationship with all students; consistent application of the requirements set at the beginning of the semester (without mid-semester changes) in all subjects, for all instructors, in accordance with the University-wide policy.

2.5. The principle of visualisation

Adhering to it facilitates understanding of certain problems, increases interest in the subject matter and ultimately helps to develop positive motivation to learn and individual student activity. This means in particular the use of modern teaching (technology) tools and technological equipment.

2.6. The principle of gradual progression from easier to harder

This means arranging the curriculum material in such a way that the basic, elementary and easier knowledge is gradually progressed from the more basic to the more difficult; the knowledge needed to understand new subject units is given earlier. This also develops systematic, logical thinking and reasoning, can develop the habit of continuous learning and indirectly implements the principle of systematicity.

3. Educational objectives and methods at the university

The formulation of "long term" educational and training objectives is necessary in order to enable the trainers of the various disciplines to plan their own courses, their medium and short term activities, and to promote the desired changes in the attitudes and competences of their students. The traditional subject fiche, which consists of a list of topics or literature to be read, does not meet this objective, as it does not specify the competences that students are expected to acquire.

Based on [8] and updating it, the links between university teaching objectives, teaching methods or student activities and the assessment system can be outlined as a kind of guideline, as shown in table 1.

4. Elements of the university educational–personal development process

The University's objectives are pursued through the planned organisation of

- educational and training process, subordinated to the general and specific objectives of the training. The education and training process is based on the following components [7]:
- the curricula (the content of the training),
- the forms and methods of imparting knowledge (the delivery of the training),
- the formulation of attitudes, the development of competences the forms and methods of training
- the organisation and funding of studies,
- the university students,
- university teachers.

The right concept of curricula is essential to achieve the detailed, substantive objectives of training. The development of sound curricula for each specialisation is based on a "specialisation model", which is developed by means of a detailed analysis of the industrial needs of the specialisation, its functional content and the knowl-

Table 1. *The links between university educational objectives, teaching methods or student activities and the evaluation system.*

Educational Objectives	Teaching Methods / Student Activity	Evaluation / Feedback
Knowledge		
Student have to:		
– have a basic knowledge of their subject terminology	– lectures; compulsory literature; practical work; demonstration, etc.	– multiple-choice exams; correct use of terms in papers; seminar debates, etc.
– be familiar with the basic laws and concepts of the subject	– lectures; compulsory literature; practical work; demonstration, etc.	– correct references to relevant laws, concepts, etc.; justifications, proofs; essay writing, etc.
– understand the usability of their subject	– links with research, industry, professionals in the field; experiments, projects (where and when appropriate)	– evaluation of reports on project work, etc.
– know the fundamentals and applications of the subjects related to their subject	– general studies; reading of 'background' literature	– synthesis of information from different sources
Skills		
University education should enable students to:		
– to express their ideas in writing in an adequate manner	– papers (essays); laboratory reports, etc.	– their informative assessment
– present clearly and concisely	– presentation of papers; discussion and debate in seminar groups; consultations, etc.	– criticism from other students
– be able to formulate judgements and opinions independently	– encountering and recognising contradictions; confronting opposing views; using the seminar to explain the student's assumptions, etc.	– e.g. "compare and contrast" questions in exams; evaluation of arguments made, etc.
– understand how to acquire information effectively	– use of libraries, internet, leaflets, abstracts, etc.; preparation for studies, projects; open-ended experiments	– informative comments on performance; "open book" exams
– be able to think imaginatively and in abstract categories	– research projects; wrestling with unsolved problems; using scientific concepts in proofs, discussions, debates	– quality of written work (possibly publications); grasp of problems; appreciation of originality
– understand how to interact with colleagues and other professionals in relation to their future career	– peer, combined projects; role-playing, group debates to elucidate group interactions	– peer evaluation of the student's behaviour and behaviour of other students
– develop adaptability to changes in knowledge and attitudes (both in general technical developments in the field and new insights in your own field)	– exposure to new ideas, concepts (not accepting everything as 'fact')	– post-graduation monitoring
Attitudes		
The sense of purpose in university education is designed to promote in students:		
– enthusiasm for learning	– reading literature of your choice; extra-curricular activities (e.g. professional clubs and classes...)	– expanding extra-curricular activities; identifying new problems for their own research work
– a scientific need for accuracy	– contact with teachers and researchers who embody this precision; continuous monitoring of own results	– rewarding punctuality in exams with a mark
– an awareness of the moral, economic and scientific problems of society	– general cultural studies; projects; sociology, economics, faculties...	– impressively, based on the student's written work and seminar discussions

edge, characteristics, technical and economic aspects required, with particular attention to the most effective implementation of the engineering tasks of each industrial post (e.g. in dual training).

Curricula, based on the "degree model", delimit the range of knowledge, skills and competences required for students to complete a degree course, in terms of theoretical and practical preparation.

The curriculum based on the “department model” outlines the whole knowledge and skills necessary for students graduating from that given department, in theoretical and practical aspects as well. Consequently, the academic curriculum specifies the number and frame of theoretical subjects, special subjects, complementary subjects, human subjects, quantity of the necessary practice, the global quantity and correct proportions of the instructional contents in such a way that those fit into the whole and divided sections of the training period.

The study plans are defined in their final form:
- the number of subjects to be taught and their logical sequence in each semester;
- the number of hours of lectures and practicals in each subject;
- the basic requirements (examinations, mid-year grades, signatures) and the credits to be obtained;
- the number and duration of the work placements or internships to be carried out in production.

The study plans are used as a basis for the development of the so-called framework curricula for each subject, which define the teaching content in each subject that is essential for the course. The individual lecturers and tutors draw up the detailed curricula for each subject on the basis of these framework curricula.

The teaching process must be flexible and adapted to the people involved, to the specific and changing circumstances of each subject, each of which has its own methodological characteristics.

The material basis for the teaching and training process is adequate, with modern laboratory equipment, the provision of textbooks and notes, well-stocked libraries and reading rooms, modern lecture and practical rooms and laboratories, well-organised workshops and dormitories. The correct organisation of the course of studies is equally important, and includes:
- grouping students according to criteria that ensure rapid integration of the community and the development of a sense of collective responsibility for the learning outcomes;
- developing a reasonable timetable for compulsory classes, taking into account the economic use of students' time;
- the proportionate distribution of semester requirements (complex and detailed);
- reasonable examination scheduling;
- careful, detailed overview of the content of the curriculum.

In [9] it is pointed out that nowadays there is a steady emergence of university students who are younger than the Internet of mass public services. For them, the use of the Internet and computers, the versatile use of multimedia and mobile devices are a natural part of everyday life. They first encounter the internet and digital technologies as children and from then on, their use becomes a dominant part of their lives. All this is of course significant.

This has a significant impact on their perception of their role as students and on the way they think about higher education.

Of course, engineering education must be organised with this in mind, but it is also important to bear in mind that the development of "technical acumen" and practical skills is only a virtual process. In a virtual environment, using 'online' methods or distance materials cannot be effective and efficient.

The authors of [10] aim to help higher education institutions to apply strategy management methodologies that have been tried and tested in other sectors and industries and which are relevant for higher education institutions, and to improve their strategy management practice in general. This will be facilitated by practice-oriented descriptions of the methods and examples from higher education.

5. Conclusions

Without the active attitude of students, their self-aware attitude to learning and their motivated participation in the teaching and training process, the teaching staff cannot achieve the desired results. However, it is also the teaching staff community that is responsible for the whole training process, its content and scope, the methods used to achieve the training objectives, ensuring that it is properly organised, and for managing and exploiting the cooperation of young people. This requires committed teachers who are aware of the objectives and tasks, and who have the necessary scientific, pedagogical and moral skills.

References

[1] Bagyinszki Gy., Bitay E.: *Mérnökképzés oktatási módszerei*. MTK 13. (2020) 19–23. https://doi.org/10.33895/mtk-2020.13.02

[2] Bagyinszki Gy., Bitay E.: *Tananyag- és oktatásszervezés a műszaki képzésekben*. MTK 11. (2019) 23–26. https://doi.org/10.33895/mtk-2019.11.02

[3] Bagyinszki Gy., Bitay E.: *Anyagtudományi gyakorlat-modulok a gépész- és mechatronikai mérnök képzésben*. Műszaki Tudományos Füzetek 16. (2011) 5-16. https://doi.org/10.36243/fmtu-2011.04

[4] Bitay E., Bagyinszki Gy.: *Oktatási anyagok és didaktikai eszközök a mérnökképzési gyakorlatokban*. MTK 15. (2021) 7–10. https://doi.org/10.33895/mtk-2021.15.02

[5] Bitay E., Bagyinszki Gy.: *Hegesztőrobotokra vonatkozó ismeretek oktatásának módszertani szempontjai*. Műszaki Tudományos Füzetek 19. (2014) 73–76. https://doi.org/10.36243/fmtu-2014.011

[6] Wincenty Okoň: *Felsőoktatási didaktika*. Felsőoktatási Pedagógiai Kutatóközpont, Budapest, 1973.

[7] Kietliňskja Z.: *A műszaki felsőoktatás pedagógiája*. Felsőoktatási Pedagógiai Kutatóközpont, Budapest, 1974.

[8] R. Beard: *Tanítás és tanulás a felsőoktatásban*. Felsőoktatási Pedagógiai Kutatóközpont, Budapest, 1974.

[9] Ollé J.: *Egy módszer alkonya: a katedrapedagógia végnapjai a felsőoktatásban*. NFKK Füzetek 5. „Korszerű felsőoktatási pedagógiai módszerek, törekvések", Budapesti Corvinus Egyetem Nemzetközi Felsőoktatási Kutatások Központja, 2010. november, 22–31.

[10] Mészáros Á. (ed.): *Felsőoktatási stratégiai módszertani kézikönyv*. Oktatáskutató és Fejlesztő Intézet Budapest, 2011.

sciendo

Műszaki Tudományos Közlemények vol. 17. (2022) 6–10.
DOI: Hungarian: https://doi.org/10.33895/mtk-2022.17.02
English: https://doi.org/10.33894/mtk-2022.17.02

EME MTSZ MTK

IMPLEMENTATION IN JAVA OF ALGORITHMS FOR SEMIDEFINITE OPTIMIZATION

Zsolt DARVAY,[1] Adrienne GARFIELD [2]

[1] *Babeș-Bolyai University, Faculty of Mathematics and Computer Science. Cluj-Napoca, Romania, darvay@cs.ubbcluj.ro; Transylvanian Museum Society, Department of Mathematics and Computer Science*

[2] *Babeș-Bolyai University, Faculty of Mathematics and Computer Science. Cluj-Napoca, Romania, adriennegarfield2000@gmail.com*

Abstract

We discuss the possibility of solving the semidefinite optimization problem using interior-point algorithms. We present the primal and dual semidefinite programming problems, and then determine the interior-point condition and the optimality criteria. We analyze the central path system and the modification of this, using the method of algebraically equivalent transformation. We use the Nesterov-Todd scaling technique to obtain the proper search directions. We give a modified version of the Nesterov-Todd step interior-point algorithm based on the implementation point of view. We present some numerical results based on a code implemented in the Java programming language. We compare the results obtained for the identity map and the square root function within the framework of the algebraically equivalent transformation technique.

Keywords: *semidefinite optimization, interior-point algorithm, central path, algebraically equivalent transformation.*

1. Theoretical foundations

1.1. The semidefinite optimization problem

Semidefinite optimization (SDO) is a particular case of convex optimization, which has several applications, for example, in the field of combi-natorial optimization. In the field of engineering such problems are met in the case of structural optimization. In artificial intelligence the pattern separation using ellipsoids leads to SDO problems [1].

Denote by $\mathbb{R}^n$, $\mathbb{R}^{n\times n}$, and S^n the set of n-dimensional column vectors, matrices, and symmetric matrices, respectively. For each $X, S \in \mathbb{R}^{n\times n}$ we introduce the following algebraic operation:

$$X \circ S = \mathrm{Tr}(X^T S),$$

where X^T denotes the transpose of the matrix X. If the matrix $X \in S^n$ is positive semi-definite, then we write this in the form $X \succcurlyeq 0$. The notation $X \succ 0$ is used to denote that X is positive definite.

The SDO problem can be given in the following way:

$$\begin{aligned} &min\ C \circ X, \\ &A_i \circ X = b_i,\ i = 1,2,\ldots,m, \\ &X \succcurlyeq 0, \end{aligned} \tag{1}$$

where A_i, $C \in S^n$ and $b_i \in \mathbb{R}$ for all $i = 1,2,...,m$. This means that we are looking for a positive semidefinite matrix X, which satisfies the equality constraints and the value of the expression $C \circ X$ is minimal. Problem (1) is called primal problem.

1.2. Dual problem

We can assign a dual problem to the primal one, which is about the maximization of a linear objective function subject to the equality constraints expressed with the matrices A_i, and C:

$$\begin{aligned} &max\ b^T y, \\ &\sum_{i=1}^{m} y_i A_i + S = C, \\ &S \succcurlyeq 0. \end{aligned}$$

In case of the dual problem, we search for the column vector $y \in \mathbb{R}^m$ and the positive semi-definite symmetric matrix S to fulfil the feasibility constraints and to maximize the linear function $b^T y$.

1.3. Condition for the starting point

In the following, we deal with the primal-dual problem pair, which we solve with a path-following interior-point algorithm. It is important to mention that the interior point condition (IPC) must be already satisfied for the starting point (X^0, y^0, S^0). The IPC is:

$$A_i \circ X^0 = b_i, \quad X^0 \succ 0, \quad i = 1,2,..,m,$$
$$\sum_{i=1}^{m} y_i^0 A_i + S^0 = C, \quad S^0 \succ 0.$$

1.4. Optimality criteria

It can be proved that if the IPC holds, then the following system determines the optimal solution [2]:

$$A_i \circ X = b_i, \quad i = 1,2,\dots,m, \quad X \succcurlyeq 0,$$
$$\sum_{i=1}^{m} y_i A_i + S = C, \quad S \succcurlyeq 0,$$
$$XS = 0.$$

The first two equations of the optimality condition are called feasibility conditions, and the third one is the complementarity condition.

1.5. Central path

The system corresponding to the central path is obtained by replacing the null matrix in the complementarity condition of the optimality criteria with the expression μI_n, where $\mu > 0$ is a positive real number and I_n is the identity matrix of size n. AThe obtained equality is called centrality equation. The system describing the central path can be specified as follows:

$$A_i \circ X = b_i, \quad i = 1,2,\dots,m, \quad X \succcurlyeq 0,$$
$$\sum_{i=1}^{m} y_i A_i + S = C, \quad S \succcurlyeq 0, \qquad (2)$$
$$XS = \mu I_n.$$

It can be proved that if the IPC holds, then for every positive real number μ system (2) has a unique solution [2]. The solutions obtained for different values of the parameter μ determine the points of the central path. The interior-point algorithm will proceed along this path.

1.6. Search directions

Search directions play an important role in introducing different versions of interior-point algorithms. An entire class of search directions can be given by the algebraically equivalent transformation of the system defining the central path [3, 4].

This method consists of the following. First divide by the parameter μ the centrality equation given by the third equation of system (2). Next apply a continuously differentiable and invertible function $\varphi : (0,\infty) \to \mathbb{R}$ to both sides of the equation. Thus, we arrive at the following system [5]:

$$\begin{aligned} A_i \circ X &= b_i, \quad i = 1,2,\dots,m, \quad X \succcurlyeq 0, \\ \sum_{i=1}^{m} y_i A_i + S &= C, \quad S \succcurlyeq 0, \\ \varphi\left(\frac{XS}{\mu}\right) &= \varphi(I_n). \end{aligned}$$

Note that the function φ is applied in the following way in the case of each symmetric and positive semidefinite matrix $U \in S^n$. We use the fact that U can be written in the form $U = Q^T \Lambda Q$ where

$\Lambda = \mathrm{diag}(\lambda_1, \lambda_2, \dots, \lambda_n)$

is the diagonal matrix formed by the eigenvalues and Q is an orthonormal matrix, thus $Q^T = Q^{-1}$. In this case

$$\varphi(U) = Q^T \mathrm{diag}\big(\varphi(\lambda_1), \varphi(\lambda_2), \dots, \varphi(\lambda_n)\big) Q.$$

According to the analysis provided by Wang and Bai [5] the search directions are given by the system

$$\begin{aligned} A_i \circ \Delta X &= 0, \quad i = 1,2,\dots,m, \\ \sum_{i=1}^{m} \Delta y_i A_i + \Delta S &= 0, \\ \Delta X + X \Delta S S^{-1} &= \mu \left(\varphi'\left(\frac{XS}{\mu}\right)\right)^{-1} \left(\varphi(I_n) - \varphi\left(\frac{XS}{\mu}\right)\right) S^{-1}. \end{aligned} \qquad (3)$$

1.7. Nesterov–Todd scaling

System (3) defining the search directions does not have a unique solution $(\Delta X, \Delta y, \Delta S)$ for which ΔX is a symmetric matrix. Since the solution needs to be found in the space of symmetric matrices, it is therefore necessary to scale the system. There are several scaling methods. In the following, we use the scaling introduced by Nesterov and Todd [6, 7].

According to the method, it is necessary to introduce a symmetric matrix P which will provide an approximation of the previous system. The matrix can be given by the following two equal expressions:

$$P := X^{½} (X^{½} S X^{½})^{-½} X^{½} = S^{-½} (S^{½} X S^{½})^{½} S^{-½}.$$

Thus, we obtain the system:

$$A_i \circ \Delta X = 0, \quad i = 1,2,\dots,m,$$
$$\sum_{i=1}^{m} \Delta y_i A_i + \Delta S = 0,$$
$$\Delta X + P\Delta S P^T = \mu\left(\varphi'\left(\frac{XS}{\mu}\right)\right)^{-1}\left(\varphi(I_n) - \varphi\left(\frac{XS}{\mu}\right)\right)S^{-1}. \tag{4}$$

We would like to transform the left-hand side of the third equation of system (4) into a simple sum of two matrices. To this end, we introduce the

$$D = P^{\frac{1}{2}},$$
$$D_X = \frac{1}{\sqrt{\mu}} D^{-1}\Delta X D^{-1}, \tag{5}$$
$$D_S = \frac{1}{\sqrt{\mu}} D\Delta S D \tag{6}$$

matrices. Observe that equalities (5) and (6) can also be used to determine the search directions ΔX and ΔS if D_X and D_S are given.

Applying the scaling technique and introducing the above notations, we get the following system:

$$\bar{A}_i \circ D_X = 0, \quad i = 1,2,\dots,m,$$
$$\sum_{i=1}^{m} \Delta y_i \bar{A}_i + D_S = 0,$$
$$D_X + D_S = P_V,$$

where

$$\bar{A}_i := \frac{1}{\sqrt{\mu}} D A_i D, \quad i = 1,2,\dots,m,$$
$$V = \frac{1}{\sqrt{\mu}} DSD,$$
$$P_V = \sqrt{\mu} D^{-1}(D\varphi'(V^2)D^{-1})^{-1} \cdot \cdot (\varphi(I_n) - D\varphi(V^2)D^{-1})S^{-1}D^{-1}.$$

2. Implementation characteristics

2.1. Residual vectors and residual matrices

In the case of the implementation of interior-point algorithms, we cannot always assume that the feasibility conditions will be satisfied in each iteration of the algorithm. This means that not necessarily the 0 vector and the null matrix do appear on the right-hand side of the first two equations of system (4). Since the equality $A_i \circ X = b_i$ does not always hold, it is therefore necessary to introduce the following notation:

$$r_i^b = A_i \circ X - b_i, \quad i = 1,2,\dots,m.$$

Note that in this way we have introduced the residual vector r^b, whose components are the above differences. The same should be done with the equation

$$\sum_{i=1}^{m} y_i A_i + S = C$$

to which we assign the residual matrix R^C:

$$R^C = \sum_{i=1}^{m} y_i A_i + S - C.$$

The first two equations of system (4), which determines the search directions will be modified accordingly:

$$A_i \circ \Delta X = -r_i^b, \quad i = 1,2,\dots,m,$$
$$\sum_{i=1}^{m} \Delta y_i A_i + \Delta S = -R^C,$$
$$\Delta X + P\Delta S P^T = \mu\left(\varphi'\left(\frac{XS}{\mu}\right)\right)^{-1}\left(\varphi(I_n) - \varphi\left(\frac{XS}{\mu}\right)\right)S^{-1}. \tag{7}$$

By introducing the

$$\bar{r}_i^b = \frac{r_i^b}{\mu}, \quad i = 1,2,\dots,m,$$
$$\bar{R}^C = \frac{1}{\sqrt{\mu}} D R^C D$$

notations the scaled form of system (7) can be written as:

$$\bar{A}_i \circ D_X = -\bar{r}_i^b, \quad i = 1,2,\dots,m,$$
$$\sum_{i=1}^{m} \Delta y_i \bar{A}_i + D_S = -\bar{R}^C, \tag{8}$$
$$D_X + D_S = P_V.$$

2.2. Step length

The theoretical algorithm introduced by Wang and Bai [5] works with full Nesterov-Todd steps, which means that the new (X,y,S) triple is obtained from the original one by adding the directions given by $(\Delta X, \Delta y, \Delta S)$. In this case, the parameter μ is reduced by using the factor $(1-\theta)$ where $0<\theta<1$. The choice of θ reveals that it is a short-step algorithm. However, from the implementation point of view, it is more efficient to choose the value of the next μ based on the matrices X and S as follow:

$$\mu = \sigma\frac{X \circ S}{n},$$

where $0<\sigma<1$ is a fixed parameter. Furthermore, by choosing the step length, we ensure that the

obtained X and S remain in the cone of the positive semidefinite matrices. For this purpose, for any $M \in S^n$ let $\lambda(M)$ be the column vector formed from the eigenvalues of the matrix M and let us introduce the notation $\lambda_{min}(M) = min(\lambda(M))$, which gives the minimal eigenvalue of the matrix M. Similarly, we can introduce the notation $\lambda_{max}(M)$ which specifies the largest eigenvalue of the matrix M. The step length is determined by modifying the method given by Tütüncu, Toh and Todd [8]. Introducing the notation

$$\alpha(M) = \begin{cases} \dfrac{-1}{\lambda_{min}(M)}, & \lambda_{min}(M) \le -1 \\ 1, & \lambda_{min}(M) \in (-1, +\infty) \end{cases} \quad (9)$$

the step length for the matrix X will be

$$\alpha_X = \alpha(X^{-1}\Delta X), \quad (10)$$

and the step length calculated for the vector y and the matrix S will be

$$\alpha_S = \alpha(S^{-1}\Delta S). \quad (11)$$

Observe that the values calculated by (10) and (11) will also be reduced by a constant factor $0 < \rho < 1$ thus ensuring that X and S remain inside the cone of positive semidefinite matrices.

2.3. Stopping criterion

he stopping criterion of the algorithm is divided into three parts. The first concerns that the relative duality gap given by expression

$$\text{relgap} = \frac{X \circ S}{1 + |C \circ X| + |b^T y|} \quad (12)$$

should be smaller than a fixed real number $\varepsilon > 0$. Let us introduce the notation

$$A \circ X = \begin{bmatrix} A_1 \circ X \\ A_2 \circ X \\ \dots \\ \dots \\ A_m \circ X \end{bmatrix}$$

Since it may happen during the algorithm that the feasibility condition is not satisfied in a given iteration, we provide two related measures as part of the stopping criterion. The primal infeasibility is defined by the expression

$$\text{pinfeas} = \frac{\|A \circ X - b\|}{1 + \|b\|} = \frac{\sqrt{\sum_{i=1}^m (A_i \circ X - b_i)^2}}{1 + \sqrt{\sum_{i=1}^m b_i^2}} \quad (13)$$

while the dual infeasibility is expressed using

$$\text{dinfeas} = \frac{\|\sum_{i=1}^m y_i A_i + S - C\|}{1 + \|C\|} \quad (14)$$

where for each matrix $M \in S^n$ we have

$$\|M\| = \sqrt{\left(\lambda_{max}(M^T M)\right)} = |\lambda_{max}(M)|.$$

Note that for a primal feasible solution the value of pinfeas is zero. Similarly, in the case of a dual feasible solution, the value of dinfeas is zero. Therefore, as part of the stopping criterion, we will investigate whether the values of pinfeas and dinfeas are smaller than a given real number $\varepsilon > 0$.

3. The algorithm

Based on the presented theoretical description, we modify the interior-point algorithm introduced by Wang and Bai [5] to obtain an efficient implementation.

Interior-point algorithm for SDO

Let $\varepsilon > 0$ be the accuracy parameter, $0 < \rho < 1$ constant factor that reduces the step size, and $0 < \sigma < 1$ constant factor that reduces the value of μ.

Suppose that for the triple (X^0, y^0, S^0) the IPC holds and let $\mu_0 = \dfrac{X^0 \circ S^0}{n}$;

begin

$X := X^0$; $y := y^0$; $S := S^0$;

$\mu := \mu_0$;

relgap := 1; pinfeas := 1; dinfeas := 1;

while relgap $\ge \varepsilon$ **or** pinfeas $\ge \varepsilon$ **or** dinfeas $\ge \varepsilon$ **do**

begin

determine the triple $(D_X, \Delta y, D_S)$ using (8);

determine the matrix ΔX using (5);

determine the matrix ΔS using (6);

calculate the step length α_X using (10);

calculate the step length α_S using (11);

$X := X + \rho\, \alpha_X \Delta X$;

$y := y + \rho\, \alpha_S \Delta y$; $S := S + \rho\, \alpha_S \Delta S$;

$\mu = \sigma\, (X \circ S)/n$;

determine the value of relgap *using (12);*

determine the value of pinfeas *using (13);*

determine the value of dinfeas *using (14);*

end

end.

4. Numerical results

The interior-point algorithm for SDO was tested on the examples published on the website **[9].** In the first version, the algebraically equivalent transformation method was used with the identity function, while in the second version, the square root function was used. **Table 1.** presents the obtained results.

It can be concluded that the iteration numbers do not significantly differ from each other, but in some cases the method based on the square root function works more efficiently than the one based on the identity map.

Table 1. *Obtained results for the values* $\varepsilon = 10^{-7}$, $\rho = 0.95$, $\sigma = 0.3$.

Problem	Function φ	Dimension of the matrix	Number of iterations
sdp01	$\varphi(t) = t$	n=20	21
sdp01	$\varphi(t) = \sqrt{t}$	n = 20	18
sdp02	$\varphi(t) = t$	n = 30	19
sdp02	$\varphi(t) = \sqrt{t}$	n = 30	18
sdp03	$\varphi(t) = t$	n = 40	17
sdp03	$\varphi(t) = \sqrt{t}$	n=40	15

Acknowledgment

The authors express their gratitude to the Transylvanian Museum Society for the support provided to the research work.

References

[1] Vandenberghe L., Boyd S.: *Semidefinite Programming*. SIAM Review. 38/1. (1996) 49–95. https://doi.org/10.1137/1038003

[2] Klerk E. de: *Aspects of Semidefinite Programming. Interior Point Algorithms and Selected Applications.* Kluwer Academic Publishers, Dordrecht, 2002.

[3] Darvay Zs.: *A new Algorithm for Solving Self-Dual Linear Optimization Problems*. Studia Universitatis Babeş-Bolyai, Series Informatica, 47/1. (2002) 15–26.

[4] Darvay Zs.: *New Interior Point Algorithms in Linear Programming*. Advanced Modeling and Optimization, 5/1. (2003) 51–92.

[5] Wang G. Q., Bai Y. Q.: *A New Primal-Dual Path-Following Interior-Point Algorithm for Semidefinite Optimization.* Journal of Mathematical Analysis and Applications, 353/1. (2009) 339–349. https://doi.org/10.1016/j.jmaa.2008.12.016

[6] Nesterov Yu. E., Todd M. J.: *Primal-Dual Interior-Point Methods for Self-Scaled Cones*. SIAM Journal on Optimization, 8/2. (1998) 324–364. https://doi.org/10.1137/S1052623495290209

[7] Nesterov Yu. E., Todd M. J.: *Self-Scaled Barriers and Interior-Point Methods for Convex Programming.* Mathematics of Operations Research, 22/1. (1997) 1–42. https://doi.org/10.1287/moor.22.1.1

[8] Tütüncü R. H., Toh K. C., Todd M. J.: *Solving Semidefinite-Quadratic-Linear Programs Using SDTP3.* Mathematical Programming, Ser. B 95/2. (2003) 189–217. https://doi.org/10.1007/s10107-002-0347-5

[9] Darvay Zs., Garfield A.: *Examples of Semidefinite Optimization Problems.* 2022. (accessed on: 2022. november 17.) https://www.cs.ubbcluj.ro/~darvay/sdp/

sciendo

Műszaki Tudományos Közlemények vol. 17. (2022) 11–15.
DOI: Hungarian: https://doi.org/10.33895/mtk-2022.17.03
English: https://doi.org/10.33894/mtk-2022.17.03

EME MTSZ MTK

ALGEBRAICALLY EQUIVALENT TRANSFORMATION TECHNIQUE FOR WEIGHTED LINEAR COMPLEMENTARITY PROBLEMS

Zsolt DARVAY,[1] Zsanett JAKAB[2]

[1] *Babeș–Bolyai University, Faculty of Mathematics and Computer Science. Cluj-Napoca, Romania, darvay@cs.ubbcluj.ro; Transylvanian Museum Society, Department of Mathematics and Computer Science*

[2] *Babeș–Bolyai University, Faculty of Mathematics and Computer Science. Cluj-Napoca, Romania, zsanett28@yahoo.com*

Abstract

We study the algebraically equivalent transformation technique using an application implemented in the Java programming language that solves weighted linear complementarity problems. In general, in the case of the algebraically equivalent transformation, we divide the nonlinear equation of the system that characterizes the central path, the so-called centrality equation, by the barrier parameter. However, in this case, we divide, component-wise, the centrality equation by the right-hand side vector, which depends on the barrier parameter. We apply the same continuously differentiable and invertible function to both sides of the obtained equation and generate different search directions using Newton's method. We analyze the numerical results provided by our application in the case of applying the algebraically equivalent transformation technique using the identical map and the square root function.

Keywords: *weighted linear complementarity problem, algebraically equivalent transformation, interior-point algorithm.*

1. Description of the weighted linear complementarity problem

The weighted complementarity problem (*WLCP*) significantly extends the concept of the usual linear complementarity problem (*LCP*). *WLCP* was introduced by Potra [1] in 2012.

Let $\mathbb{R}^n_+$ be the set of n-dimensional vectors consisting of non-negative real numbers. Suppose that $M \in \mathbb{R}^{n\times n}$ is a monotone matrix, i.e. $x^T Mx \geq 0$ for each vector $x \in \mathbb{R}^n$.

Similar to the well-known complementarity problem, the following system can be considered [2]:

$$\begin{aligned} &-Mx + s = q,\\ &xs = w,\\ &x \geq 0, s \geq 0, \end{aligned}$$

where $x, s, q \in \mathbb{R}^n$ and $w \in \mathbb{R}^n_+$.

It can be observed that in the case of the weighted problem, the xs component-wise product must be equal to the vector w, consisting of non-negative real numbers. In addition, the relation $-Mx + s = q$ must be fulfilled, as well as the fact that the components of the vectors x and s are non-negative real numbers.

Interior-point algorithms usually follow the central path, but in the case of WLCP, we introduce a special path. Assuming that the initial x_0 and s_0 interior points are given and

$$\mu^0 = \frac{(x^0)^T s^0}{n},$$

we introduce the following vector depending on the positive parameter μ [1, 2]:

$$w(\mu) = \left(1 - \frac{\mu}{\mu_0}\right) w + \frac{\mu}{\mu_0} c, \text{ where } c = x_0 s_0.$$

Thereby, the central path, which designates the direction, can be specified as follows:

$$\begin{aligned} &-Mx + s = q,\\ &xs = w(\mu), \qquad (1)\\ &x > 0, s > 0, \end{aligned}$$

where $\mu \in (0, \mu^0]$. The existence and uniqueness of the central path can be proved assuming that the matrix M is monotone and the starting interior point (x^0, s^0) exists [3].

In the following, we will introduce a possible modification of the above system.

2. Algebraically equivalent transformation technique

Let $e = [1\ 1 \ldots 1]^T$ be an n-dimensional all-one vector. Considering the algebraically equivalent transformation technique [4, 5], in the usual case, we proceed by dividing the centrality equation $xs = \mu e$ by the barrier parameter μ and then applying a continuously differentiable and invertible function $\varphi: (0, \infty) \to \mathbb{R}$ to both sides of the equation. Thus, we obtain the equation $\varphi\left(\frac{xs}{\mu}\right) = \varphi(e)$. On the other hand, in the case of the WLCP, the centrality equation is given by $xs = w(\mu)$ therefore we will divide it component-wise by the right-hand side vector $w(\mu)$. Moreover, we apply the function φ, so system (1) takes the following form:

$$\begin{aligned} &-Mx + s = q, \\ &\varphi\left(\frac{xs}{w(\mu)}\right) = \varphi(e), \\ &x > 0, s > 0. \end{aligned}$$

Using Newton's method, the search directions Δx and Δs can be uniquely determined by the system [3]:

$$\begin{aligned} s\Delta x + x\Delta s &= w(\mu) \cdot \frac{\varphi(e) - \varphi\left(\frac{xs}{w(\mu)}\right)}{\varphi'\left(\frac{xs}{w(\mu)}\right)}, \\ -M\Delta x + \Delta s &= 0. \end{aligned} \qquad (2)$$

It can be established that by introducing the function φ, the matrix of the system of linear equations that defines the search directions will always be the same, only the right-hand side vector depends on the function φ. In the implementation, we use two types of functions φ, the identical map and the square root function: $\varphi(t) = t$, $\varphi(t) = \sqrt{t}$.

To analyze the algorithm, the function δ must also be introduced, which defines the neighborhood of the given point on the central path. This gives us a proximity measure that expresses the distance of points x and s from the central path:

$$\delta(x, s, \mu) = \left\| \frac{w(\mu)}{\mu} - v^2 \right\|, \text{ where } v = \sqrt{\frac{xs}{\mu}}, \mu > 0.$$

In the following, we will describe the modified version of the algorithm from the theoretical and the implementation point of view.

3. The algorithm

First, we present the full-step interior-point algorithm, and then we introduce a modified version from the point of view of implementation, which is suitable for obtaining effective solution of weighted linear complementarity problems. The theoretical algorithm can be written as follows [2].

Theoretical algorithm for WLCP

The pair (x^0, s^0) is given, such that $-Mx_0 + s_0 = q$. We assume that $x^0 > 0$, $s^0 > 0$, as well as $\delta(x^0, s^0, \mu^0) \le \tau$, where $\tau \in (0,1)$ and $\mu^0 = \frac{(x^0)^T s^0}{n}$.

$x = x^0$, $s = s^0$;
while $\|xs - w\| > \varepsilon$ **do**
  $\mu = (1 - \theta)\,\mu$;
  Determination of $(\Delta x, \Delta s)$ based on system (2);
  $x = x + \Delta x$;
  $s = s + \Delta s$;
end while

The input data of the algorithm are the starting interior points, which are denoted by the vectors x^0 and s^0; the variable $0 < \theta < 1$, which is responsible for the reduction of the barrier parameter μ; the parameter $0 < \tau < 1$, which adjusts the neighborhood of the central path and the value $\epsilon > 0$, which determines the stopping criteria. In addition, it is necessary to give the matrix M and the vector q corresponding to the conditions of the problem. An initial value μ^0 must be assigned to the initial point pair (x^0, s^0). Starting from this pair, we can continue the cycle until the specified condition is met. Within the cycle, the value of μ must be reduced, and the simplest method for this is to multiply it by a number smaller than 1, in this case by $(1 - \theta)$. In addition, the directions Δx and Δs are calculated from system (2). In this case, we always define the new points x and s with a full-Newton step.

Since the implementation of full-Newton step for interior-point algorithms is usually not efficient enough, we make several modifications to obtain methods with lower running time. In the implemented version of the algorithm, we use a multiplication factor $0 < \sigma \le 1$ for μ^0 to accelerate its reduction. Furthermore, the current and max-

imum number of iterations and the parameters ε, ρ and σ are also displayed as input data. To increase the efficiency of the implemented algorithm, we do not use a full-Newton step, but calculate the maximum step lengths $\alpha(x)$ and $\alpha(s)$ using the minimum ratio test. Subsequently, we consider the minimum of $\alpha(x)$ and $\alpha(s)$ and the obtained positive real number α gives the length of the step, which is multiplied by a constant $\rho \in [0,1]$.

Based on the current points x and s, μ is calculated as described in article **[6]**, assuming that $e^T c \neq e^T w$.

Modified algorithm for WLCP

The vectors $x^0 > 0$, $s^0 > 0$ are given, such that $-Mx_0 + s_0 = q$.
Let $0 < \sigma \leq 1$ and $\mu^0 = \frac{(x^0)^T s^0}{n}$.

We assume that $\delta(x^0, s^0, \mu^0) \leq \tau$, where $\tau \in (0,1)$.
Let $0 < \rho < 1$ and $\varepsilon > 0$.
$x = x^0$, $s = s^0$;
$iter = 0$, $max\_iter = 3000$;
do

$$\mu = \sigma \cdot \left| \frac{\mu_0 (x^T s - e^T w)}{e^T c - e^T w} \right|;$$

Determination of $(\Delta x, \Delta s)$ based on system (2);
Determination of $\alpha(x)$ and $\alpha(s)$;
$\alpha = \min\{\alpha(x), \alpha(s)\}$;
$x = x + \rho \cdot \alpha \cdot \Delta x$;
$s = s + \rho \cdot \alpha \cdot \Delta s$;

$$gap = \left| \frac{x^T s - e^T w}{e^T c - e^T w} \right|;$$

$$infeasibility = \frac{\|Mx - s + q\|}{1 + \|q\|};$$

$iter = iter + 1$;
while ($gap \geq \varepsilon$ *or* $infeasibility \geq \varepsilon$) *and* $iter < max\_iter$);

4. Numerical results

In the following, we present numerical results for various weighted complementarity problems.

1. problem

The first problem is the same as problem 1 studied by Asadi and Mansouri **[7]**, with the difference that instead of $w = 0$, we now consider a non-zero weight vector.

$$n = 4,\ q = \begin{pmatrix} 4.0 \\ 4.0 \\ -2.0 \\ -1.0 \end{pmatrix},\ w = \begin{pmatrix} 15.0 \\ 10.0 \\ 12.0 \\ 23.0 \end{pmatrix},$$

$$M = \begin{pmatrix} 1.0 & -2.0 & 1.0 & -1.0 \\ 2.0 & 0.0 & -2.0 & 1.0 \\ 1.0 & 2.0 & 0.0 & -3.0 \\ 2.0 & -1.0 & 3.0 & 3.0 \end{pmatrix}.$$

2. problem

The second problem is the modified version of problem 5.2 studied by Mansouri and Pirhaji **[8]**. In this case, we also work with a weight vector $w \neq 0$:

$$n = 7,\ q = \begin{pmatrix} -1.0 \\ -3.0 \\ 1.0 \\ -1.0 \\ 5.0 \\ 4.0 \\ -1.5 \end{pmatrix}, w = \begin{pmatrix} 10.0 \\ 12.0 \\ 15.0 \\ 35.0 \\ 15.5 \\ 12.0 \\ 20.2 \end{pmatrix},$$

$$M = \begin{pmatrix} 1.0 & 0.0 & -0.5 & 0.0 & 1.0 & 3.0 & 0.0 \\ 0.0 & 0.5 & 0.0 & 0.0 & 2.0 & 1.0 & -1.0 \\ -0.5 & 0.0 & 1.0 & 0.5 & 1.0 & 2.0 & -4.0 \\ 0.0 & 0.0 & 0.5 & 0.5 & 1.0 & -1.0 & 0.0 \\ -1.0 & -2.0 & -1.0 & -1.0 & 0.0 & 0.0 & 0.0 \\ -3.0 & -1.0 & -2.0 & 1.0 & 0.0 & 0.0 & 0.0 \\ 0.0 & 1.0 & 4.0 & 0.0 & 0.0 & 0.0 & 0.0 \end{pmatrix}.$$

3. problem

The last problem is studied by Achache **[9]**, but in this case we use the assumption $w \neq 0$ as well.

$$n = 500,\ q = \begin{pmatrix} -1.0 \\ -1.0 \\ \cdots \\ \cdots \\ -1.0 \\ -1.0 \end{pmatrix}, w = \begin{pmatrix} v_0 \\ v_1 \\ \cdots \\ \cdots \\ v_{498} \\ v_{499} \end{pmatrix},$$

$$M = \begin{pmatrix} 1.0 & 2.0 & \ldots & 2.0 & \ldots & 2.0 \\ 0.0 & \ddots & 2.0 & \ldots & 2.0 & \ldots \\ \ldots & 0.0 & 1.0 & 2.0 & \ldots & 2.0 \\ 0.0 & \ldots & 0.0 & 1.0 & 2.0 & \ldots \\ \ldots & 0.0 & \ldots & 0.0 & \ddots & 2.0 \\ 0.0 & \ldots & 0.0 & \ldots & 0.0 & 1.0 \end{pmatrix},$$

where v_i, $1 \leq i \leq n$ are randomly generated positive real numbers.

To determine the directions, we first use the identical map $\varphi(t) = t$, then the square root function $\varphi(t) = \sqrt{t}$. Furthermore, in the first case, let $\varepsilon = 10^{-6}$, $\rho = 0.95$ and $\sigma = 0.3$, for which the obtained values are presented in **Table 1** in the case of WLCP problems.

It can be observed that in the case of the problem with a 4×4 matrix, when applying the square root function, we need more iterations than in case of the identical map. The opposite can be said for the other two problems (**Table 1**).

Similar observations can be concluded for **Table 2** as for **Table 1**, but by reducing the value of ε, the number of iterations increases, since during this modification we want to obtain the values of x and s with greater accuracy.

In the case of increasing the value of ρ, the method using the identical map proved to be the

Table 1. *Results for values of $\varepsilon = 10^{-6}$, $\rho = 0.95$, $\sigma = 0.3$.*

Problem	Function φ	Size of matrix	Nr. of iterations	Running time (ms)
1	$\varphi(t) = t$	$n = 4$	6	1.382
1	$\varphi(t) = \sqrt{t}$	$n = 4$	14	1.947
2	$\varphi(t) = t$	$n = 7$	15	3.918
2	$\varphi(t) = \sqrt{t}$	$n = 7$	10	2.977
3	$\varphi(t) = t$	$n = 500$	19	7117.815
3	$\varphi(t) = \sqrt{t}$	$n = 500$	18	7474.826

Table 2. *Results for values of $\varepsilon = 10^{-8}$, $\rho = 0.95$, $\sigma = 0.3$.*

Problem	Function φ	Size of matrix	Nr. of iterations	Running time (ms)
1	$\varphi(t) = t$	$n = 4$	10	1.614
1	$\varphi(t) = \sqrt{t}$	$n = 4$	19	2.362
2	$\varphi(t) = t$	$n = 7$	20	3.276
2	$\varphi(t) = \sqrt{t}$	$n = 7$	19	3.756
3	$\varphi(t) = t$	$n = 500$	23	9283.661
3	$\varphi(t) = \sqrt{t}$	$n = 500$	22	8764.180

Table 3. *Results for values of $\varepsilon = 10^{-6}$, $\rho = 0.98$, $\sigma = 0.3$.*

Problem	Function φ	Size of matrix	Nr. of iterations	Running time (ms)
1	$\varphi(t) = t$	$n = 4$	11	1.646
1	$\varphi(t) = \sqrt{t}$	$n = 4$	14	2.134
2	$\varphi(t) = t$	$n = 7$	15	2.772
2	$\varphi(t) = \sqrt{t}$	$n = 7$	14	3.013
3	$\varphi(t) = t$	$n = 500$	18	7102.162
3	$\varphi(t) = \sqrt{t}$	$n = 500$	18	7119.939

Table 4. *Results for values of $\varepsilon = 10^{-6}$, $\rho = 0.95$, $\sigma = 0.9$.*

Problem	Function φ	Size of matrix	Nr. of iterations	Running time (ms)
1	$\varphi(t) = t$	$n = 4$	138	15.872
1	$\varphi(t) = \sqrt{t}$	$n = 4$	140	21.080
2	$\varphi(t) = t$	$n = 7$	139	18.307
2	$\varphi(t) = \sqrt{t}$	$n = 7$	140	19.608
3	$\varphi(t) = t$	$n = 500$	143	100614.3
3	$\varphi(t) = \sqrt{t}$	$n = 500$	143	105317.7

most effective for the first problem. The second problem was solved by the method based on the square root function in fewer iterations, while in the case of the third problem, the number of iterations was the same (**Table 3.**).

Based on **Table 4**, it can be concluded that the program reached the solutions after more iterations than in the previous case, but this was expected, since by increasing the parameter σ we decelerated the decrease of the variable μ.

5. Conclusions

Regarding the solution of the WLCP, we introduced the algebraically equivalent transformation technique. With the help of an application written in the Java programming language, we established that the function describing the direction can influence the results provided by the WLCP solver. The technique of algebraically equivalent transformation was analyzed from the perspective of the identical map and the square root function. It can be concluded that the number of iterations depends on the accuracy parameter ε, as well as on the values of the parameters σ, which reduces the barrier parameter, and ρ which adjusts the length of the step.

Acknowledgment

The authors express their gratitude to the Transylvanian Museum Association for the support provided to the research work.

References

[1] Potra F. A.: *Weighted Complementarity Problems - a New Paradigm for Computing Equilibria.* SIAM Journal on Optimization, 22/4. (2012) 1634–1654. https://doi.org/10.1137/110837310

[2] Asadi S., Darvay Zs., Lesaja G., Mahdavi-Amiri N.: *A Full-Newton Step Interior-Point Method for Monotone Weighted Linear Complementarity Problems.* Journal of Optimization Theory and Applications, 186/3. (2020) 864–878. https://doi.org/10.1007/s10957-020-01728-4

[3] Potra F. A.: *Sufficient Weighted Complementarity Problems.* Computational Optimization and Applications, 64/2. (2016) 467–488. https://doi.org/10.1007/s10589-015-9811-z

[4] Darvay Zs.: *A new Algorithm for Solving Self-Dual Linear Optimization Problems.* Studia Universitatis Babeş-Bolyai, Series Informatica, 47/1 (2002) 15–26.

[5] Darvay Zs.: *New Interior Point Algorithms in Linear Programming.* Advanced Modeling and Optimization, 5/1. (2003) 51–92.

[6] Darvay Zs., Orbán A.-Sz.: *Implementation of the Full-Newton Step Algorithm for Weighted Linear Complementarity Problems*. Műszaki Tudományos Közlemények, 15/1. (2021) 15–18. https://doi.org/10.33894/mtk-2021.15.04

[7] Asadi S., Mansouri H.: *Polynomial Interior-Point Algorithm for P∗(κ) Horizontal Linear Complementarity Problems*. Numerical Algorithms, 63/2. (2013) 385–398. https://doi.org/10.1007/s11075-012-9628-0

[8] Mansouri H., Pirhaji M.: *A Polynomial Interior-Point Algorithm for Monotone Linear Complementarity Problems.* Journal of Optimization Theory and Applications, 157/2. (2013) 451–461. https://doi.org/10.1007/s10957-012-0195-2

[9] Achache M.: *Complexity Analysis and Numerical Implementation of a Short-Step Primal-Dual Algorithm for Linear Complementarity Problems*. Applied Mathematics and Computation, 216/7. (2010) 1889–1895. https://doi.org/10.1016/j.amc.2010.03.015

Műszaki Tudományos Közlemények vol. 17. (2022) 16–19.
DOI: Hungarian: https://doi.org/10.33895/mtk-2022.17.04
English: https://doi.org/10.33894/mtk-2022.17.04

GENERATION OF SINUSOIDAL ALTERNATING CURRENT OF VARIABLE FREQUENCY AND INTENSITY FOR MEASURING THE ELECTROMAGNETIC CHARACTERISTICS OF ELECTRIC MOTORS

Patrícia ELEK,[1] Attila SZÁNTÓ,[2] Gusztáv Áron SZIKI[3]

[1] *University of Debrecen, Faculty of Engineering. Debrecen, Hungary,, epatri014@gmail.com*
[2] *University of Debrecen, Faculty of Engineering. Debrecen, Hungary,, szanto.attila@eng.unideb.hu*
[3] *University of Debrecen, Faculty of Engineering. Debrecen, Hungary,, szikig@eng.unideb.hu*

Abstract

The electric vehicle drive is nowadays considerably widespread in everyday road transport. These vehicles have an important component: the electric motor. The motors are tested using a simulation program for which knowledge of its electromagnetic and dynamic parameters are needed. These data are usually not provided by the manufacturers; therefore, it must be determined experimentally by measurements. For this purpose, at the Faculty of Engineering of the University of Debrecen there is the structure of a complex measuring system in progress. With this system, we can determine the motor parameters required for the simulation for all electric motors used in the automotive industry. In this publication, we will present a method designed to produce one of the characteristic electromagnetic parameters of electric motors; the variable frequency and strength sinusoidal alternating current required to determine the inductance of windings.

Keywords*: electric motor, measuring system, motor test bench, simulation.*

1. Introduction

Nowadays, more and more attention is being paid to alternative propulsion vehicles, and electric / hybrid propulsion. [1] This is due not only to the development of technology, but also to our more environmentally conscious lifestyle, as we all want a cleaner world free of harmful substances.

There are several designs of alternative vehicle drives, but most of them are powered by some kind of electric motor.

The Faculty of Engineering of the University of Debrecen also conducts a lot of research on alternative drives, and the Faculty team has started and achieved success in several races with electric-powered, self-designed racing cars. For the conscious development of vehicles, a vehicle dynamics simulation program is essential [2, 3], with which we can calculate the performance and driving dynamics of the electric motor as well as the car, and thereby optimize the technical characteristics of the vehicle for a given competition goal. This requires knowledge of vehicle parameters, including the characteristics of the electric motor that drives the vehicle.

The performance and other characteristics of an electric motor depend on a number of electromagnetic and dynamic parameters that are not normally provided by the manufacturer. Consequently, they must be determined experimentally. [4–8]

It is very important for successful measurements to have a complex, validated measuring system. For this purpose, the Faculty of Engineering of the University of Debrecen is in the process of building a measuring system [9], with which we can determine the motor parameters required for the simulation in the case of all electric motors used in the automotive industry.

In this publication we deal with the determination of one of the electromagnetic parameters

of electric motors, the inductance of windings, which depends on the intensity of the current flowing through the windings. Described in detail are plans for a power source for generating a variable frequency and intensity sinusoidal current to excite the motor windings while measuring the voltage induced therein. This equipment complements our previously built measuring system.

2. Determination of inductance of windings

The simulation of different types of electric motors (SWDC, BLDC, PMSM, IM) requires knowledge of the inductances of the motor windings as an input parameter. [10] This is not usually provided by the manufacturers, so should be determined experimentally. The measuring arrangement assembled for this purpose is illustrated in figure 1.

For the measurements, a sinusoidal AC voltage would be applied to the stator or rotor winding in the motor, and then the voltage across the winding ($U(t)$) and the current flowing through it ($I(t)$) would be measured with the NI 9239 measurement data acquisition card. The measurement would be performed at different current intensities. Based on this, the magnetic flux of the winding ($\Psi(t)$) can be calculated by the following procedure [4, 5]:

$$\psi(t) = \int_0^t (U(\tau) - I(\tau) \cdot R) d\tau + \psi(0) \qquad (1)$$

The calculation would be performed with the Simulink module of the MATLAB program. Knowing the functions $\Psi(t)$ and $I(t)$, the magnetic flux can be given as a function of the current intensity. The current derivative of the magnetic flux gives the inductance $L(I)$ as a function of the current, which can be given to the simulation program with “Lookuptable”.

In the following, the plans of the previously mentioned AC power source required to perform the measurements are described.

3. The planned power source

To perform accurate measurements, we need to produce sinusoidal alternating current with variable frequency (5-50 Hz) and intensity (0-200 A). One way to do this would be to use a frequency converter. For this, we have a Morgensen MSI200A-004G/5R5P-4 device, the output voltage signal of which was examined using an HAMEG HM303-6 analog oscilloscope. The measured voltage signal is illustrated in figure 2.

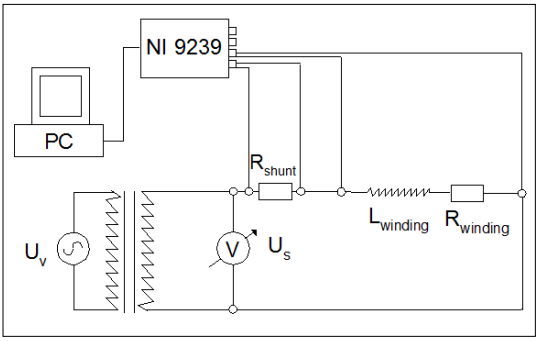

Figure 1. *Measurement layout for determining inductances.*

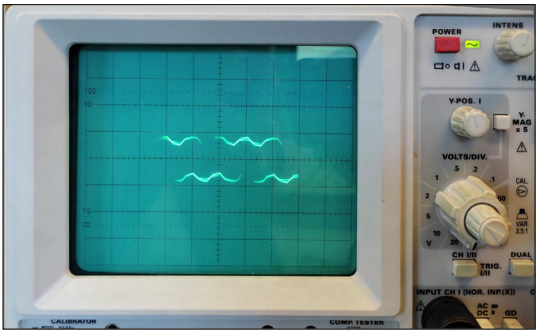

Figure 2. *Frequency converter output voltage signal.*

The voltage signal generated by the frequency converter, as shown in the figure, is not sinusoidal, so it cannot be used directly for measurements. It has also been observed that the frequency converter can only reach the set frequency a certain time after switching on, so this is not suitable for measurements, as it is not advisable to load the winding for a longer period of time at high current intensities. Furthermore, it only supplies voltage to its output when it is connected to a three-phase motor. Thus, to solve the above problems, we plan to build a system that is suitable for producing purely sinusoidal alternating current.

3.1. Schematic diagram of the arrangement

Figure 3 shows a schematic drawing of the designed power source.

The sinusoidal alternating current required for the measurements would be generated by a separately excited generator. A variable DC voltage would be applied to the excitation windings (stator) of this, thereby changing the voltage at the output of the generator, and thus the alternating current applied to the excitation of the windings.

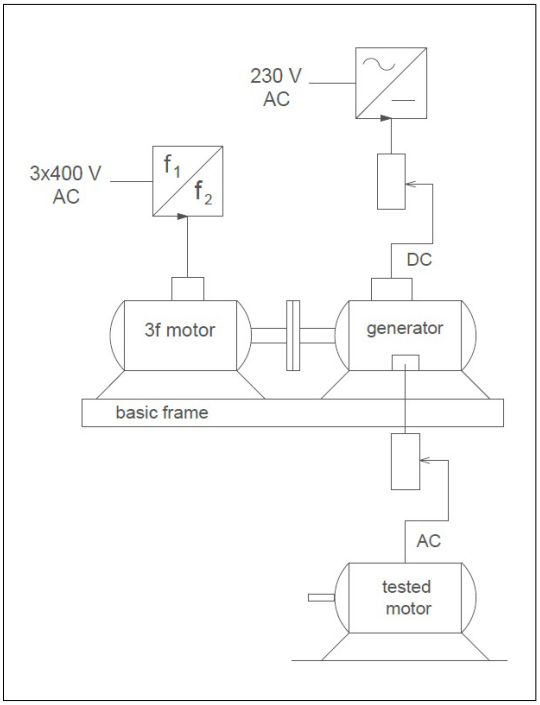

Figure 3. *Schematic diagram of the power source.*

Variable resistors can also be used in the measuring circuit to more accurately set the desired current intensities on the tested motor. In addition, a transformer can be used to achieve high current intensities if required.

The generator would be driven by a 3-phase asynchronous motor through a clutch. This motor would be connected to the previously mentioned frequency converter, thus ensuring the setting of different RPMs and thus different output frequencies.

The whole system would be fixed to a basic frame designed by us, which would be connected to our previously built measuring system, which is suitable for testing electric motors

3.2. The selected components

A Morgensen MSI200A-004G/5R5P-4 frequency converter with a power of 4/5.5 kW is planned to drive the motor (**figure 4**).

This would drive the Morgensen MSE3-90L-2 2.2 kW three-phase asynchronous motor shown in **figure 5.** The performance of the motor is designed to be adequate to perform the measurements.

The generator, according to our plans, would be an EVIG separately excited generator (**figure 6**).

Figure 4. *Morgensen MSI200A-004G/5R5P-4 frequency converter.*

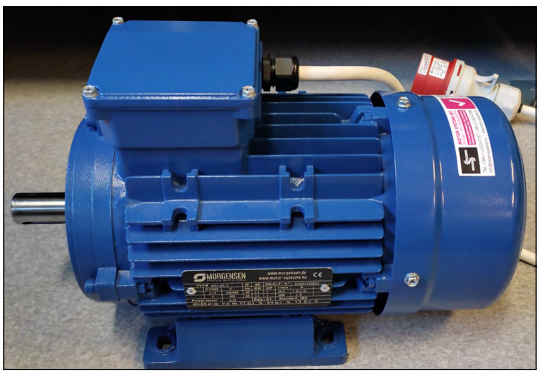

Figure 5. *Electric motor for driving the generator.*

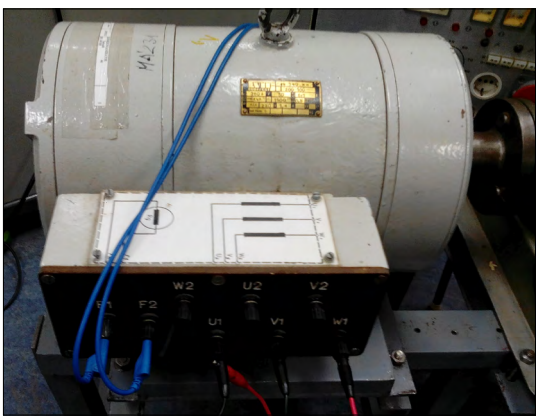

Figure 6. *The separately excited generator.*

External excitation is required to control the magnitude of the alternating current at the output of the generator at a given RPM (frequency). This can be done with a DC current of 0-230 V connected to the excitation windings. To do this, a rectifier and a toroidal transformer will be added to the system.

4. Conclusion

In this paper, we deal with the determination of one of the electromagnetic characteristics of electric motors used in the automotive industry, the inductance of windings. To determine this experimentally, a purely sinusoidal alternating current of variable frequency and intensity is required. To do this, we examined a frequency converter available to us, which, based on our measurements, revealed that the voltage generated by it was not directly suitable for performing the measurements.

Therefore, we have planned to create a system that can generate alternating current that meets our requirements. The main elements of this are a 3-phase asynchronous motor driven by a frequency converter and a separately excited generator connected to it. We presented the structure and operation of the planned measurement arrangement and the devices selected for it.

We plan to build this measuring arrangement in the Laboratory of Machine Elements of the Faculty of Engineering of the University of Debrecen, thus supplementing our previously established measuring system suitable for the experimental testing of electric motors. Once the system is set up, we will measure the inductance of the windings of the motors used in vehicle drives, and then use the measured data in simulation programs as input data.

Acknowledgement

Supported by the ÚNKP-21-3 new national excellence program of the ministry for innovation and technology from the source of the national research, development and innovation fund.

The research was supported by the thematic excellence programme (TKP2020-NKA-04) of the ministry for innovation and technology in Hungary.

References

[1] Szántó A., Síki G. Á.: *Review of Modern Vehicle Powertrains and Their Modelling and Simulation in MATLAB/Simulink*. International Journal Of Engineering and Management Sciences / Műszaki és Menedzsment Tudományi Közlemények, 5/2. (2020) 232–250.

[2] Szántó A., Sziki G. Á., Hajdú S., Gábora A., Sipos K. B: *Járműdinamikai szimuláció és optimalizáció*. Műszaki Tudományos Közlemények, 9. (2018) 219–222. https://doi.org/10.33895/mtk-2018.09.50

[3] Szántó A., Síki G. Á., Hajdu S.: *Dynamics Simulation of a Prototype Race Car Driven by Series Wound DC Motor in Matlab-Simulink*. Acta Polytechnica Hungarica, 17/4. (2020) 103–122. https://doi.org/10.12700/APH.17.4.2020.4.6

[4] Sziki G. Á., Sarvajcz K., Kiss J., Gál T., Szántó A., Gábora A., Husi G.: *Experimental Investigation of a Series Wound Dc Motor for Modeling Purpose in Electric Vehicles and Mechatronics Systems*. Measurement, 109. (2017) 111–118. https://doi.org/10.1016/j.measurement.2017.05.055

[5] Hadziselimovic M., Blaznik M., Štumberger B., Zagradišnik I.: *Magnetically Nonlinear Dynamic Model of a Series Wound DC Motor*. Przeglad Elektrotechniczny, 87/12b. (2011) 60–64.

[6] Síki G. Á., Szántó A., Mankovits T.: *Dynamic Modelling and Simulation of a Prototype Race Car In MATLAB/Simulink Applying Different Types of Electric Motors*. International Review of Applied Sciences and Engineering, 12/1. (2020) 1–7. https://doi.org/10.1556/1848.2020.00145

[7] Szántó A., Szántó A., Sziki G. Á.: *Review of the Modelling Methods of Series Wound DC Motors*. Műszaki Tudományos Közlemények, 13. (2020) 166–169. https://doi.org/10.33894/mtk-2020.13.31

[8] Szántó A., Kiss J., Mankovits T., Síki G. Á.: *Dynamic Test Measurements and Simulation on a Series Wound DC Motor*. Applied Sciences, 11/10. (2021) 1–18. https://doi.org/10.3390/app11104542

[9] Szántó A., Décsei R., Kujbus M., Fejes L., Papcsák N., Sziki G. Á.: *Design of a Measuring System Suitable for Measuring the Electromagnetic and Dynamic Characteristics of Electric Motors*. Műszaki Tudományos Közlemények, 15. (2021) 99–102. https://doi.org/10.33894/mtk-2021.15.19

[10] Szántó A., Síki G. Á.: *Mérőrendszer fejlesztése villanymotorok elektromágneses és dinamikai jellemzőinek méréséhez és teszteléséhez*. Proceedings of the Conference on Problem-based Learning in Engineering Education, Debrecen, University of Debrecen Faculty of Engineering, (2021) 61–71.

sciendo

Műszaki Tudományos Közlemények vol. 17. (2022) 20–24.
DOI: Hungarian: https://doi.org/10.33895/mtk-2022.17.05
English: https://doi.org/10.33894/mtk-2022.17.05

EME MTSZ MTK

JÓZSEF GALAMB, DESIGNER OF FORD T-MODEL AND HIS RELATIONSHIP WITH HOMELAND

József GÁTI,[1] János KUTI,[2] Krisztina NÉMETHY[3]

[1] *Óbuda University, Donát Bánki Faculty of Mechanical and Safety Engineering, Budapest, Hungary, gati@uni-obuda.hu*

[2] *Óbuda University, Donát Bánki Faculty of Mechanical and Safety Engineering, Budapest, Hungary, kuti.janos@bgk.uni-obuda.hu*

[3] *IBS, International Business School, Budapest, Hungary, knemethy@ibs-b.hu*

Abstract

In October 1908, a Ford Model T designed by József Galamb and companions, rolled out of the assembly line and achieved for the company a worldwide success it still enjoys today. The car's ease of use and reliable construction, as well as its affordable price, won the favour of buyers so much that the model was produced until 1927. The increasingly successful Hungarian chief designer of the Ford Motor Company, József Galamb never forgot his homeland. When he returned home, he supported his brothers in building up and running a Ford site and assembly plant in Makó, and established scholarships, gave lectures to members of the professional community, and supported the Reformed Church in Makó.

Keywords*: József Galamb, Ford Model T, Ford Motor Company.*

1. Preparation for the technical career

József Galamb was born on the 3rd of February in 1881, into a Reformed Family in Makó. His father was József Galamb and his mother Erzsébet Putnoki. Graduating from the Elementary Civic Boys' School in Makó, József Galamb studied in the metal industry department of the Szeged State Vocational School of Wood and Metal Industry. He continued his studies at the Royal Hungarian State Higher Industrial School in Budapest which he and his 28 colleagues completed in 1900/1901. (today's Óbuda University, Donát Bánki Faculty of Mechanical and Safety Engineering).

After that he went to the Iron Factory in Diósgyőr as a technical draftsman, then in 1901, he entered the military service in Pula, where he served on a gunboat under the command of Miklós Horthy. After his discharge, he worked for a short time at Magyar Automobil PLC. in Hódmezővásárhely and in Arad. In 1903 he traveled to Western Europe on a scholarship and then on a self-funded study trip. He toured the large machine factories in Dresden, Berlin, Hamburg, Bremen, Belgium, the Netherlands, Düsseldorf, and finally visited the Adler Car Factory in Frankfurt am Main. Here, he heard the news that there would be a World Exhibition in 1904 in Saint Louis.

2. Starting a successful career

He arrived in New York on October 6, 1903, where he took a job in a box factory. The World's Fair in St. Louis made such an impact on him that he was determined to stay in America. After a short detour, he traveled to Detroit to look for a job, from three offers- C Cadillac, Silent Northern, and Ford- he chose the latter, joining them on December 11, 1905. The engineers who applied at the time were asked not for their degree but for a test drawing. So he began working on the design of the N-model. He designed a new cooler, a circulating pump.

In 1952, Joseph Galamb recorded her audio memoirs for the Ford Museum. A cite from this:

„At the beginning of 1907, Mr. Ford said to me, Joe, I have an idea. Let's design a new car. Take your drawing board to a separate room and let's start designing a new model. No one needs to know about it. The first thing I need is a new

Figure 1. *József Galamb in 1905 in Pittsburgh.*

Figure 2. *The T-Model from 1922 restored by Óbuda University, Donát Bánki Faculty of Mechanical and Safety Engineering.*

transmission because I'm unsatisfied with what's been there so far, it's not practical enough. Then of course we didn't know it was going to be the T model! Or I worked on the design of the gear shift for half a year." [1]

On October 1, 1908, the first car for sale rolled off the production line. The car, which has become world-famous as Tin Lizzie, was produced for nearly 20 years, more than 15 million were sold, and in 1997 an international jury chose the Ford model T above the Porsche 911, Volkswagen Beetle, Citroën DS and Morris Mini for Car of the XX. Century.

The ease-of-use, reliable design and the affordable price pleased buyers so much that the model was manufactured until 1927. Production demand could only be met by assembly line.

The engine of the world's first production car is the Otto-system four-cylinder, four-stroke, thermosiphon water-cooled engine. Its maximum power is 15 kW, which it achieved at 1450 RPM. Consumption is 13.5 liters of fuel per 100 km, with a top speed of 65 km / h. The most ingenious technical solution employed in the car was the planetary gearbox, designed by József Galamb.

Cite from polish writer, Alfred Liebfeld's book, titled Henry Ford is the' God: „It turns out that the new car will meet not only the needs of the rural population but also the urban population. Its construction was so simple that anyone could sit behind the wheel and, as promised, make minor repairs themselves." [2]

The price of the T-model dropped from the initial $ 825 to $ 575 in four years, and later reached the $ 355 minimum.

An important Fordson tractor, designed by József Galamb and Jenő Farkas, played an important role in the mechanization of American agriculture.

In addition to the above, József Galamb also designed many other constructions: he was involved in the development of other Ford car models, trucks and track cars, as well as working on prototype experiments and designing new factory departments. He was also involved in the design of a submarine finder and light tanker during World War I. [3]

Machine design work of Galamb is well characterized by his patent activity. A total of 27 patents filed with the United States Patent Office between 1920 and 1952 reflect carefully edited, clear, accurate engineering work.

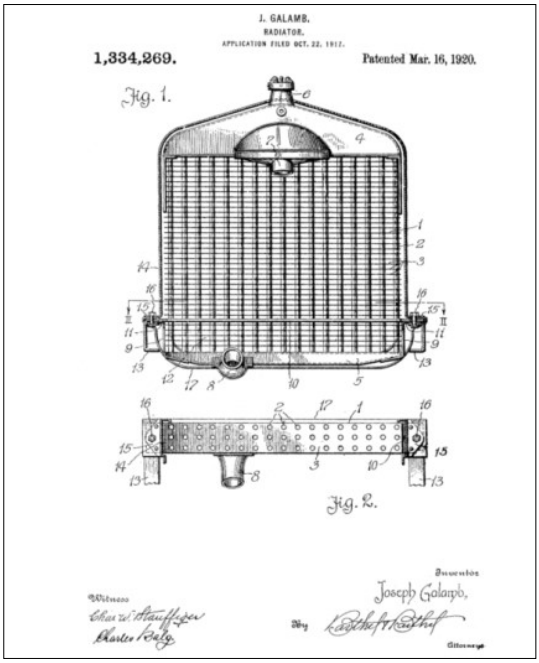

Figure 3. *Patent sketch of the radiator.*

The four decades of chief engineering work of József Galamb, an engineer, is an example of American wonder and success.

In 1905, Ford was still a small factory with 300 employees, and by 1944 it had become one of the largest U.S. giants. In the mid-1910s, 250 cars a day were produced, and twenty years later production was 10,000 cars a day.

3. Relationship with the homeland

According to the birth certificate of the Galamb family with roots in Makó, József Galamb was the second child of his parents, and five more (four sons and one daughter) followed him in line (his two brothers died early). Persuaded by a Reformed teacher the intelligent peasant farmer supported the further education of two oldest sons, Alexander and Joseph. The eldest son, Sándor, became a lawyer.

József Galamb first re-visited his homeland in the autumn of 1911. His mother and siblings welcomed him after his eight-year absence with great love. It was then that the famous picture of the four Galamb boys was taken in the Homonnai studio. He became an American citizen in 1915.

In 1921, he founded a scholarship of 100,000 crowns to support further education. According to the Articles of Association:" József Galamb, born in Makó and currently a resident of Detroit, completed his upper vocational school studies on a scholarship; (North America, Michigan); he provided a scholarship foundation of 100,000 crowns for the poor but well-educated students of the mechanical engineering department of the upper industrial school and paid this amount to the public fund of the city of Makó". [4]

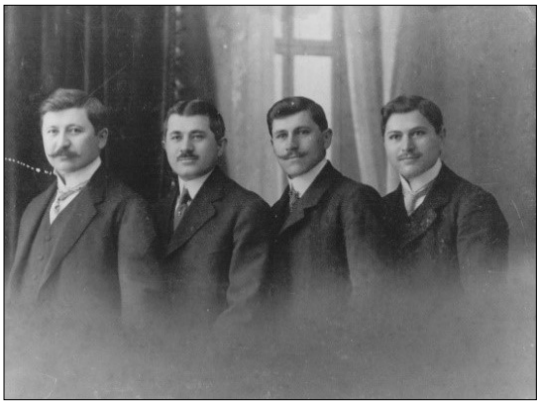

Figure 4. *Galamb Brothers in Makó: Sándor, József, János, Ferenc (from left to right)*

John took his younger brother out to America, and he also worked for Ford for two years. After World War I, in 1921, Joseph Galamb sent six Fordson tractors to his Makora brothers to work on and promote Ford products. This is how the family business was founded, run by two younger Galamb brothers, John and Francis. József Galamb visited Makó to start the business in the autumn of 1922, on which occasion the Pénzvilág published a longer interview.

The Makó site was located on the corner of Deák Ferenc Street. Colorful Ford cars were painted on the exterior wall of the repair shop in the late 1920s, traces of which can still be found on the facade to this day. The workshop and service of the warehouse were managed by János, and the commercial tasks were managed by Ferenc. With the increase in turnover, a Galamb warehouse was opened in Békéscsaba, where 35 mechanics worked [4].

During his return visit, József Galamb not only visited his family but also gave lectures at the Hungarian Association of Engineers and Architects and at the Technical Academy. He brought films with him, which allowed professionals to learn about Ford's factory production and the technical features of the products.

The appearance of the Ford caravan in Hungary served to promote the Ford brand. The car line

representing the best in Ford's range has traveled across Europe. On May 1, 1926, a caravan of 25 different cars arrived in Hungary having set off from Trieste. Then József Galamb visited to Makó again. This time the governor greeted him at an interrogation in the Castle. It turned out that they had first met on the mechanical training school ship 25 years earlier. After their official meeting, Miklós Horthy invited József Galamb to his private suite. He met the governor's family and talked for more than four hours. They planned that after graduating from university, István Horthy, the son of the Governor would go on a study trip to Detroit [5].

During the First World War, the bells of Makó also fell victim to metal shortages, and after removal, they were melted down for military purposes. Sándor Galamb, the pastor of the Reformed Church, played a significant role in their replacement.

In the tower of the Reformed Church in October 1927, the so-called On the Horthy Bell, which was “cast for the public use of the Reformed Church in Makó,” it ranks first in the list of donors “Dr. the name of the valiant Sándor Galamb ”, next to which is the inscription“ Galamb József Amerika” [6].

István Horthy, the governor's eldest son, obtained his degree in mechanical engineering in 1928. The young man, who spoke fluent English, German and French, was well prepared for the American study trip.

Governor Horthy inaugurated the World War I Heroes Memorial in Makon on September 29, 1929. Here the Governor asked Alexander Galamb to write to his brother that Stephen had graduated and could go to America. On his intervention, Henry Ford wrote to the governor with his own hand that his son could come, welcoming him to Detroit. From the autumn of 1929, the later deputy governor worked first as a simple worker, then in the tractor assembly department, and finally in the experimental design department. He spent a total of 18 months at Ford.

His last homeland visit was in 1932. Even then, he gave a lecture at the headquarters of the Hungarian Association of Engineers and Architects, and once again screened a film about Ford products. This was his last visit to Hungary, he recovered from a heart attack in 1944 and applied for his retirement. On December 4, 1955, at the age of 74, a retired chief engineer from one of the world’s largest automotive corporations died.

Figure 5. *Ford depot from the yard in Mako.*

Figure 6. *Advertising of the Ford caravan in Szeged.*

Figure 7. *Horthy bell cast from the donations of the Reformed Makó.*

References

[1] Galamb Józseffel folytatott angol nyelvű, hangszalagra felvett beszélgetés kézirata a Ford Archívumból. Riporter Owen Bombard, Pontchartrain, 1952. január 30.; február 6. Fordította Terplán Zénó egyetemi tanár

[2] Liebfeld A.: *Henry Ford, az „isten”*. Kossuth Kiadó, Budapest, 1973.

[3] Gáti J.: *Galamb József. Ford T-modell, a XX. század autója*. Magyar Örökség Díj nyolcvankettedik díj-átadó ünnepsége. Laudáció. Magyar Tudományos Akadémia, 2016. március 19.

[4] Halmágyi P.: *Egy világra szóló karrier. Galamb József életútja.* Makói História, József Attila Múzeum Kulturális Lapja, Makó, 2006.

[5] Gáti J., Horváth S., Legeza L.: *A XX. század autója. 100 éves a Ford T-modell.* Budapest Műszaki Főiskola, Budapest, 2008.

[6] Harangzúgás, a Makói Református Egyház lapja, Makó, 1927. október 9.

sciendo

Műszaki Tudományos Közlemények vol. 17. (2022) 25–30.
DOI: Hungarian: https://doi.org/10.33895/mtk-2022.17.06
English: https://doi.org/10.33894/mtk-2022.17.06

EME MTSZ MTK

PHOTOVOLTAIC SYSTEMS: CONTROL STRATEGIES FOR GRID CONNECTION

Tamás KEREKES

Aalborg University, Faculty of Engineering and Science, Department of Energy; Aalborg, Denmark, tak@energy.aau.dk;

Abstract

Renewable energy is one of the best solutions for generating clean energy. Wind and solar installations have seen a huge increase in the last decades and will be the major power production technology in the future, phasing out classical power production such as coal and gas, which result in the increase of CO2 and other greenhouse gases. This article gives an overview on how grid connected renewable energy systems, like a photovoltaics, can play an important role in the energy supply of the future. Also it shows that such renewable energy sources need to be combined with storage in order to be able to comply with grid codes and make the energy system of the future clean and secure.

Keywords*: renewable energy, grid-connected, current control.*

1. Introduction

Renewable energy has been a very hot topic during the last two decades. Converter based renewable energy is mainly linked to wind and solar applications, where the wind turbine (WT) generator or the photovoltaic (PV) plant is connected to the electrical grid using power electronic converters. These converters are needed in order to convert the alternating current (AC) from the WT generator or the direct current (DC) from the PV plant into a fixed frequency AC electrical grid.

Looking into yearly installations there have been a total of 97.5GW of new WT installed worldwide in 2021 [1]. Though, this has been surpassed by new PV installations, since about 168 GW of new PV plants have been installed in 2021, according to [2]. Looking at the globally installed cumulative capacity of WT and PV installations, at the end of 2021 there were 837 GW of WT and 940 GW of PV installations worldwide.

Looking at PV plants, one would imagine a few PV panels installed on rooftops. This is true for systems installed in residential and commercial buildings, where such systems have a capacity from a few kWp to around hundreds of kWp, depending on building size.

Nevertheless, PV installations have reached GWp capacities and their peak production can match the production of traditional coal power plants or even that of nuclear reactors, given the fact that sunshine is available in the specific location.

The biggest PV plants are listed in **Table 1.** nevertheless there are many smaller PV systems in the range of up to several hundred kWp capacity either as residential or commercial installations. This means that nowadays a huge capacity of the electrical power production is now distributed over a wider area, while in the past electrical energy was produced in a central power plant and distributed over long transmission lines to the consumers, that could be several hundreds of km away.

PV plants are modular and are made up of thousands of PV panels connected in PV strings, these PV strings are then connected in parallel into PV arrays. These PV arrays are then connected to the electrical grid through a PV inverter. In most cases such PV plants use three-phase inverters and connect to the medium voltage (MV) voltage grid though a MV/LV transformer station [3].

2. Grid codes and requirements

Grid connected systems need to comply with rules and requirements that are defined by the local electrical grid owner. These requirements define DC voltage injection, voltage imbalance, voltage amplitude, frequency deviation, faults and harmonics in a three-phase system in order to make sure that a grid connected unit will not disturb the grid and will not have a negative impact in grid voltage quality.

Looking into the IEEE 1547 Standard for Interconnection and Interoperability of Distributed Energy Resources with Associated Electric Power Systems Interfaces published by IEEE, back in 2003, one can read, that converters connected to the grid [4]:

- shall not actively regulate voltage;
- shall disconnect on abnormal voltage or frequency of the electrical grid.

This was the rule since at that time there were only 2.8 GWp of PV and 39GW of WT installations worldwide contributing only to a very small share in the total energy mix.

Table 1. *Largest PV plant installations worldwide*

Name	Country	Capacity MW_{DC} or MW_{AC}	Land size km^2	Year
Bhadla Solar Park	India	2,700	160	2020
Longvangxia Dam Solar Park	China	2,400		2015
Huanghe Hydropower Hainan Solar Park	China	2,200	50	2020
Pavagada Solar Park	India	2,050	53	2019
Benban Solar Park	Egypt	1,650	37	2019
Tengger Desert Solar Park	China	1,547	43	2016
Noor Abu Dhabi	United Arab Emirates	1,177	8	2019
Mohammed bin Rashid Al Maktoum Solar Park	United Arab Emirates	1,013		2020
Kurnool Ultra Mega Solar Park	India	1,000	24	2017
Datong Solar Power Top Runner Base	China	1,000		2016
NP Kunta	India	900		2020

With the increasing share of renewable energy in the energy mix, the grid codes have also evolved. In 2014, the IEEE 1547 standard was updated and mentioned that converters connected to the grid:

- may actively regulate voltage;
- may ride through abnormal voltage or frequency;
- may provide frequency response.

This means that grid connected systems are now capable of supporting the electrical grid with ancillary services, thereby making the electrical network stronger, better and safer.

With the continuous increase in the installed renewable energy systems, the IEEE 1547 grid code requirement has been updated again in 2018, where it is mentioned that grid connected systems are now required to fulfil the following:

- shall be capable of actively regulating voltage;
- shall ride through abnormal voltage/frequency;
- shall be capable of frequency response.

With these ancillary services, grid connected converters have taken an active part in the grid, not only injecting power in the grid, but also adjusting their behavior depending on the actual grid parameters, the same way traditional power plants would do.

3. Control of grid connected converters

Grid connected converters have several layers of control algorithms. The main control layer is the low-level control and is common for all grid connected converters. This is usually made up of a DC voltage control loop, grid synchronization and a current control loop. The theory about these loops can be found in many publications and books, such as [5], and will not be discussed here in detail. Grid current control focuses on THD limits imposed by standards, stability in case of grid impedance variations and ride-through grid voltage disturbances. DC voltage control deals with the adaptation to grid voltage variations and ride-through grid voltage disturbances. Finally, grid synchronization has the purpose of synchronizing to the grid using a phase locked loop (PLL) or frequency locked loop (FLL), required for grid connection or reconnection after a grid event, like a grid fault.

These control algorithms, shown in **Figure 2** are all needed for grid connected applications to

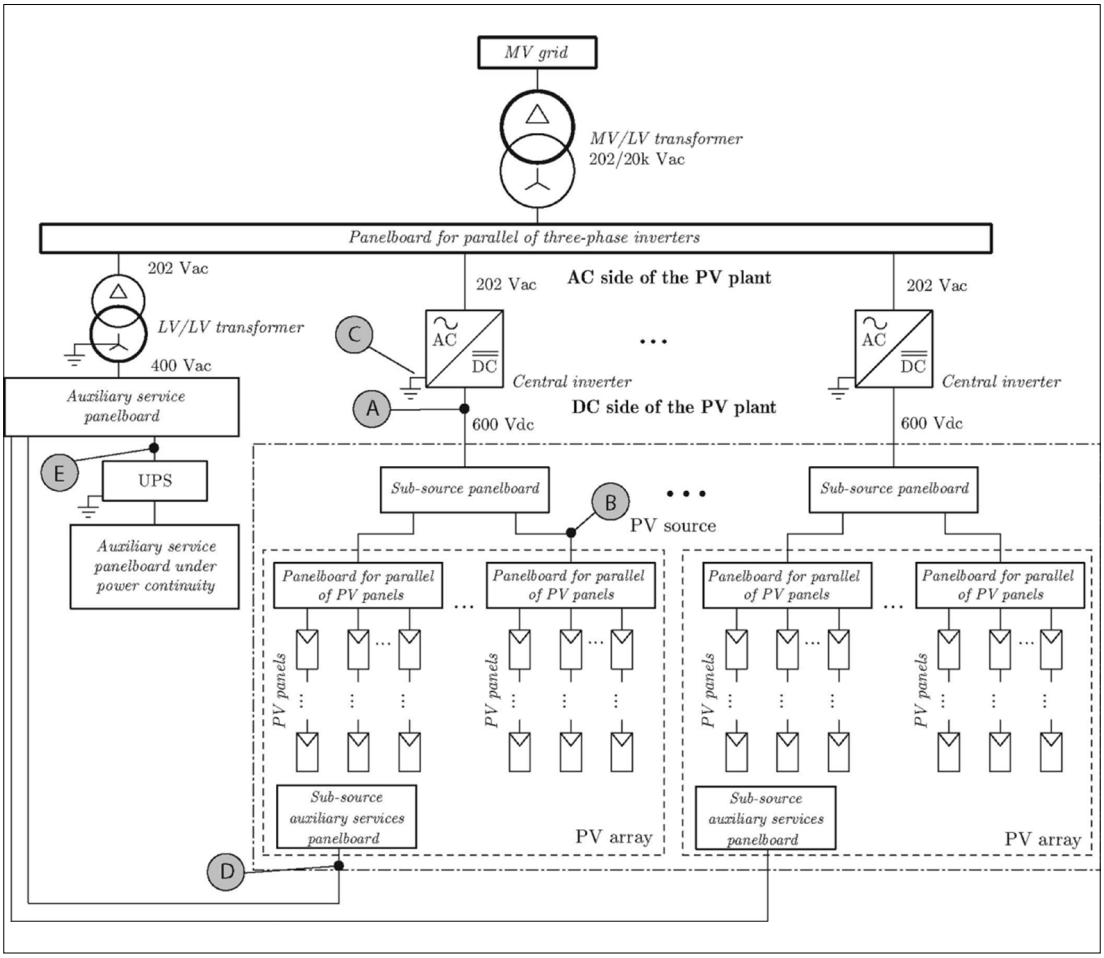

Figure 1. *Single line diagram of a PV plant.*

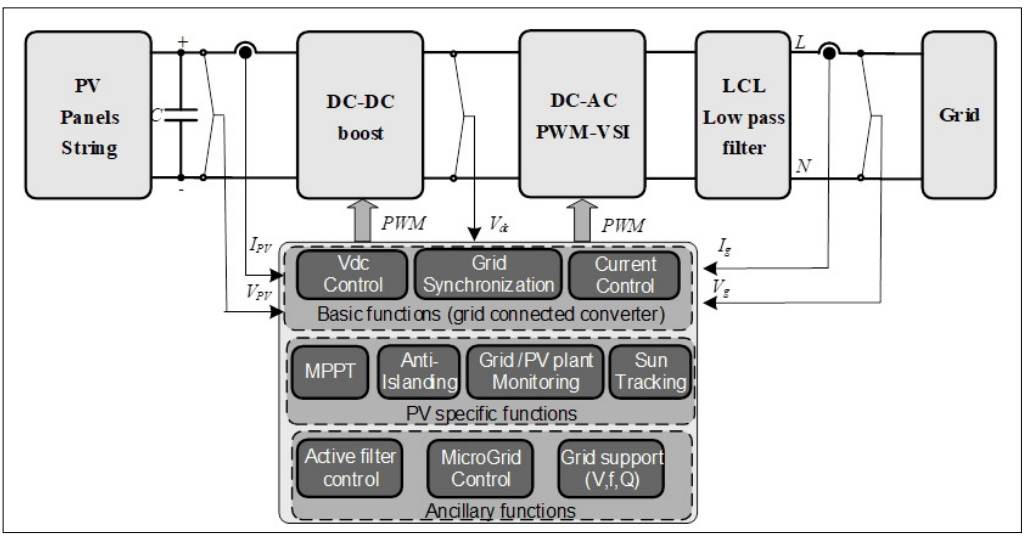

Figure 2. *Control loops in a grid connected converter application.*

make sure that grid requirements such as IEEE 1547 are followed.

In case of PV applications, there are specific PV functions, including:

- Maximum Power Point Tracking (MPPT), which requires a very high MPPT efficiency in steady state (typical > 99%), fast tracking during rapid irradiation changes (dynamical MPPT efficiency) and a stable operation at very low irradiation levels;
- Anti-Islanding (AI), to disconnect from the grid in case of specific grid events, if this is required by grid codes and standards;
- Grid Monitoring for operation at unity power factor and fast voltage/frequency detection as required by standards;
- Plant Monitoring with the scope of diagnostic of the PV panel array or partial shading detection.

Such specific PV related functions ensure that the PV array is operating at optimum conditions while also following the grid codes and requirements defined in the specific standards.

Controlling the power flow in a grid connected converter requires two loops. An outer power loop (PQ controller) shown in **Figure 3** that will calculate the required current references (id* és iq*) based on the P* and Q* reference values. Using the calculated current reference values, the inner loop (Current controller) shown in **Figure 3** then will calculate the required voltage references (Vd* and Vq*). These voltage references will be transformed to their three-phase equivalent values and used in the pulse width modulator (PWM). The PWM will generate the duty cycles that control each individual transistor in the three-phase power electronic converter, as also shown in **Figure 2.**

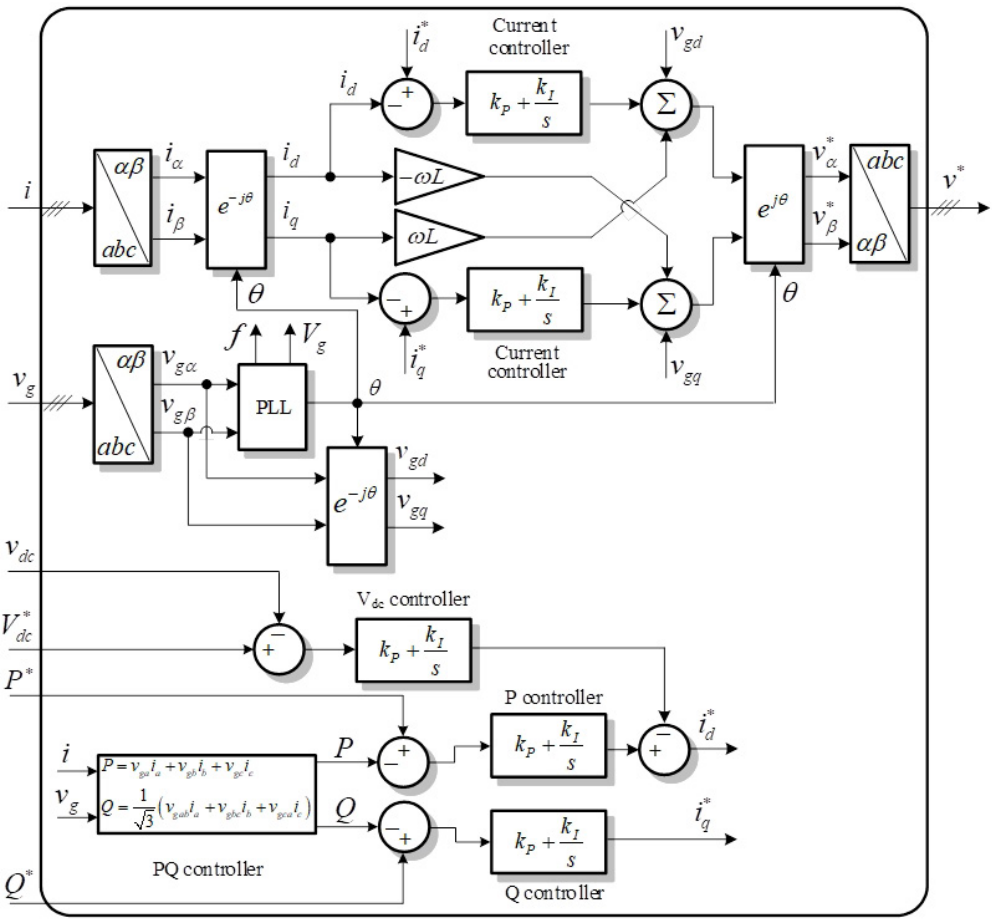

Figure 3. *Control of grid side current using a traditional PI controller and DQ transformations.*

Controlling the current and the power flow is just one of the tasks grid connected systems need to do. Grid codes also specify how fast the injected power is allowed to change, when connected to the grid. This is done in order to limit the power fluctuations that would influence grid security in a negative way. Taking into account that PV systems have no inherent inertia, any change in the received sunlight intensity will be directly visible on the output power of the converter and lead to very steep power fluctuations.

Simulating such a scenario has been achieved using a 5.7 kWp PV system. As can be seen in **Figure 5** the output power from the PV systems follows the sunlight pattern and will cause voltage fluctuations on the electrical grid. This is an unwanted side effect, and the power ramp rate needs to be limited. While the positive ramp rate can be limited in case of increasing power, just by limiting and clamping the power output of the converter, the negative ramp rate cannot be limited, since the energy stored in the power electronic converter is not enough. This means that during such scenarios the PV system will not match the grid codes and requirements.

Such power fluctuations can be limited using storage, in the form of a battery system. In this particular case, if a 10 kW and 2.5 kWh battery system is added, then, depending on the battery management system (BMS), the fluctuations can be limited to a level that is within the limits defined by the grid codes. The model of such a system is presented in **Figure 6.** and the results of the output power using the hybrid system, can be seen in **Figure 7**.

Comparing the results from **Figure 5** and **Figure 8** one can see the P_{out} reduces fluctuations when using storage since the battery filters and compensates these power fluctuations coming from the PV array. Also, if the impedance of the cables between the PV system and the low voltage (LV) distribution transformer is taken into account, then these power fluctuations will lead also to voltage fluctuations, that again are limited by the grid code. These voltage fluctuations are due to the increased active power (P) and can be compensated for using reactive power (Q). This means that the PV inverter needs to be sized accordingly, so that the current rating of the transistors will be able to carry the combined current both from the active and reactive power during all scenarios.

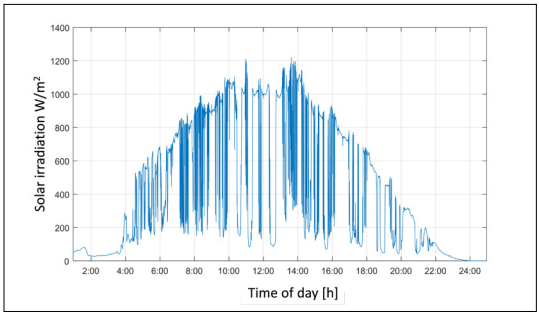

Figure 4. *Solar irradiation profile on a sunny day with passing clouds.*

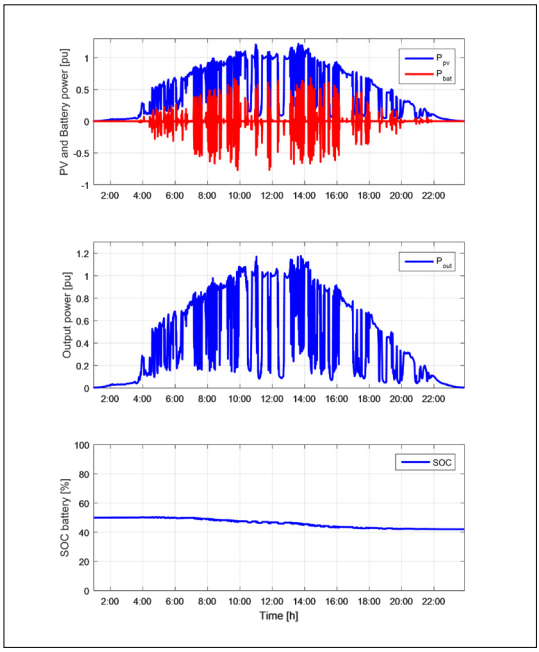

Figure 5. *PV system output power during sunny day with passing clouds shown by P_{out}.*

4. Conclusion

Renewable energy is one of the best solutions in generating clean energy. Wind and solar installations have seen a huge increase in the last decades and will be the major power production technology in the future, phasing out classical power production such as coal and gas, that result in the increase of CO_2 and other greenhouse gases. The intermittency of renewable energy, though, is a challenge. Therefore, different renewable energy sources need to be combined with energy storage solutions to make energy production a success in the future.

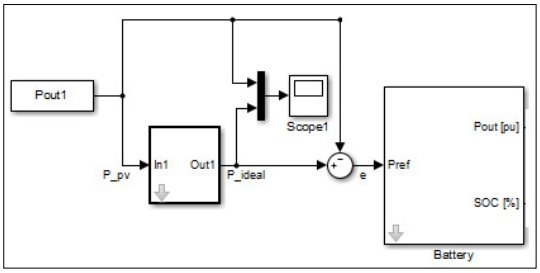

Figure 6. *PV production including battery model.*

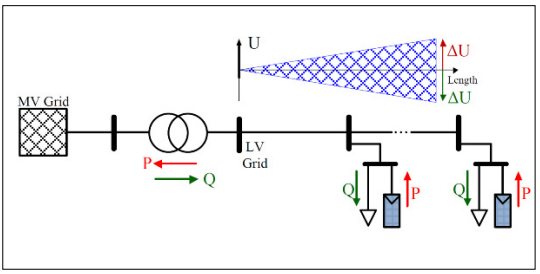

Figure 7. *Grid voltage influenced by grid impedance in the LV grid.*

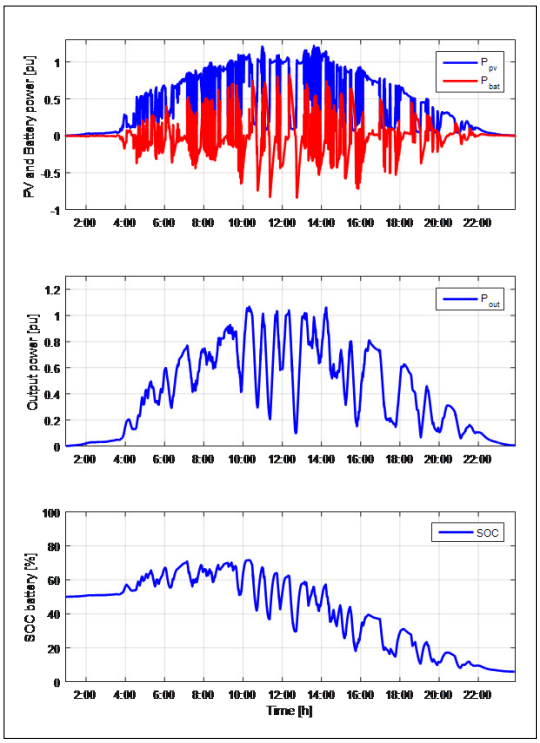

Figure 8. *Simulation results showing P_{PV}-PV power, P_{bat}-battery power, P_{out}-power injected in the grid and the battery state of charge (SOC)*

References

[1]. Global Wind Energy Council: *Global Wind Report 2022*;

[2]. *Global Market Outlook for Solar Power 2022–2026*; SolarPower Europe; ISBN NUMBER 9789464518610;

[3]. Araneo R., Lammens S., Grossi M., Bertone S.: *EMC Issues in High-Power Grid-Connected Photovoltaic Plants*, IEEE Transactions on Electromagnetic Compatibility, 51/3. (2009) 639–648.

[4]. *IEEE Standard for Interconnection and Interoperability of Distributed Energy Resources with Associated Electric Power Systems Interfaces*; IEEE 1547;

[5]. Teodorescu R., Liserre M., Rodríguez P.: *Grid Converters for Photovoltaic and Wind Power Systems*. John Wiley & Sons Ltd. 2010. https://doi.org/10.1002/9780470667057

sciendo

Műszaki Tudományos Közlemények vol. 17. (2022) 31–36.
DOI: Hungarian: https://doi.org/10.33895/mtk-2022.17.07
English: https://doi.org/10.33894/mtk-2022.17.07

EME MTSZ MTK

ON RESEARCH AND TRAINING IN MACHINERY DIAGNOSTICS IN ENGINEERING EDUCATION

Imre KOCSIS,[1] Dóra SIPOS[2]

[1] *University of Debrecen, Faculty of Engineering, Department of Basic Technical Studies, Debrecen, Hungary, kocsisi@eng.unideb.hu*

[2] *University of Debrecen, Faculty of Engineering, Department of Basic Technical Studies, Debrecen, Hungary, dorasipos@eng.unideb.hu*

Abstract

We have a decades-long tradition of examining the operation and maintenance issues of mechanical engineering systems at the Faculty of Engineering at the University of Debrecen. In the last decade, technical diagnostic research has come to the fore, especially bearing diagnostics, a lot of experience has been gathered in this field and many results have been achieved. With the development of the tools of technical diagnostics, the presentation of the topic at all levels of engineering education, and the establishment of industrial relations, an environment has been created in which it is possible to answer the current questions on the topic. Technical diagnostics, which is largely applied informatics (and mathematics) – together with several other engineering topics – also raises educational questions, which we intend to answer by transforming some elements of the training.

Keywords*: engineering education, technical diagnostics, teaching engineering mathematics.*

1. Introduction

There is a decades-long tradition of examining the operation and maintenance issues of mechanical engineering systems at the Faculty of Engineering at the University of Debrecen. In the last decade, technical diagnostic research has come to the fore, especially bearing diagnostics, a lot of experience has been gathered in this field and many results have been achieved. With the development of the tools of technical diagnostics, the presentation of the topic at all levels of engineering education, and the establishment of industrial relations an environment has been created in which it is possible to answer the current questions on the topic, including the integration of technical diagnostic tools into digitized manufacturing and operating systems, with a focus on the use of smart devices, machine-to-machine communication, process monitoring (replacing classical condition monitoring) and real-time diagnostic-based applications. Technical diagnostics, which is largely applied informatics (and mathematics) – together with several other engineering topics – also raises educational questions, which we intend to answer by transforming some elements of the training.

2. The role and tools of technical diagnostics

2.1. The role of technical diagnostics

The quality of maintenance is a key determinant of productivity and profitability in the operation of manufacturing companies. The use of the latest tools in technical diagnostics can provide a significant advantage by effectively supporting predictive maintenance, which appears in high levels of availability and machine condition and low frequency of unexpected breakdowns.

The possibilities of technical diagnostics have always been determined by the state of the art of measurement tools (electronics, computing: data transmission and storage capacity, signal processing algorithms), which have evolved along with IT. Because of its crucial role in profitability, tech-

nical diagnostics has always been one of the fastest to adopt new IT solutions, for which industrial funding has been (and will continue to be) constantly guaranteed.

The high level of automation in industrial production, the use of high-performance machinery and high productivity requirements further increase the importance of technical solutions that enhance the reliability of the processes.

Diagnostic tools and data are becoming integrated parts of digitalised production systems and smart factories. Moreover, the experience gained in condition monitoring and computer aided maintenance management systems forms the basis for such developments.

2.2. Levels of vibration diagnostics

Vibration-based condition monitoring is the most widely and effectively used diagnostic method.

Based on the purpose, the 'subtlety' of the tools, and the value of the information provided by the investigations, three fundamentally different levels of vibration diagnostics can be identified.

The simplest test is to determine the "vibration level" based on average values (most commonly the root mean square – RMS – of the vibration velocity) or peak values (such as peak or peak-to-peak). At this level, the severity of the overall condition of the machinery can be determined, and failures cannot be identified. If the vibration exceeds a given 'alarm level', the machine should be stopped and the cause of the increased vibration level should be investigated. For example, the ISO 2372 and ISO 10816 standards define general vibration velocity levels for different classes of machinery, which, if exceeded, are a warning to the operator. These limits are independent of the operating conditions and age of the machine; they are for information purposes only. For machines where high-energy vibrations 'only' lead to a reduction of the life-time of certain components, but do not affect operation in the short term (e.g. in the case of subordinate electric motors, pumps), information about the severity (or, preferably about the aggravation) of the vibrations may be sufficient to take the necessary maintenance decisions.

Condition monitoring tools based on vibration measurements are now widely used and are based on the detection of failure symptoms. Their application represents the second level, where the aim is to identify typical failures of machinery as early and as accurately as possible. The key issue here is the detection at the right time which means that corrective intervention is possible in the period between the detection of the fault and its aggravation leading to a breakdown. The length of this period can be a few days or a half a year depending on the process. In the case of a high-performance automatic machines, the critical time may be as short as a few minutes and real-time interventions based on diagnostic measurements may be needed to control the production process (to stop the process or to correct the malfunction).

Symptoms of most mechanical and many electrical failures are specific patterns (line systems) in the frequency spectrum, but some statistical features calculated from the time signal can also be effective in detecting certain problems. A particularly important area is the application of the shock pulse method in bearing diagnostics and gear diagnosis.

Modern condition monitoring systems are able to identify a wide range of faults and determine their severity, based on the symptoms. This information allows maintenance activities to be optimised.

The third level is represented by specific tests using special methods. Available systems and signal processing algorithms provide a detection method for a given set of failures. Otherwise, new solutions in the measurement system and in the processing algorithms are required. For example, in bearing diagnostics alone, hundreds of specialised diagnostic methods have appeared, including an increasing number that use specific combinations of transformations, filtering methods and machine learning tools.

For example, a doctoral thesis **[1]** provides a method for detecting grinding defects and estimating the size of defects in the manufacture of tapered roller bearings, which is effective in noisy environments as well. In the thesis, the design and application of special wavelets and MRA are the basic tools, but also support vector machines and artificial neural networks are used to classify manufacturing defects.

2.3. Evolution of technical diagnostics tools

Since the 1950s, the tools of technical diagnostics have evolved from sensory diagnostics to automated testing and decision-making based on machine-to-machine communication in digitalised manufacturing.

In the old days, given low level of the productivity requirements and the precision of the

machines, reactive maintenance (run-to-failure operation) was acceptable. This approach was replaced by preventive (scheduled) maintenance based on life-time characteristics, such as failure rate diagrams (‘bath curves’) which were prepared on the basis of large statistical samples for commonly used machines (e.g. electric motors).

An obvious limitation of the effectiveness of this statistical approach was that it could not take into account the specific operating conditions leading to a high risk of too early or too late intervention.

With the advent of IT tools becoming available to industry, it was possible to implement condition-based predictive maintenance and develop in-service condition monitoring tools.

The development of technical diagnostics has been uninterrupted since the 1970s, and today online systems, wireless sensors, remote diagnostics, continuous data reporting, diagnostics-based process monitoring, IoT diagnostics tools as an integrated part of digitalised manufacturing systems are widespread in smart factories.

Until the 1980s, the development of maintenance was mainly driven by technical development, but later on, organisational approaches such as reliability-based maintenance, risk-based maintenance or TPM, as well as computer-based maintenance management systems, became increasingly important.

Today, in the era of Industry 4.0 and digitalisation, technical development is again the basis for progress, but these are mainly IT-based developments, as opposed to the mechanical and electrical developments of the past.

3. Teaching technical diagnostics

3.1. The changing role of mathematics in engineering education

The demands of modern engineering, especially the need for the widespread use of machine learning tools, are putting mathematics and its teaching in a new position.

In engineering courses, which are trying to keep pace with the rapid changes in technology, more and more subjects are already appearing in undergraduate engineering courses, which rely heavily on certain higher-level abstract mathematical skills. Examples of such topics are engineering diagnostics and control theory.

Meanwhile, a significant proportion of engineering students are also struggling to master basic calculation methods. This discrepancy can be resolved by reformulating the goals of mathematics education and applying new approaches and methodological tools. It must be recognised that while a large part of the theory that forms the backbone of classical mathematics education in engineering is not encountered by engineers in the course of their careers, they should have a working knowledge of some of the methods of applied mathematics. **[2]**

Professors of engineering are calling for a transformation in the teaching of engineering mathematics. László Tóth, a former professor of mechanics at the University of Debrecen, has stressed in several lectures that "Mathematics should be given to engineering students as a tool." Today, there is a wealth of mathematical software available, so that in practice, a multitude of problems can be solved if we know how to use the tools. For a long time, without an appropriate tool, mathematics was only an elegant background for engineering work, calculations were practically infeasible in daily work, decisions were typically based on engineering estimates, practice and experience in the field.

The numerical (and sometimes symbolic, analytical) methods built into software now allow ‘exact’ calculations, with great economic benefits. Here we need to go into the meaning of ‘accuracy’. Although symbolic (analytical) calculations do indeed provide an accurate answer to mathematical problems that can be solved, in many cases, when studying real systems, the only way to arrive at a solvable problem is to make significant neglections and create simplified models. Thus, even if the solution is accurate in some sense, it is only an approximate solution to the original technical problem, and it is often not even possible to check how much the deviation from the exact solution is. Numerical methods are declared to give only an approximate solution, but the 'error' can usually be reduced arbitrarily by using a more detailed model, which of course usually leads to a drastic increase in computation time.

Engineering mathematics education has to face the fact that "In the future, many more engineers will need to know mathematics that few people understand in depth", as Péter Korondi, professor of mechatronics at the University of Debrecen, has emphasised in several lectures. The masses cannot be expected to understand abstract mathematics, but it is essential that mathematics is available as a tool for engineers, at least for those who do development work. And as we live in an age of smart devices, where the built-in knowl-

edge gives the product its utility, more and more people are becoming developers at some level.

3.2. Effective mathematics education in engineering education

The essential elements of our approach are:
- formulating the desired competences;
- structuring the mathematics curriculum on the basis of competences;
- defining and measuring efficiency;
- formulating cross-curricular projects and publishing them (mainly) as homework;
- refreshing the mathematical knowledge required for the professional courses in the context of technical problems, project-based learning of mathematics in professional courses;
- preparing specific maths workbooks to support learning and relearning maths which help independent learning as well.

For example, understanding computations in discrete-time system models can be formulated as a competence.

In this case, the competence-based structuring of the curriculum means a pair-wise discussion of derivation and numerical derivation.

And the effectiveness of teaching is measured by students' ability to recognise and perform the necessary calculations when solving technical problems.

Cross-curricular homework assignments help students to understand the connections between mathematical and technical concepts and to apply the methods they have learned.

A good understanding of the use of mathematical software (in particular Matlab) as an everyday tool (calculator and engineering development environment) should be introduced at the beginning of the course in the mathematics courses.

3.3. Project-based learning of mathematics in the context of technical diagnostics

In many cases, students' mathematical knowledge is already well lost when learning specialised professional subjects, and, on the other hand, the specific needs of applications are not even brought up when learning mathematics. While the teaching of mathematics should aim to cover a wide range of applications, this cannot be done for every single application, partly because of the limited time available and partly because some applications only affect a small group of students by specialisation.

In the mechanical engineering training under review in this article, there is a gap of at least two years between the study of mathematics and its application in diagnostics. This raises not only the question of what needs to be learned (as a new material) in the context of diagnostics, but also what needs to be relearned in mathematics. [2]

The theoretical part of vibration diagnostics (**Figure 1.**) which is the main part of the diagnostics course, includes signal processing (applied mathematics). Thus, the learning and relearning of the related mathematics can be linked to a professional project. In this way, we can both highlight the usefulness of previously learned knowledge and motivate students to acquire new knowledge.

Main topics in vibration diagnostics:
- harmonic vibrations (amplitude, period, frequency, phase);
- displacement, velocity, acceleration, superposition;
- symptoms in the time domain;
- symptoms in the frequency domain (**Figure 2**);
- complex investigations in time-frequency domain, shock pulse method (**Figure 3**);
- signal conditioning.

Closely related topics in math:
- sine and cosine functions (range, period, sign, zeros);
- basic function transformations;
- differential and integral calculus;
- basic statistics;
- Fourier theory;
- wavelet transform, multiresolution analysis;
- filters.

A typical project that can be used as a framework for learning mathematics: condition assessment of a drive (electric motor, gearbox) (**Figure 4**). Steps:

1. Planning
   - identification of measuring points;
   - selection of measurement techniques for each measuring point;
   - provide the data needed to apply the measurement techniques;
   - add the desired evaluation methods to the measurement plan, set the required measurement parameters.
2. Measurement
3. Assessment of the condition of the machinery components inspected on the basis of the measurement results

Figure 1. *Laboratory measurement: test bench and measuring system.*

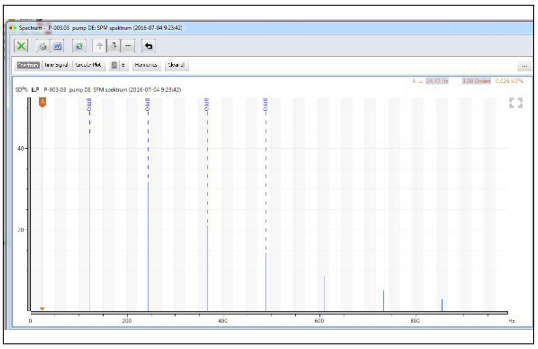

Figure 2. *A symptom in the spectrum* [4]

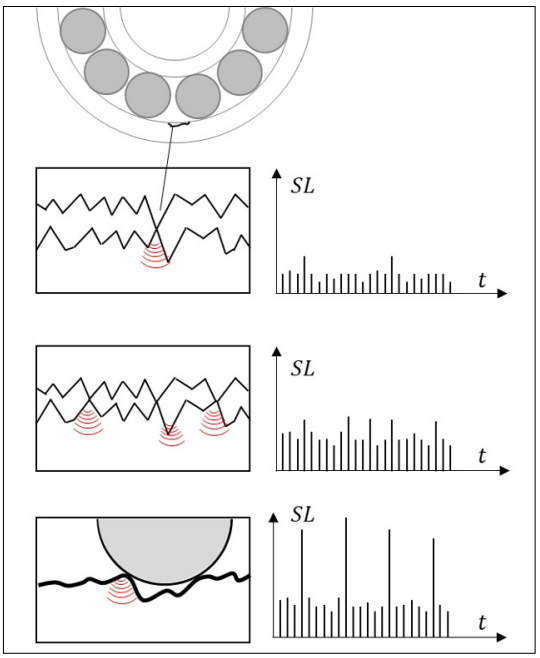

Figure 3. *Bearing testing by shock pulse method* [4]

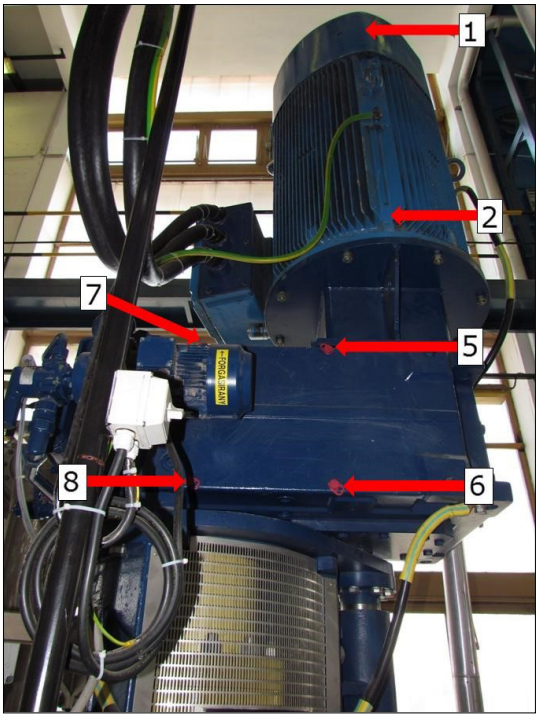

Figure 4. *Operational measurement: testing bearings in a drive train.*

General

Name	1000 Hz, 1600 lines
Short time memory	Full spectrum
Long time memory	Full spectrum
SPM spectrum type	Shock level (SL)

Settings

Order tracking	No
Upper frequency, Hz	1000
Window	Hanning
Lines in spectrum	1800

Advanced settings

FFT type	Linear
Averaging type	
Zoom center	
Zoom factor	

Figure 5. *Setting spectrum parameters.* [4]

Table 1. *Related diagnostic and mathematical tools in the project:*

Diagnostics	Mathematics
skewness, kurtosis, crest factor (peak/RMS)	descriptive statistics, relative frequency histogram
frequency spectrum, frequency range, number of lines in the spectrum, windowing	Fourier series, Fourier coefficients, Fourier transform, discrete Fourier transform, FFT, window functions
shock pulse method, bearing diagnostics, gear diagnostics, electric motor faults	complex investigations in time-frequency domain, wavelet transform, multiresolution analysis, scalogram

4. Conclusions

The ever-accelerating development of engineering is a challenge for those who want to keep up with change.

In a few decades, the effective ways of acquiring knowledge have changed completely, and the viability of traditional engineering education, in which teaching methodology issues were hardly ever raised, is weakening. This is borne out by the general opinion among young people that learning 'from the internet' is much more effective. If we look at the reasons for the popularity of online professional courses or trainings, we soon realise that one of the fundamental difference is the thoughtful way in which the knowledge is delivered (assuming, of course, that both contents are professionally correct).

Institutionalised education must also keep pace with the development of methodological tools, and focus on effectiveness, i.e. the retention of knowledge that is necessary for engineering work. Nothing is more indicative of the effectiveness of teaching a subject than the ability to apply it to other subjects or to practical engineering work.

The role of mathematics in education has changed even more, as technological tools make mathematics, at least some parts of it, more usable, even indispensable. Thus, it is becoming less and less a self-serving subject, and the learning of mathematics must be integrated into professional subjects through the coordination of topics, joint projects, homework and specific (application-oriented) mathematics teaching materials.

References

[1] Deák K.: *Development of Bearing Fault Diagnostics Methodology Based on Signal Processing and Machine Learning Tools*. PhD Thesis. Debreceni Egyetem Informatikai Tudományok Doktori Iskola, Debrecen, 2020.

[2] Sipos D.: *A numerikus számítások szerepe a műszaki modellekben*. International Journal of Engineering and Management Sciences, Debrecen, 3/5. (2018) 76–83. https://doi.org/10.21791/IJEMS.2018.5.9.

[3] Sipos D.: *A matematikaoktatás hatékonyságának vizsgálata*. In: Proceedings of the Conference on Problem-based Learning in Engineering Education, Debrecen, Magyarország, University of Debrecen, Faculty of Engineering, 2021. 47–52.

[4] *Leonova Infinity User Guide*. 71792 B. SPM Instrument AB, Sweden, 2006.

sciendo

Műszaki Tudományos Közlemények vol. 17. (2022) 37–41.
DOI: Hungarian: https://doi.org/10.33895/mtk-2022.17.08
English: https://doi.org/10.33894/mtk-2022.17.08

EME MTSZ MTK

THE SIMULATION OF A PID CONTROLLED ROBOTIC DRIVE BASED ON BOND GRAPH MODELLING

Gyula KORSOVECZKI,[1] Patrik PÁL,[2] Géza HUSI[3]

University of Debrecen, Mechatronics Department, Debrecen, Hungary

[1] *korsoveczki.gyula@gmail.com*

[2] *palpatrik5@gmail.com*

[3] *husigeza@eng.unideb.hu*

Abstract

During the study, the simulation of a robotic drive was realised using the 20-sim simulation software. The assumed robotic drive consists of an ideal permanent magnetic DC motor, a gear pair to realise the speed reduction, a torque transfer torsion shaft and a differential gear pair to change the direction and inertia. The drive is controlled by a speed control loop using a PID controller. In line with the purpose and result of the study, the simulation proved the effectiveness of Bond Graph-based modelling.

Keywords*: mechatronics, robotic drive, Bond Graph, block diagram, PID, 20-sim.*

1. Introduction

Today, engineering has attained an increasingly complex level. As the available technology expands, so does the complexity of engineering systems. The process itself is aimed at being able to provide increasingly more functions. As a result, the implementation of systems requires a more detailed design or modelling process. It is necessary to find modelling language which is not resource-intensive and provides the same response as the real physical system in cases of different signals.

2. Bond Graph modelling

2.1. The model of Multi-Domain systems

Every system has its description language. Systems that operate only in one physical domain are called Single Domain systems. Modern engineering focuses on complex combined systems. There is physical or informational connection between the contained Single Domain systems and the effect of variables is transferred from one system to the other. These systems are called Multi-domain systems. Mechatronic systems are typically Multi-domain systems [1].

For Multi-Domain systems, the biggest challenge is modelling their operations. It is required to establish connections between different domains and variables to create a dynamic model. It is difficult to find connections between the description languages. The key is a physical variable that is present in all systems. This physical variable is energy [1].

2.2. The principles of the Bond Graph

A Bond graph is a special visual and mathematical description language that uses energy as its basic variable. The modelling is an effective method for Multi-Domain systems, as energy is a physical variable that is present in all Single Domain systems. The method was developed by Henry Paynter in 1959. According to the method, the two-way flow of energy can be tracked through different elements of the language. As a result, it is possible to define the equations that describe each domain, as well as the connections between them [1, 2].

2.3. The description language of the Bond Graph

The use of the Bond Graph is based on 2 power variables, effort and flow. The multiplication

of these variables gives the transferred power, which is [1–3]:

$$P(t) = e(t) \cdot f(t) \tag{1}$$

Their role is defined and is not interchangeable. The Bond Graph is based on the Bonds, which represents the physical or informational relation between the elements. The elements can be [3–5]:

– passive one-port elements (*R, C, I*)
– active one-port elements (*Se, Sf*)
– two/three-port junctions (*TF, GY*, 0, 1)

Passive elements are used to store or dissipate energy. No new energy is produced only the existing energy is used. They can be *R* elements (e.g. damping, bearings, electrical resistance). Energy can be stored in the form of potential (*C* elements) or kinetic energy (*I* elements). Passive *C* elements are spring, shaft, capacitor and *I* elements are mass, inertia, circuit coil. The one-port active elements can add new power variables to the system. The power variable can be effort or flow, and accordingly, there is Source of effort (e.g. voltage generator, gravity force) and Source of flow (current generator, applied velocity.)The third large group consists of junctions such as basic two-port (Transformers *TF*, Gyrator *GY*) and three/more-port (0 and 1 junctions) junctions. Transformers (e.g. electrical transformator, rigid lever, gear pair) convert energy from one form to another while strictly keeping the role of power variables. Gyrators (e.g. ideal PMDC motor) reverse the roles of power variables. Another large group of junctions is the three/more-port junctions. The 0 junction (e.g. serial mechanical system or a parallel electrical circuit) is an effort junction that has constant effort value. In the case of the 1 junction (e.g. parallel mechanical system or the serial electric circuit) the flow is constant and the sum of the effort is zero [4, 5]. Causality is the most important aspect of Bond Graph-based system modelling. Causality determines the direction of effort and flow along with the Bonds since it relates to the cause and consequence relations in time. The causal stroke shows the direction of effort and flow. To correctly define causality, it is necessary to know the most important rules regarding different types of elements [6–8]. The basic Bond Graph elements can be seen in Figure 1.

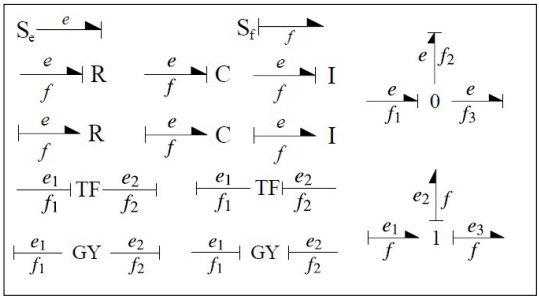

Figure 1. *The basic Bond Graph elements.* [4]

3. Drive chain of industrial robots

Industrial robots are movable mechanisms that consist of joints (constraints) and segments and have at least 3 degrees of freedom. Their motion is a constrained motion, which must be performed with exceptional precision since the repeatability of the robots is in the hundredths of millimetres. The segments are moved by the drive chain, with the following units [9]:

– energy supply or motor,
– drive unit,
– motion transforming unit,
– controlling unit.

Industrial robots can have pneumatic, hydraulic or electric drive chains. Pneumatic drives use compressed air. It is clean, explosion-proof with favourable power/weight ratio and low installation space. Disadvantages are poor signal transmission ability of compressed air, high noise levels, low positioning accuracy and difficulty in proportional control. Hydraulic drives use special liquid with higher forces. Advantages are the favourable power-to-weight ratio and the good signal transmission ability of the oil. Its disadvantages are explosion and fire hazards, noise problems, oil pollution and strong temperature dependency. The most commonly used solutions are electric drives. Their spread has been helped by the success of semiconductor technology. The requirement of low motor weight is important as the motors are part of the kinematic chain, so space and weight requirements are limited. An important criterion is the need for high torques, as industrial robots must be moved with the same dynamics throughout the load range. The motor needs to produce a wide speed range. The output typically does not have an adjustable gear ratio, so changing the speed ensures a wide range of motion. Stepper motors, DC or AC servo motors are used. The goal is to move low-speed robotic arms with low-weight but high-speed motors with high torque. Drives are used to achieve low output speed. The function of the drives is to fit the speed, fit the torque and convert motion forms. Gears (gear pairs, differential gear), drive

pulley (maximum 1/60 ratio), planetary gears and harmonic drives are used. With harmonic drives the transmission of speed up to (1/200) is available. Ball screw spindle, belt drives, chain drives and crank mechanisms are also used for this purpose [9–11].

4. The modelled drive chain

4.1. The construction of the drive chain

In the project, a drive chain was modelled using Bond graph. Its essential element is an ideal DC motor. The motor has a R_a armature resistance, a L_a armature inductance, the U_a input voltage, and an U_m electric motor voltage. The equivalent circuit is a serial circuit that has i armature current. The ideal DC motor converts the electric domain into the rotary mechanical domain. The motor produces τ_1 torque and ω_1 angular velocity values. The motor output shaft has bearing with a b_1 damping constant. Since the motor is essentially capable of moving in a wide speed range, but axes require a stable high torque and low speed, the desired speed is achieved with a gear pair. The N_1 is the input, and the N_2 gear is the output, which is supported by b_2 bearings. The torque transmission is carried out by a k torsion shaft. The axial direction of the motor is perpendicular to the axis of the motion. This is achieved by an N_3/N_4 differential gear pair. The N_3 gear is the input, the N_4 gear is the output. The differential gear pair allows us to achieve 90° motion conversion. Bearings are also on both the input and output sides with b_3 and b_4 gains. The axis to be moved is represented by inertia in the system that has J value.

4.2. The Bond Graph model of the drive chain

It is important to make the correct choice of elements and variables. The serial circuit of the motor can be modelled with 1 junction, where constant flow (current) and variable effort (voltage) is present. The voltage source can be modelled as *Se* the armature resistance as an *R* element, and the armature inductance as *I* element. Since the motor is an ideal conversion between the electric and rotary mechanical domain, it can be modelled as a GY element with k_m motor constant ratio. The mechanical part of the motor output can also be modelled with 1 junction, which includes an *R* bearing element. The speed-reducing gear pair is modelled with the *TF* element. The modulus of the TF element is the ratio of N_1/N_2 gear pair. The output bearing of the N_2 axis is modelled with 1 junction, and the b_2 bearing modelled as an *R* element. The torsion shaft for torque transmission can be modelled as a *C* element and its value is k. This connection is responsible for the torque transmission, so it can be modelled with a 0 junction. The output bearing is modelled with a 1 junction through an R element with the b_3 gain. The differential gear pair can also be modelled as a *TF* element. Its modulus value is the N_3/N_4 ratio number. Finally, the output side is modelled with 1 junction, the bearing is an *R* element and the axis is represented by *J* inertia as an *I* element. The drive chain construction and its Bond Graph model can be seen in Figure 2.

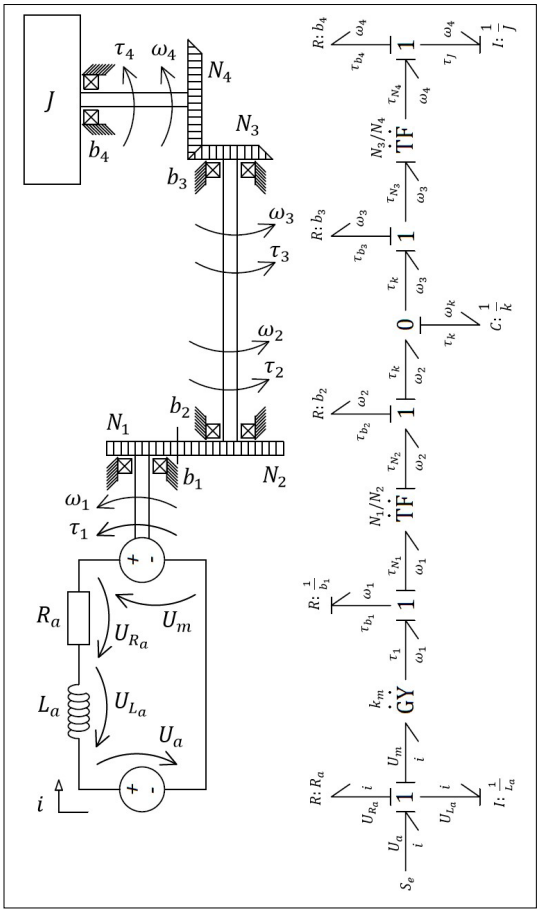

Figure 2. *The drive chain and its Bond Graph model.*

4.3. The system equations

The advantage of Bond Graph-based modelling is the possibility to define equations directly. The equations of the DC motor based on the Bond Graph are the following:

$$U_{L_a} = U_a - U_{R_a} - U_m \tag{2}$$

$$L_a \cdot \frac{di}{dt} = U_a - R_a \cdot i - k_m \cdot \omega_1 \quad (3)$$

$$\tau_{b_1} = \tau_1 - \tau_{N_1} \quad (4)$$

$$b_1 \cdot \omega_1 = k_m \cdot i - \frac{N_1}{N_2} \cdot \left(b_2 \cdot \omega_2 + \frac{1}{k} \cdot \int \omega_k dt\right) \quad (5)$$

The relations of effort and flow in the *GY* element with k_m ratio are the following:

$$U_m = k_m \cdot \omega_1 \quad (6)$$

$$\tau_m = k_m \cdot i \quad (7)$$

The equations of the *TF* element with $m_1 = N_1/N_2$ modulus are the following:

$$\tau_{N_1} = \frac{N_1}{N_2} \cdot \tau_{N_2} \quad (8)$$

$$\omega_2 = \frac{N_1}{N_2} \cdot \omega_1 \quad (9)$$

Based on these the equations, the *k* torsion shaft and the b_3 bearing have the following relations:

$$\tau_{N_2} = \tau_{b_2} + \tau_k \quad (10)$$

$$\frac{N_2}{N_1} \cdot \tau_{N_1} = b_2 \cdot \omega_2 + \frac{1}{k} \cdot \int \omega_k dt \quad (11)$$

$$\omega_k = \omega_2 - \omega_3 \quad (12)$$

$$k \cdot \frac{d\tau_k}{dt} = \frac{N_1}{N_2} \cdot \omega_1 - \frac{\tau_{b_3}}{b_3} \quad (13)$$

$$\tau_{N_3} = \tau_k + \tau_{b_3} \quad (14)$$

$$\frac{N_3}{N_4} \cdot \tau_4 = \frac{1}{k} \cdot \int \omega_k dt - b_3 \cdot \omega_3 \quad (15)$$

The differential gear pair represented by the *TF* element with N_3/N_4 modulus affects the drive by the following:

$$\tau_{N_4} = \frac{N_4}{N_3} \cdot \tau_{N_3} \quad (16)$$

$$\omega_3 = \frac{N_4}{N_3} \cdot \omega_4 \quad (17)$$

Finally, the equations of the *J* inertia and the b_4 bearing are the following:

$$\tau_J = \tau_{N_4} - \tau_{b_4} \quad (18)$$

$$J \cdot \frac{d\omega_4}{dt} = \frac{N_4}{N_3} \cdot \tau_3 - b_4 \cdot \omega_4 \quad (19)$$

4.4. Design of speed control using PID controller

To model the speed conditions of the drive chain, speed control loop was designed using a PID controller. PID controllers are widely used for linear systems. It operates based on parallel compensation. The PID controller possesses 3 components, which are proportional (*P*), integrating (*I*) and derivative (*D*) parts [12]. PID controllers need an error signal, which is the difference between the reference signal and the real output detected by a suitable sensor. In parallel compensation, the proportional part (*P*) creates an executive signal proportional to the error signal, the integral part (*I*) is proportional to the integration of the error signal, and the derivative part (*D*) creates an executive signal proportional to the derived of the error signal until the error signal reaches the switch-off threshold. PID controllers use hysteresis control [12].

The equations of the PID controller are the following:

$$e(t) = K_p \cdot e(t) + K_i \cdot \int_0^t e(t)dt + K_d \cdot \frac{de(t)}{dt} \quad (20)$$

$$e(t) = K_p \cdot \left(e(t) + \frac{1}{T_i} \cdot \int_0^t e(t)dt + T_d \cdot \frac{de(t)}{dt}\right) \quad (21)$$

5. The simulation results

After the simulation model was created, the addition of values was the next step. These values determine the behaviour of the drive chain and they are also necessary to tune the PID controller. The set values during the simulation can be seen in the **Table 1** :

Table 1. *The set values of the simulation*

R_a = 0.45 Ω	k = 0.09 Nm/rad
L_a = 0.1 mH	J = 0,0011 kgm^2
k_m = 0.067 Nm/A, Vs/rad	N_1/N_2 = 0.1
$b_1 = b_3 = b_4$ = 0.1 Nms	N_4/N_3 = 10
b_2 = 0.028 Nms	

If the drive chain operates without a controller it is opened loop and results in unstable behaviour. To solve this, a PID controller was designed and implemented. After implementation, the controller was tuned by using the Ziegler-Nichols tuning method, which is used to determine values in a closed loop. The first step of tuning is to determine the critical amplification amplitude and period time using the proportional (*P*) part. The integration time (T_i) is infinite, while the derivative time (T_d) is zero. Resonance with constant amplitude is produced at the critical amplification, since this is the border of the stability. The K_p, T_i és T_d parameters can be set based on pre-defined formulas of the Ziegler-Nichols method [12].

Figure 3. *The displayed angular velocity values.*

The displayed angular velocity results of the simulation can be seen in **Figure 3**:

The first value is the desired reference angular velocity (ω_{ref}), which is represented by a unit step signal. This is the required angular velocity of the DC motor. To present the behaviour of the PID controller the direct output angular velocity of the motor shaft was also displayed. The third displayed value was the angular velocity of the *J* inertia. This value needs to be changed according to the applied gear ratio (1/100), so the angular velocity of the inertia is a hundredth part of the output angular velocity of the motor. After a short transient state, the required value of 10 m/s should appear on the output of the PMDC motor as a result of the PID controller. The angular velocity of the *J* inertia is 1/100 of the angular velocity of the motor, thus this value is 0.1 rad/s.

6. Conclusions

During the study, a Multi-Domain system was modelled, which is an industrial robotic drive. It contains both electrical and rotating mechanical domains. It was important to ensure that the simulation should be dynamically variable. Thus, the choice of the description language of the Bond Graph, proved that it is suitable for this purpose. The description language allowed the graphical notations to translate directly into mathematical equations without a software environment. Since simulation-based visualization was also a purpose, a special software called 20-sim was used. The advantage is the low resource requirement, and the wide toolkit.

References

[1] G. Husi, A. H. Abdulkareem: *Mechatronics Systems in the Cyber-physical Space*. Debreceni Egyetem, Műszaki Kar, 2018.

[2] R. H. Bishop: *The Mechatronics Handbook*. CRC Press LLC, Florida, U.S., 2002.

[3] *Bond Graph Modelling*. 1st International and 16th National Conference on Machines and Mechanisms, iNaCoMM 2013, IIT Roorke, December 18-20, 2013.

[4] J. A. Kypuros: *System Dynamics and Control with Bond Graph Modeling*. CRC Press Taylor & Francies Group LLC, U.S., 2013.

[5] S. Das: *Mechatronic Modeling and Simulation Using Bond Graphs*. CRC Press Taylor & Francis Group LLC, Boca Raton, 2009.

[6] W. Borutzky: *Bond Graphs for Modelling, Control and Fault Diagnosis of Engineering Systems*. Second edition, Springer International Publishing, Switzerland, 2017.

[7] D. C. Karnopp: *System Dynamics – Modeling, Simulation, and Control of Mechatronics System*. Fifth Edition, John Wiley & Sons, Inc., Hoboken, New Jersey, 2012.

[8] R. C. Dorf, R. H. Bishop: *Modern Control Systems*. Thirteen Edition, Pearson Education Inc., Hoboken, New Jersey, 2017.

[9] J. Pintér: *Ipari robotok hajtása.* Robottechnika, 4. előadás, [Online]. https://docplayer.hu/11254587-Ipari-robotok-hajtasa.html. [Accessed: 20.01.2022.].

[10] A. K. Gupta, S. K. Arora, J. R. Westcott: *Industrial Automation and Robotics: An Introduction*. Mercury Learning & Information Publishing, 2016.

[11] Z. Luo: *Robotics, Automation, and Control in Industrial and Service Settings*. Engineering Science Reference, United States of America, 2015.

[12] S. Duman, U. Guvenc: *Determination of the PID Controller Parameters for Speed and Position Control of DC Motor Using Gravitational Search Algorithm*, January 2011. https://www.researchgate.net/publication/254048079_Determination_of_the_PID_controller_parameters_for_speed_and_position_control_of_DC_motor_using_Gravitational_Search_Algorithm. [Accessed: 20.01.2022.].

sciendo

Műszaki Tudományos Közlemények vol. 17. (2022) 42–45.
DOI: Hungarian: https://doi.org/10.33895/mtk-2022.17.09
English: https://doi.org/10.33894/mtk-2022.17.09

EME MTSZ MTK

MODERN MEASUREMENT METHODS INTRODUCED IN I4.0 MANUFACTURING SYSTEMS

Daniel LEDENYAK,[1,2] Tamás ROSTA[2]

[1] *Savaria Institute of Technology, Faculty of Informatics, Eötvös Loránd University, Szombathely, Hungary, ld@inf.elte.hu*

[2] *Jozsef Cziraki Doctoral School, Simonyi Karoly Faculty of Engineering, Wood Sciences and Applied Arts, University of Sopron, Sopron, Hungary, fr0c94@uni-sopron.hu, rosta@inf.uni-sopron.hu*

Abstract

The main target of this research, as with other I4.0 related research, is to create a system by which a quantitatively lower human resources workload is achieved in manufacturing processes, thereby allowing efforts to be better focused on creating development activities. The focus of the research work is the creation of an I4.0 compatible data processing system and algorithm which can store and forward data obtained from various machine tool and measurement equipment. To establish and appropriately use these measurement values, it is important to process the data in the most optimum way. The first step is to introduce and evaluate the measurement equipment available for our system and its capabilities in the proper transfer of data. This study intends to introduce these systems, focusing on theoretical and practical attainable accuracy.

Keywords*: I4.0, CMM, CNC, measurement accuracy.*

1. Introduction

The manufacture of highly complex technical components with a large number of specifications requires companies to have rapid inspection tools to carry out conformity assessment. In this context metrology is an important resource for supporting innovation and development processes, as well as manufacturing processes, threreby allowing the monitoring of technological improvement in line with the principles of Industry 4.0. In order to guarantee the reliability of the manufacturing process and to ensure the dimensional and geometrical conformity of technical parts, companies are demanding increasingly complex metrology tools capable of ensuring the correct performance of measurement functions. The extraordinary need to ensure the dimensional and geometrical compliance of technical parts can be fulfilled by checking with coordinate measuring machines. This technology supports rapid inspection and can produce large amounts of data, improving the interaction with the manufacturing process in order to guarantee compliance. [1]

The coordinate measuring machine is a multi-axis measuring machine developed for universal application. In terms of structural design, the three-axis construction is common but there are also five-axis designs. Each axis of this machine is equipped with a position sensor and can record any desired points and the position vectors associated with the points in the coordinate system of a machine, based on the position of the measuring probe. In most cases measuring machines are of the portal design but there are also some versions with a moving table, moving column or moving bridge. The most common type of guideway is the air-bearing type which has the great advantage of low resistance due to friction, but there are also roller types. Since the measuring system of a coordinate measuring machine requires accurate positioning resolution, it is not sufficient to use the rotary encoder method commonly used on CNC machine tools. However, glass gauge positioning is necessary. The continuous supply of remote control is essential because of the air bearings. Most often the plant's air supply

is also used but in this case particular attention must be paid to air quality. [2]

The probe is in direct contact with the work piece. There are several types, the most common being the perfect spherical shape, but for special measurements there are special shaped probes (e.g. star. L-shaped. etc.) made of ruby.

This paper is concerned with the functioning and adaptability of the methods used for the advanced opportunities offered by Industry 4.0. The main aim is to assess accuracy under real-world conditions of the various I4.0 compliant measurement systems available at the Savaria Institute of Technology. Using the measurement results, a comparison is made about the accuracy of the systems based on and using these data.

2. Measuring methods

For measuring machines and machine tools, accuracy is a key performance requirement. Verification of the accuracy of measuring and inspection equipment is an important prerequisite for the quality departments in industry as production quality is based on the objective of "zero defects". Hence, it is essential to have a good knowledge of the condition of the equipment. For CMMs the DIN EN ISO 10360-2:2009 standard specifies calibration to be carried out regularly and at defined intervals. In addition, repeatability accuracy tests must be carried out.

Measurements were taken both inside the CNC machine and on the coordinate measuring machine using a block gauge and calibration ring of accuracy class 2 according to DIN EN ISO 3650 with a manufacturer's tolerance of −0.32 µm at 20°C. The uncertainty of measurement can be defined by the following standard relation given by the manufacturer:

$$U = 1{,}5 \cdot 10^{-6} \cdot L \qquad (1)$$

which in our case is:

$$U = 1{,}5 \cdot 10^{-6} \cdot 20\ mm = 0.03\ \mu m.$$

The linear coefficient of thermal expansion of the etalon material as specified by the manufacturer is $11.5 \cdot 10^{-6}\ K^{-1}$. The respective measurement types were carried out with 30 replicates and the results obtained and the differences between the different measurement methods were investigated using different statistical analyses.

Before starting the evaluation, it is of key importance to be aware of the positioning accuracy of the equipment. This is available from measurements carried out by the manufacturer or other accredited organisations. In the case of a CNC machine the linear positioning accuracy can be determined by calibration with a laser interferometer. [3–6]

For the measurements a Renishaw OMP40-2 probe unit was used. Prior to starting the measurements, it is necessary to adjust the radial runout of the probe head. Since the software can bridge a maximum of ±2.5 µm beat, which in the current case was ±0.02 µm. The achieved value was adjusted using screws on the adapter.

3. Results of measurement processes

The work piece to be measured was placed and fixed on CNC machine initially, then pre-positioned by approaching the work piece at a specified speed by touching the coordinates and moving away to a safe distance. In current work, the parallel surfaces of the gauge were touched from 1 to 1 and the distance between the points was recorded using the software by subtracting the coordinate values. Accurate clamping was ensured by the vertical compass on the vice and the parallel sides of the slit leg.

Next, measurements were taken with ring gauges. The etalon was used in this study. The bore diameter of 63.0021 mm was specified by the supplier. Before starting the operation, the position of the ring had to be determined and then the position taken as the centre was used as a starting point. During the measurement 4 points were touched by the feeler and the diameter was calculated from these points based on a theoretical circle. The results are presented in **table 1**.

For further measurements, a coordinate measuring machine located in the metrology laboratory of the Savaria Institute of Technology was used, equipped with Renishaw touch trigger probes and TouchDMIS software whose accuracy

Table 1. *Measurement results (CNC)*

	x direction	y direction	Circle
Average [mm]	20.0018	20.0000	63.0024
Average deviation [mm]	0.0021	0.0005	0.0003
Variation [mm]	0.0003	0.0006	0.0003
Minimum [mm]	20.0008	19.9991	63.0019
Maximum [mm]	20.0027	20.0013	63.0030
+2 σ variation [mm]	20.0024	20.0012	63.0030
-2 σ variation [mm]	20.0011	19.9989	63.0018

can be calculated for the given lengths from the calibration certificate issued according to DIN EN ISO 10360-2 [4]:

$$MPE = \pm(15\ \mu m + L/333), \quad (2)$$

which in our case is:

$$MPE = \pm(1.5\ \mu m + 20\ mm/333) = 1.56\ \mu m.$$

Before starting the measurements, it was checked that the error of the probe did not exceed the permissible range using the calibration sphere. This check should be carried out at prescribed intervals. depending on the use, but usually once a week.

After the calibration measurements were taken on both the gauge block and the ring gauge. Before starting the process, it was necessary to ensure a constant laboratory temperature. The measurement software has in-built temperature compensation **[4]**.

The measurements were made on the CMM using different methods, two point and two plane measurements in the case of a block gauge, and nine point and scanned measurements in the case of a ring gauges. So that not only the measuring instruments but also the measurement methods were comparable. The point-to-point measurements were made in exactly the same way as was done on the CNC machining centre. During the plane-to-plane measurement, the coordinate measuring machine software fits a theoretical plane to the points and then gives the distance between the two resulting planes.

In the case of the nine-point measurements the first 5 probes belong to the frontal surface of the calibration ring. The reason being to compensate for inaccuracies due to positioning errors of the object to be measured. During the planar probing, care must be taken to ensure that the points are not recorded on the matrices or other markings on the planar surface. By touching the additional 4 points the software defines a theoretical circle.

When determining the diameter of a circle with points, the software acts exactly as it would when measuring on a CNC machine. In the case of the scanned surface a value is obtained from the profile drawn from the 2400 points taken over the entire surface.

The results in **table 2** conclude that there are no systematic errors between our measurement systems. The variances of the observed variables are within an acceptable range for all measurement scenarios. Since the measurement uncertainty of the used measurement results is an order of magnitude lower than the accuracy of our measurement systems, it can be concluded that the two measurement systems are equivalent to each other for the current given application.

Table 2. *Measurement results (CMM)*

	Between points	Between planes	Circle (9 point)	Circle (scanned)
Average [mm]	20.0004	19.9994	63.0023	63.0024
Average deviation [mm]	0.0008	0.0002	0.0002	0.0003
Variation [mm]	0.0002	0.0001	0.0001	0.0001
Minimum [mm]	20.0003	19.9993	63.0021	63.0023
Maximum [mm]	20.0006	19.9995	63.0026	63.0026
+2 σ variation [mm]	20.0007	19.9996	63.0026	63.0026
-2 σ variation [mm]	20.0002	19.9993	63.0020	63.0022

4. Conclusion

The accuracy of the measuring system integrated in the newly calibrated milling machine easily matches the tolerance fields specified by the manufacturer. Based on experience the measurement is typically fast, and the resulting data can be easily transmitted and stored using the MES system.

Post-production measurement of work pieces is one of the most common, yet most debated areas in terms of quality assurance and product conformity. The simplest example is the application of many different sizes and tolerances and then the real need for these which is often modified only during the assembly of the product or based on the data obtained from use. An unnecessarily tight tolerance often multiplies the cost of a given machining, not to mention the unnecessary environmental impact. The integrated workpiece measuring system of the CNC milling machine used in the research is able to perform measurements with a significantly tighter tolerance as specified by the manufacturer. The CMM measuring machine is an excellent monitoring tool of the CNC machine as the measurement process can be almost the same. Based on this it can be easily integrated and process data into the production system. The institute has meanwhile integrated a 3D scan probe, a new generation of measurements. It could be a perfect, fast prefilter for classic contact measurements as it is faster, and if an error is found, the program can move on to more accurate

but slower tactile measurements without human intervention. With this, an advanced and precise quality system can be set up at our institute.

References

[1] *A koordinátamérő-gépek szerkezeti kialakítása*. CNC MEDIA. 2021 https://www.cnc.hu/2015/04/a-koordinata-merogepek-szerkezeti-kialakitasa-i/

[2] Yongjin Kwona, Tzu-Liang Tsengb, Yalcin Ertekinc: *Characterization of Closed-loop Measurement Accuracy in Precision CNC Milling*. Robotics and Computer-Integrated Manufacturing, 22. (2006) 288–296.

[3] Hau-Wei Lee, Jr-Rung Chen, Shan-Peng Pan, Hua-Chung Liou and Po-Er Hsu: *Relationship between ISO 230-2/-6 Test Results and Positioning Accuracy of Machine Tools Using LaserTRACER*. Center for Measurement Standards, Industrial Technology Research Institute (2016)

[4] Renishaw: Touch Trigger Probes. 2021 https://www.renishaw.com/en/touch-trigger-probes--6652

[5] COORD3 Metrology. Industrial Metrology System. 2021 https://coord3.com/en/cmm-universal-2/

[6] Akira-Seiki. Vertical Machining Center V2.5XP. 2021 https://www.akiraseiki.com/vertical-machining-center-v/vmc-v2-5xp.html

Műszaki Tudományos Közlemények vol. 17. (2022) 46–49.
DOI: Hungarian: https://doi.org/10.33895/mtk-2022.17.10
English: https://doi.org/10.33894/mtk-2022.17.10

DEVELOPMENT OF INDUSTRIAL GRADE HORIZONTAL POLARGRAPH

Hunor MENYHÁRT,[1] Zoltán FORGÓ[2]

[1] *Sapientia Hungarian University of Transylvania, Faculty of Technical and Human Sciences, Department of Mechanical Engineering, Târgu Mureș, Romania,, menyhart.hunor@student.ms.sapientia.ro*

[2] *Sapientia Hungarian University of Transylvania, Faculty of Technical and Human Sciences, Department of Mechanical Engineering, Târgu Mureș, Romania,, zforgo@ms.sapientia.ro*

Abstract

This article describes the basis for a horizontal compact drawing robot, its use in the industry, constituent parts and how these parts and methods – drawn from electronics, mechanics and informatics – combine to make up the entirety of this machine.

Keywords*: horizontal polargraph, drawing robot, Arduino.*

1. Introduction

In the industry, much emphasis is necessarily placed on maximizing reliability and, above all, performance. Simplifying certain tasks can be the difference between profit or loss.

Many processes can be performed quickly with experienced and skilled workers, but skilled labour is often too expensive or simply unattainable if there is not enough interest in the industry. Untrained or less skilled workers are often unable to work at the same speed and precision, or in case of complex problems may be unable to find a solution in these situations.

Because of this, in many places we replace the role of humans with robots, so we can mathematically guarantee the solution of most problems.

One such problem can appear in the manufacture of curved sheet parts. The component design engineer often designs the piece and passes it to a specialist at the plasma machine to be cut down. However, when it reaches the specialist, whose understanding may be different from that of the designer, one by one he has to walk through the piece and record the bending lines by hand. This is a very time-consuming job and the more inexperienced the specialist, the higher the frequency of errors, even to the point that the part can be ruined. Furthermore, it often does not help if the manufacturer of the part and the person performing the bending are one and the same , since he does not know exactly the bending lines from memory every time.

This problem requires an automatic system that eliminates the human factor, for example, a drawing robot.

So our machine has to meet a few criteria in order to make industrial and practical sense of its use:

– has to have a large workspace;
– installing it on the work area and starting it cannot take more than 5 minutes;
– It should be easy to manage and intuitive.

On the market, the various drawing machines have huge support structures, which increases precision, but this precision is not necessary for us to this extent, and in the case of constant and larger plates in their field of work, due to the size of these machines, their installation in the work area requires up to 3-4 people and occupies a huge area.

The so-called polar graph **[1]** is suitable for the task of adjusting the variable work space, but the biggest problem is that gravity is used to move on the x axis and the engines direct the working point in only one direction.

For this reason, a new solution to this task should be found, since the existing possibilities are unsatisfactory. This is where a new solution comes into play, a rethinking of an existing idea or technology.

What we are looking for is a tape that can hold its weight against gravity, exert force in an axis direction and, in the event of unscrewing, it is able to fold and bend. With this, we are able to create a compact polar graph with two motors, two storage wrists and two tapes that can work on the horizontal plane, thus making it substantially easier to install and practical in the production process.

2. Parameters and geometric design

2.1. The geometric working space of the machine and its calculation

First of all, we need to get the distance between the two wrists, which is given by the formula (1).

Then we can calculate the active length of the tapes and determine the direct geometry in which the endpoint of the drawing device and the equipment is determined by the formula (3) to calculate the position of the working point. **(Figure 2)**

$$b = l1 * cos\ cos\ \theta 1 + l2 * cos\ cos\ \theta 2 \quad (1)$$

$$l1 = \left(\frac{l2 * cos\ cos\ \theta 2}{b}\right) \quad (2)$$

$$x = \left(\frac{(l1^2 - l2^2)}{b}\right) \quad (3')$$

$$y = \left(\frac{1}{\sqrt{2}} * \sqrt{l1^2 + l2^2 - \frac{b^2}{2} - \frac{(l1^2 - l2^2)}{2 * b^2}}\right. \quad (3'')$$

2.2. Practical workspace

The machine is controlled from both sides, with the help of the two engines we can reach any point within the working area. **Figure 3**)

The area consists of 3 priority zones, the first zone is the primary work space, which is the sum of a rectangle and a polynomial triangle, this area can be reached by both wrists so that it can be worked on.

Only one wrist has access to the secondary area, so although the length of each tape would be enough to reach the entire area, the entire area is inaccessible to the finished machine.

The last area is the area outside the primary and secondary areas that the machine cannot reach.

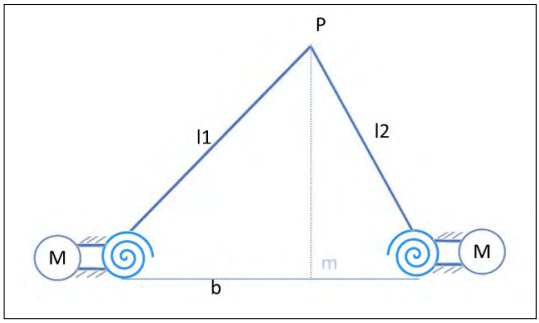

Figure 1. *Machine parameters - top view.*

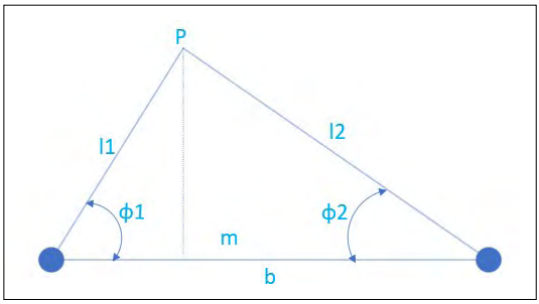

Figure 2. *Geometrical parameters from top view.*

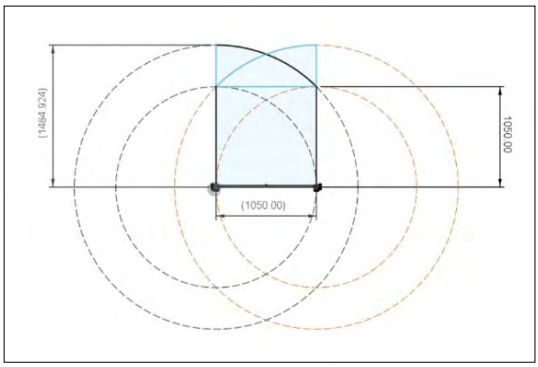

Figure 3. *The entire machine workspace from above.*

3. Implementation

3.1. Tape spring

These tapes hold their shape in one direction and bend into the other (**Figure 4**). this is a special mechanical property in robotics that can create compact low-load moving arms. **[2, 3]**

If the force does not exceed the critical value, the arm is able to exert a force in one direction with the axis, this is unsuitable for high-performance tasks, but our light drawing pencils can be moved without any problems **[4]**. (**Figure 5**)

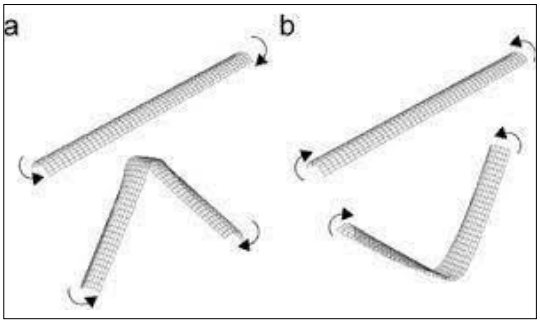

Figure 4. *Tape springs and types of movement.*

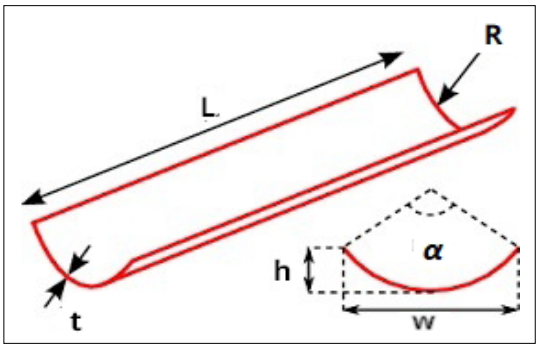

Figure 5. *Construction of a strip spring.*

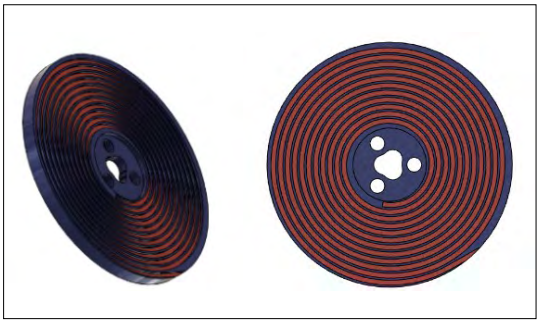

Figure 6. *Geometric structure of the wrist disc.*

Figure 7. *Before and after assembly of the entire wrist.*

3.2. Wrist

Our machine's wrist has given up storing and then successfully compressing the tape into its convex configuration and using two plates with spiral indentation. (**Figure 6**)

The folding discs are made of metal for a higher sturdiness and for better sliding, they are connected by a plastic reel whose height precisely follows the width of the tape. **[5]** (**Figure 7**)

Due to its design, when the wrists are turned, the force acting on the tape forces the spiral wall to force it into a convex shape. Because of this, the plate is able to exert more force along its axis, as well as its side.

Figure 8. *A NEMA17 stepper motor.*

3.3. Stepper motor

Its role is to rotate the wrist thereby moving the plates out so that it reaches a sufficiently large linear force that moves the pencil.

For this role, we use a NEMA17 bipolar motor with a step of 1.8°, (**Figure 8**) for high accuracy and ease of handling.

The stepper motor is controlled by an A4988 2A-force engine controller, as this controller is easily accessible and easily replaced in the event of a problem. The advantages also include the fact that the controller can control the engine at sufficient speed and accuracy.

3.4 Drawing structure

There is a structure located at the end of the tapes, the first part consists of the 2-cylinder joint, which receives the tapes and allows them to rotate ,the second part holds the frame of the SR 90

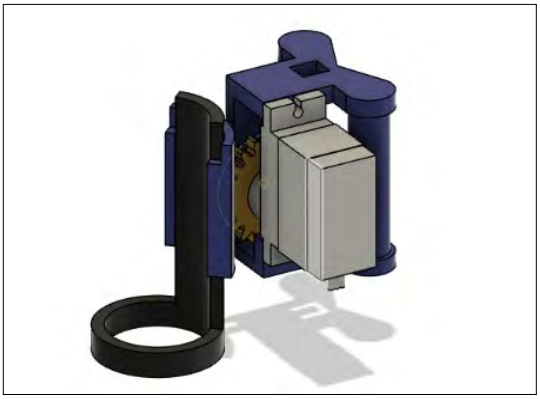

Figure 9. *Design of the drawing structure.*

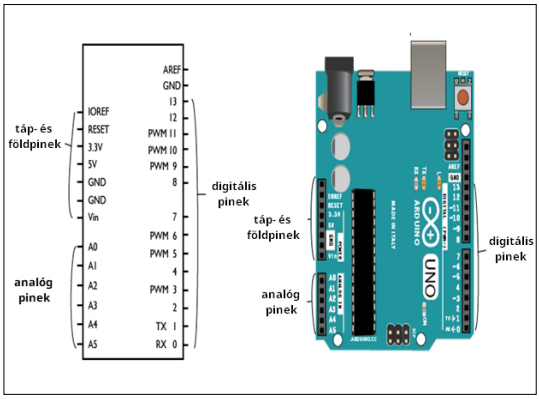

Figure 10. *Cable layout and graphic presentation of an ARDUINO UNO.*

servo motor, at the end of which it can move up a cylindrical platform with a gear and rack, which may contain drawing tools of different sizes and shapes. (**Figure 9**)

3.5 Arduino and control

We use an Arduino Uno (**Figure 10**) to control the machine and, to reach the more compact contractor, we use a CNC shield, which establishes a direct connection with the Arduino.

Then the engine controllers and the associated stepper motors are added to them.

4. Conclusions

In order for the industry to develop, new technologists need to enable easier and faster production in order to keep up with market demand. The drawing machine can fulfil a small task in this chain, but this need cannot be fully supported without tests.

References

[1] Polargraph UK,Polargraph on Hiatus 2019, http://www.polargraph.co.uk/,(Letöltve 2021.02.15)

[2] *Project Scribble-Theorz Craft*, 2021, https://invalidentry.engineer/blog/project-scribble-part-1/ (Letöltve 2022.04.17)

[3] S.J.I. Walker, Guglielmo Aglietti: *A Study of Tape Spring Fold Curvature for Space Deployable Structures.* Engineering Proceedings of the Institution of Mechanical Engineers Part G Journal of Aerospace 221/3 (2007) 313–325. https://doi.org/10.1243/09544100JAERO209

[4] Dewalque F., Collette J. P., Brüls O.: *Mechanical Behaviour of Tape Springs Used in the Deployment of Reflectors around a Solar Panel.* Acta Astronautica, 123. (2016) 271–282. https://www.sciencedirect.com/science/article/abs/pii/S0094576515302952

[5] Ekelöw J.: *Design and Manufacturing of Thin Composite Tape Springs.* 2014. (Letöltve 2021.02.03) http://www.diva-portal.org/smash/get/diva2:805332/FULLTEXT01.pdf

Műszaki Tudományos Közlemények vol. 17. (2022) 50–54.
DOI: Hungarian: https://doi.org/10.33895/mtk-2022.17.11
English: https://doi.org/10.33894/mtk-2022.17.11

EXAMINATION OF AGING OF ALSI1MGMN TYPE ALUMINIUM ALLOY

Mohammed MUDABBIRUDDIN,[1] Tünde Anna KOVÁCS[2]

[1] *Óbuda University, Doctoral School on Materials Sciences and Technologies, Budapest, Hungary, mohammed.mudabbir@uni-obuda.hu*

[2] *Óbuda University, Bánki Donát Faculty of Mechanical and Safety Engineering, Budapest, Hungary, kovacs.tunde@bgk.uni-obuda.hu*

Abstract

In the world of manufacturing, aluminium alloy is mostly used because of its suitable properties, such as mechanical behaviour and machinability. The formation of the cluster, the erosion and corrosion, the precipitation process, artificial ageing and other factors are also discussed in this study. From the practical point of view, the main objective of this experimental study is the investigation of the ageing process of AlSi1MgMn (EN AW 6082 T6) aluminium alloy. To investigate the compound precipitation in the aluminium alloy, a heat treatment process is conducted after which a hardness test is performed and hardness values evaluated to obtained the optimal hardness value according to ageing time and temperature. Significant results have been obtained in the hardness test, however, the metallography shows no clear significant result. For better results, more tests are suggested.

Keywords*: AlSi1MgMn, ageing, heat treatment, hardness.*

1. Introduction

The ageing of materials generally depends on the material properties, while the ageing of technical systems depends on their application. Ageing can be classified into three groups: thermal, mechanical and electrical. The main causes of ageing can be erosion and corrosion, wear and tear, and lack of maintenance which can cause a sudden failure and can lead to damage whole system **[1]**. Time-dependent failure rates can also depend on the weather. To overcome this problem and to increase the efficiency of any technical system, the prediction of failure on bus cable ageing is very important. Fatigue property plays a very important role in predicting ageing of the used material and mechanical properties, authors presented their work for this problem. To understand material behaviour, mathematical modelling can be used.

In today's "Industry 4.0" environment, aluminium alloys are mostly used in various fields of application due to their excellent properties: low density, adequate strength and hardness, excellent castability and corrosion resistance. These properties make Al–Si–Mg alloys a sought-after material for various applications in the construction, automotive, and aerospace industries. The main areas of application are high-stress applications, lattice structures, bridges, cranes, transport applications, copper barrels, beer barrels and milk barrels. It should be borne in mind that the mechanical properties of AlMgSi alloys primarily depend on processing technology.

Over the years, many authors have studied aluminium alloys and the dependence of their mechanical properties on different heat treatment conditions. Extensive research on the properties of aluminium alloys has been presented. Forging and plastic forming is presented in **[2],** and these methods were also used to analyze the strength of the 6082 Al alloy. In order to estimate the fatigue life, a short-cycle fatigue test is performed for AlMgSi alloys with different chemical com-

positions and microstructures [3] literature. Previous work shows that cracking in this type of alloy is due to the presence of magnesium and chromium. In an alloy with a high magnesium content, the phenomenon of the formation of precipitates occurs more often than in an alloy with a low magnesium content during the natural ageing process. The AlMgSi alloys family are aged to improve properties, the goal is not hardness, but increased ultimate tensile strength and yield strength [4, 5]. During the artificial ageing of AlMgSi alloys, the precipitation process was studied with experimentally. Alloys of this type are widely used as structural materials, so it is worthwhile to improve the production process and the properties of the material. The crack growth behaviour of aluminium alloy 6082-T6 is studied in the literature [6]. Applying the "Paris" law, fatigue crack growth can be observed in the samples. In this study, the effect of two types of incisions, curved U-incision and V-incision, are considered. Using Paris law in test specimens, fatigue crack growth rate is obtained. Two types of notches are taken into consideration for this study i.e. Curved U-notch and V-notch. Results show that the curved U-notch shows a higher value of stress as compared to V-notch. An ageing model is executed to predict the ageing life under different stress values. The fatigue test was performed and compared with 2017A-T4 and 6082-T6 aluminium alloys. Based on mean torsion stress, after statistical analysis, this model uses measured data to estimate ageing. Based on the heat treatment time and temperature, precipitation behaviour is examined by differential scanning calorimetry, Scanning Electron Microscopes (SEM), Transmission Electron Microscopes (TEM) metallographic analyses, and hardness testing [8]. Aluminium alloys such as 6082-T6, 6060, 6005A, and 6063 were used for the test with varying cooling rates. The behaviour of the precipitates in a certain cooling speed range showed the same result. The literature [9] examines the ageing behaviour of aluminium alloy 6082 with the help of Vicker microhardness measurements, mild micro ageing, and tensile strength test analysis [9]. During material testing, the microscopic image after etching does not provide a clear answer concerning the hardening of the material. The effect of welding techniques and the effects of alloys are examined in the literature [10].

2. Material and heat treatment

2.1. AlMgSi (6082-T6)

Precipitation of alloys that can be refined, such as aluminium, is expected to contain scattered fine precipitates, which can range from spherical to lamellar. Therefore, an aluminium-based alloy - AlMgSi (6082-T6) - is used for further analysis. Aluminium alloy 6082-T6 is an alloy for cold working means it is a member of the aluminium-magnesium-silicon alloy family. It is typically formed by extrusion and rolling. They are usually heat-treated to create a material with greater strength but less breathability. It is difficult to produce thin-walled, complex shapes from the 6082 alloys using extrusion. Aluminium alloy 6082-T6 is a medium-strength alloy with excellent erosion and corrosion resistance properties. Among the 6000 series alloys, it has the highest strength.

The chemical composition and material properties of T6-6082 aluminium alloy are listed in Tables 1 and 2.

Table 1. *Chemical Composition*

Element	Percentage %
Al	95.2 - 98.3%
Cr	0.25% max.
Cu	0.1% max.
Fe	0.5% max.
Mg	0.6 - 1.2% max.
Mn	0.4 - 1% max.
Si	0.7 - 1.3% max.
Ti	0.15% max.
Zn	0.2% max.
Other	0.15% max.

Table 2. *Material Properties*

Properties	Value
Density	2.71 g/cm^3
Young's Modulus	71 GPa
Ultimate tensile strength	140–330 MPa
Yield strength	280 MPa
Hardness Vickers	35-100 HV
Brinell Hardness	84 HB
Melting Point	555 °C

2.2. Heat Treating

The most important heat treatment used to increase the strength of aluminium alloys is age-

ing, which includes solvent annealing, rapid cooling, and ageing. The research aims to study the ageing process of the used aluminium alloy. First, the 6082-T6 sample was cut into 5 different parts, each 4x3.5 cm in size. These samples were labelled according to their heat treatment. The samples were then heated in an oven at 550 °C for one and a half hours (solvent annealing). All the samples were taken out after heating and then cooled in cold water. Solvent annealing was performed at 550 °C for 1 hour for each piece. After this process, it was heat treated using different ageing times. The duration is respectively 1 hour, 5 hours, 10 hours and 24 hours at a constant temperature of 200 °C. After ageing, these samples were individually cooled to room temperature in still air, and then a hardness test was performed on each sample, using Vickers hardness measurement. **Figure 1** shows the temperature-time diagram of the performed heat treatment process.

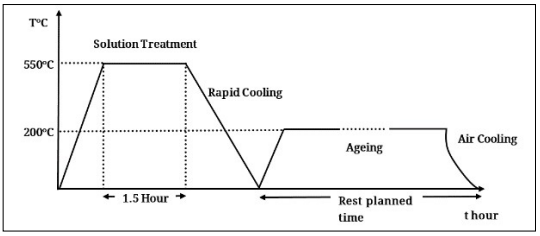

Figure 1. *Ageing heat treatment process diagram*

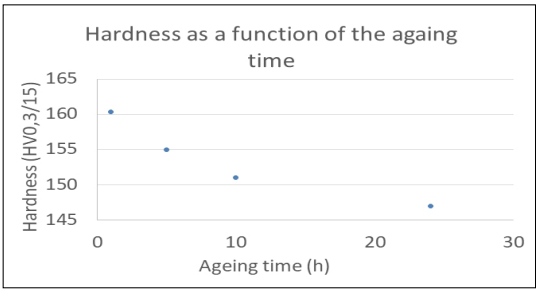

Figure 2. *Graphical representations of obtained hardness values*

3. Results and Discussion

3.1.Hardness test

FFatigue failure depends on many factors, such as the type and condition of the material, the geometry of the structural elements, the type of loading or the state of stress. During the experiments, four aged samples, one hardened sample and one control sample without heat treatment were examined (**Table 3**). The load used for hardness measurement is 300 g, and the test time is 15 seconds (HV0.3/15). Five measurements were taken on each sample, and the hardness value was determined by calculating the average. The obtained values were designed on a graph, as a function of ageing time and hardness (**Figure 2**).

Table 3. *Hardness Vickers value of each sample*

No. of Samples	Description	Reading in HV03/15
1	Original Control Sample	101.63
2	Solution treated at 550°C and Quenched	144.33
3	Ageing at 200°C for 1 hours	160.33
4	Ageing at 200°C for 5 hours	155
5	Ageing at 200°C for 10 hours	151
6	Ageing at 200°C for 24 hours	147.66

The hardness measurement results are shown in a diagram. We wanted to show the effect of the ageing time on the hardness as a function of the ageing time. The diagram clearly shows that the highest hardness was obtained after 1 hour of ageing. Longer ageing heat treatment caused a decrease in hardness.

3.2.Metallography

– Preparation of the microscopic examination: 1. Making a cross-section 2. Casting the piece 3. Grinding 4. Polishing and 5. Etching.

After the hardness test, all the samples were embedded so that grinding and polishing could be performed afterwards, and then the microscopic examination was performed. The casting of the piece is done with a resin material to give it the final shape for further preparation. The cast samples were prepared by sanding them with coarse sandpaper. For the sanding process, we progressed from 80-grit sandpaper to fine 2500-grit sandpaper. Keller's reagent, which is a mixture of nitric acid, hydrochloric acid and hydrofluoric acid, was used for about 10-15 seconds for etching. After etching, we perform a microstructural examination using an optical microscope.

Figures 3–8. shows images of all age-hardened aluminium alloys. These images are taken by optical microscope with 1000x zoom (50 μm).

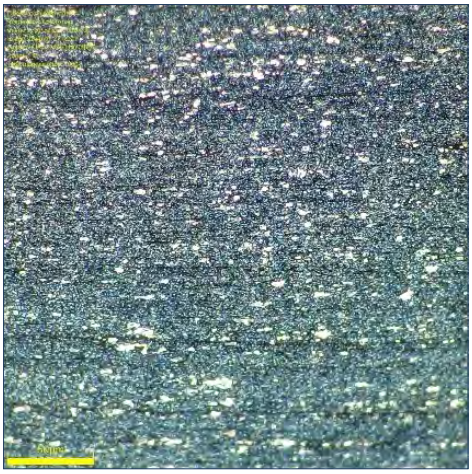

Figure 3. *Control Sample*

Figure 4. *Quenched Sample 2 at 550°C for 1 hour*

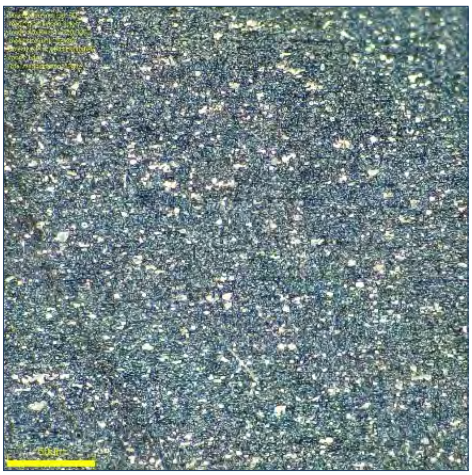

Figure 5. *Sample 3 At 200°C for 1 hour*

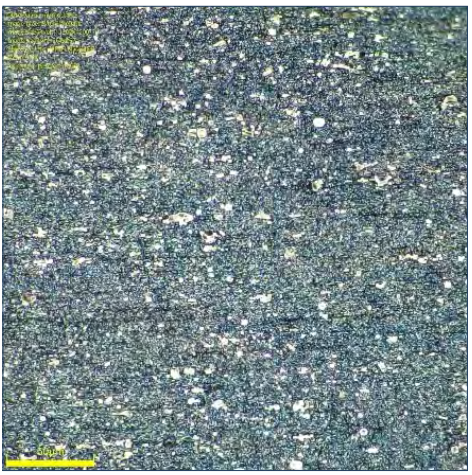

Figure 6. *Sample 4 At 200°C for 5 hour*

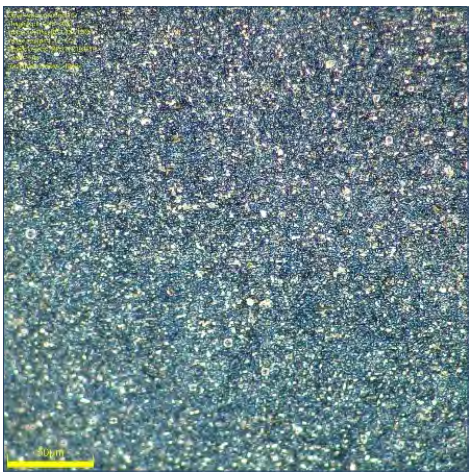

Figure 7. *Sample 5 At 200°C for 10 hour*

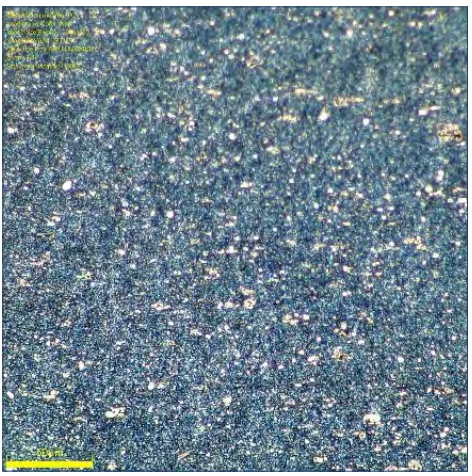

Figure 8. *Sample 6 At 200°C for 24 hour*

4. Conclusion

In this study, AlMgSi (6082) aluminium alloy was aged by heat treatment and evaluated by hardness measurement. We have explained the process step by step. Overall, it can be said that during the test, it can be noticed in the hardness measurements that the hardness of sample 3 is the highest, therefore ageing at 200 °C for 1 hour can be considered as the optimal ageing heat treatment.

After the hardness measurements, we tried to observe the precipitates with the metallographic tests. No significant results were visible in metallography. This metallographic examination was performed with an optical microscope, for better results it would be recommended to use other techniques, such as a scanning electron microscope or a transmission electron microscope.

References

[1] M. Mudabbiruddin., L. Pokoradi: *Aging of Technical Systems – Literature Review.* Journal of Production Engineering, 24/1. (2021) 69–74. https://doi.org/10.24867/JPE-2021-01-069

[2] N. Kumar, G. M. Owolabi, R. Jayaganthan: *Al 6082 Alloy Strengthening through Low Strain Multi-axial Forging*. Materials Characterization, 155. (2019) 109-761. https://doi.org/10.1016/j.matchar.2019.06.003

[3] L. P. Borrego, L. M. Abreu, J. M. Costa, J. M. Ferreira: *Analysis of Low Cycle Fatigue in AlMgSi Aluminium Alloys*. Engineering Failure Analysis, 11/5. (2004) 715–725. https://doi.org/10.1016/j.engfailanal.2003.09.003

[4] J. Kim, J. Im, M. Song,I. Kim.: *Effects of Mg Addition and Pre-aging on the Age-Hardening Behavior in Al-Mg-Si.* Metals, 8/12. (2018) 10-46. https://doi.org/10.3390/met8121046

[5] M. Stipcich, A. Cuniberti, V. Noseda Grau.: *Electrical Resistometry Study of an AlMgSi Alloy under Artificial Aging*. Journal of Alloys and Compounds, 542. (2012) 248–252. https://doi.org/10.1016/j.jallcom.2012.07.031

[6] J. A. F. O. Correia, A. M. P. De Jesus, A. S. F. Alves, G. Lesiuk, P. J. S. Tavares, P. M. G. P. Moreira.: *Fatigue Crack Growth Behaviour of the 6082-T6 Aluminum Using CT Specimens with Distinct Notches*. In: Procedia Structural Integrity. Vol. 2. Catania, Italy, 2016. 3272-3279. https://doi.org/10.1016/j.prostr.2016.06.408

[7] K. Kluger.: *Fatigue Life Estimation for 2017A-T4 and 6082-T6 Aluminium Alloys Subjected to Bending-Torsion with Mean Stress*. International Journal of Fatigue, 80. (2015) 22–29. https://doi.org/10.1016/j.ijfatigue.2015.05.005

[8] B. Milkereit, N. Wanderka, C. Schick, O. Kessler.: *Continuous Cooling Precipitation Diagrams of Al-Mg-Si Alloys*. Materials Science and Engineering A, 550. (2017) 87–96. https://doi.org/10.1016/j.msea.2012.04.033

[9] M. Fujda, M. Matvija, M. Glogovský, I. Orišenko.: *Natural Aging Behaviour of the EN AW 6082 and Lead Free EN AW 6023 Aluminium Alloys*. Manufacturing Technology, 17/5. (2017) 19–20. https://doi.org/10.21062/ujep/x.2017/a/1213-2489/MT/17/5/701

[10] G. Cornacchia, S. Cecchel.: *Study and Characterization of EN AW 6181/6082-T6 and EN AC 42100-T6 Aluminum Alloy Welding of Structural Applications: Metal Inert Gas (MIG), Cold Metal Transfer (CMT), and Fiber Laser-MIG Hybrid Comparison.* Metals, 10/4. (2020) 1–21. https://doi.org/10.3390/met10040441

sciendo

Műszaki Tudományos Közlemények vol. 17. (2022) 55–59.
DOI: Hungarian: https://doi.org/10.33895/mtk-2022.17.12
English: https://doi.org/10.33894/mtk-2022.17.12

EME MTSZ MTK

STUDY OF A COMPRESSOR REFRIGERATION CIRCUIT

István-Sándor SZABÓ,[1] Judit PÁSZTOR,[2] Rudolf-László FARMOS[3]

[1] *Sapientia Hungarian University of Transylvania, Faculty of Technical and Human Sciences, Târgu Mureş, Romania, szabo.l.istvan@student.ms.sapientia.ro*

[2] *Sapientia Hungarian University of Transylvania, Faculty of Technical and Human Sciences, Târgu Mureş, Romania, pjudit@ms.sapientia.ro*

[3] *Sapientia Hungarian University of Transylvania, Faculty of Technical and Human Sciences, Târgu Mureş, Romania, farmos_rudolf@ms.sapientia.ro*

Abstract

An important part of technical education is the presentation of processes through experiments and demonstration tools. This direct sensual experience is one of the sources of knowledge acquisition. The illustration provides a deeper understanding of the curriculum, making the cognitive process more intense. In this study we present a refrigerator model we have designed and implemented. Measurements are then performed on a real refrigerator to study the compressor refrigeration process. The locations where data were acquired are shown on the model.

Keywords*: compression refrigeration system, model, refrigeration cycle, temperature measurement.*

1. Presentation of a compressor refrigerator

The presentation equipment is a teaching tool suitable for illustrating the structural relationships, parts, and operating principles of objects. The didactic requirement of the presentation equipment is to be suitable for purposeful and versatile observation, and to be able to present the processes both as a whole and in detail.

The equipment showing the compressor refrigerator visually helps those participating in technical education to understand and record the structure and operation of the machines.

A compressor is a machine capable of increasing the pressure of gases. It is driven by a power machine, often an electric motor. It can be found in almost every household: it is present in refrigerators, air conditioners, cars, and most air-powered tools [1].

With the refrigerator, a lower temperature than the environment can be artificially produced and permanently maintained [2].

1.1. Principle construction and operation of a compressor refrigerator

The principle structure of the compressor refrigerator is shown in Figure 1. The main parts of the refrigerator are the compressor, the condenser, the expansion valve and the evaporator, which form a closed system. Refrigerant circulates in the closed system [2].

The refrigerant can be gas or vapour. The most common refrigerant is vapour [3–4]. We will only discuss this hereinafter. The refrigerant is present in different states during the cooling process.

The compressor increases the pressure and temperature of the wet vapour refrigerant, so the high-pressure and high-temperature vapour continues to flow toward the condenser. The condenser is a large surface area heat exchanger. The superheated high-pressure vapour arriving here gives off its heat to the environment, and then cools and condenses. The liquid refrigerant passes through a throttle valve, which maintains the pressure difference, and where the medium expands, causes its pressure to drop and thus its temperature. It begins to boil at a lower temperature due to the lower pressure. It takes heat from its surroundings for evaporation. The heat is absorbed in the evaporator. The refrigerant arriving here is in the form of wet vapour which evaporates here completely while absorbing heat from the medium to be cooled. It leaves the evaporator as cold vapour. The compressor usually includes

a recuperator, in which the incoming cold vapour is preheated by the outgoing hot vapour, so that a higher temperature refrigerant arrives at the compressor. As long as the compressor ensures the circulation of the refrigerant, these processes take place, thus the environment of the evaporator cools down, while that of the condenser heats up.

1.2. Compressor presentation

We used the compressor of a refrigerator to create the demonstration equipment. We opened the compressor and took it out of the housing, so the piston, cylinder head, valves, in this case the flow passages of the coolant, spray oiling, and the drive motor are visible, **Figure 2.**

In order to properly illustrate the cylinder head, valves and suction side muffler, we replaced the original mounting bolts and created the correct distance for visual inspection.

1.3. Presentation equipment of a refrigerator

We also used parts of an old refrigerator to create the refrigerator demonstration equipment. The presentation equipment contains the basic parts of the refrigeration circuit: the compressor, the condenser, the evaporator, the throttle valve formed as a common body with the evaporator. The equipment is completed with the dryer and the pipelines, **Figures 3** and **4**).

The condenser is usually large, so we only used a part of it.

The dryer filters the refrigerant passing through it and extracts any moisture from it **[2]**. To demonstrate its construction, the cover was cut lengthwise, the filters were cleaned, and then the silica gel balls were fixed with instant glue.

The evaporator is a 120×400×300 mm aluminium box with a tube system in its wall, where the refrigerant circulates. The throttle valve can be observed on its surface, which is trained on the entry side.

The pipes were attached to each other with a transparent flexible PVC hose for easy installation.

2. Examination of the refrigeration cycle

In order to study the refrigeration cycle, we examined the elements of a real refrigerator together. The refrigerator is a closed system, so it is only possible to measure the temperature. We have developed a measurement system for this.

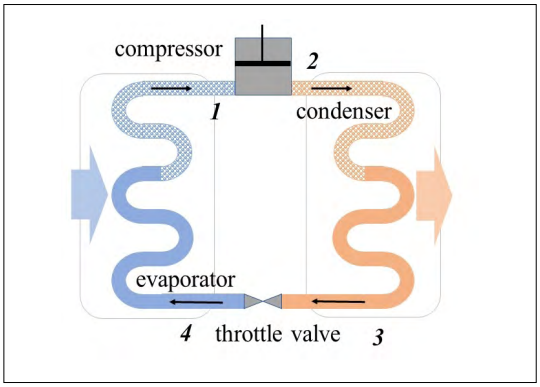

Figure 1. *The principle construction and operation of a refrigerator.*

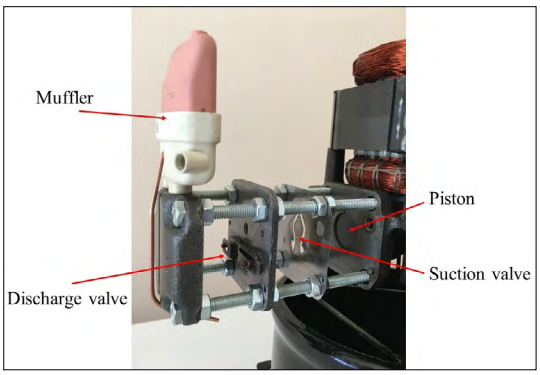

Figure 2. *Implemented compressor presentation equipment.*

Figure 3. *Presentation of dryer.*

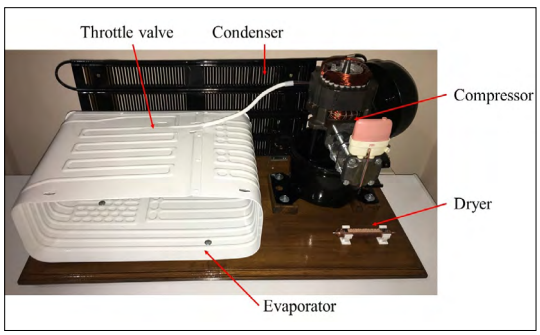

Figure 4. *Implemented refrigerator demonstration equipment.*

2.1. Measurement system

The test was carried out on an LDK refrigerator with a volume of 43 L, Figure 5. The condenser of the tested refrigerator is built into the side walls, the evaporator-freezer part is small. Refrigerant is isobutane, designation: R600a. Isobutane boils at −11.7 °C at normal, atmospheric pressure and can be liquefied at 25°C with a pressure of 3.5 bar [5].

The main components of the measuring unit: Arduino Mega2560, 7 DS18B20 temperature sensors, 3.2" diameter touchscreen colour TFT LCD display.

The purpose of the measuring program is to create an easy-to-understand interface that shows the user the temperature values measured by all sensors at the same time [6]. The temperature changes are also illustrated by a graphic interface. For easier tracking, each sensor has its own color code. Navigation is possible between 4 pages on the user interface, which is made possible by the touch-sensitive display.

The flowchart of the program is shown in Figure 6.

2.2. Measurement

In order to test the refrigerator, the seven sensors were fixed in important places in terms of operation: before the compressor and after the compressor, on the condenser, in front of the dryer, after the dryer, in front of the throttle and after the throttle. The temperature sensors were fixed with aluminum adhesive tape and heat-conducting paste.

After starting the refrigerator, the sensor data is saved in a *.txt file; these can be followed on the fourth page of the screen, Figure 7.

The temperature change of the refrigerant during the operation of the refrigerator at the measurement locations can be followed in Figure 8.

Figure 8. shows the measurement locations and identifies the elementary processes of the cooling cycle:

- S4-S1: Temperature increase by compressor;
- S1-S5-S2-S3-S6: Temperature drop by condenser;
- S6-S7: Temperature drop by throttle;
- S7-S4: Temperature increase by evaporator.

2.3. Refrigerant cycle test

Knowing the pressure and enthalpy of the refrigerant is of practical importance for the illustration and investigation of the change in the state of the refrigerant along the refrigeration

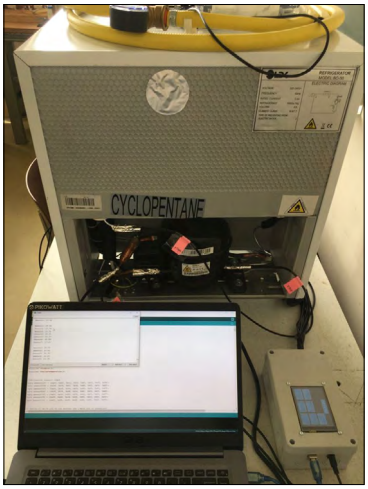

Figure 5. *The tested refrigeration machine and data collection.*

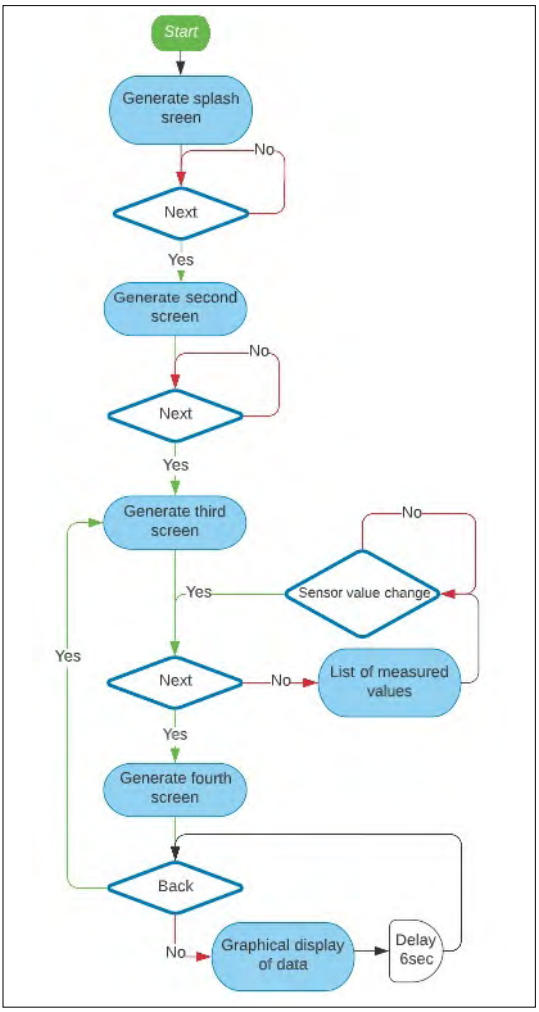

Figure 6. *Flowchart of the program.*

cycle [4, 7, 8, 9]. Enthalpy, whose symbol is H, is a caloric state indicator with energy dimension, and its unit is [*J*].

Based on the temperature, the saturated vapor pressure of the refrigerant can be determined, this was based on the characteristic of the saturated vapor pressure of isobutane. The saturated vapor pressure values for the R600a, isobutane refrigerant at a given temperature can be found in the literature [5]. Using these values, we formed an approximate polynomial, Figure 9.

The relation of the approximate polynomial:

$$p = 4 \cdot 10^{-6}\, t^3 + 8 \cdot 10^{-4}\, t^2 + 0.562\, t + 1.5624 \text{ [bar]} \quad (1)$$

The saturated vapor pressure values for the temperature values after the compressor and after the throttle were determined with the relation (1). The data are given in Table 1. The expected data of R600a refrigerant, which can be found in the literature, have also been indicated there.

The refrigeration circuit processes can be clearly illustrated on the p-h diagram, Figure 10, where *h* is the specific enthalpy, [J/kg].

The pressure-increasing effect of the compressor and the enthalpy increase can be followed in section S4-S1 of the diagram. The refrigerant turns into superheated vapor. The calculated pressure of 5.6 bar is acceptable based on literature data.

In section S1-S5-S6, the temperature on the condenser decreases (Figure 8). The refrigerant changes from a vapor state to a liquid state (Figure 9). Isobaric heat release, enthalpy reduction occurs.

On the S6-S7 section can be seen the pressure drop across the throttle. The temperature value measured after the choke matches the literature data (Table 1, Figure 8). If we start from the assumption that the refrigerant after the throttle is in a vapor state, it can be seen that the determined pressure of 0.6 bar can be realistic (Table 1, Figure 10).

In section S7-S4, the refrigerant evaporates, isobaric heat absorption takes place and the enthalpy increases.

Table 1. *Determined saturated vapour pressure values*

Sensor number	Sensor place	Temperature (°C)	Calculated pressure (bar)	Literature data
1	After compressor	41.75	5.60	40 ÷ 60 °C max. 8 bar
7	After throttle	−23.66	0.61	−25 ÷ −20 °C 0.5 ÷ 1 bar

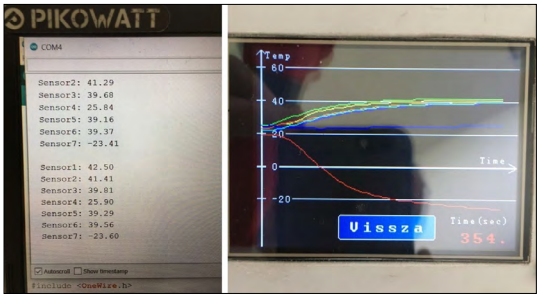

Figure 7. *Displayed data.*

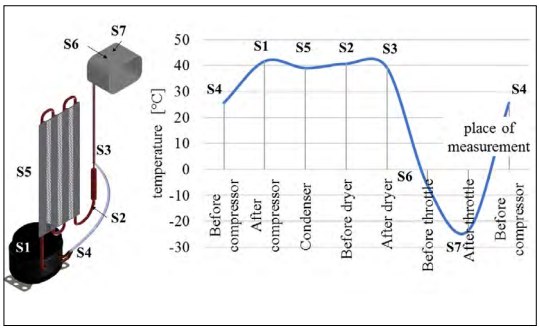

Figure 8. *Refrigerant temperature change at the measurement locations along the circuit.*

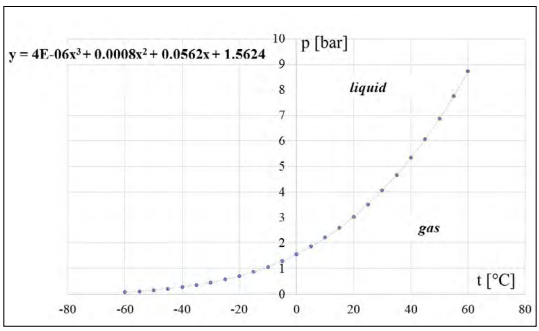

Figure 9. *R600a, isobutane saturated vapor pressure diagram.*

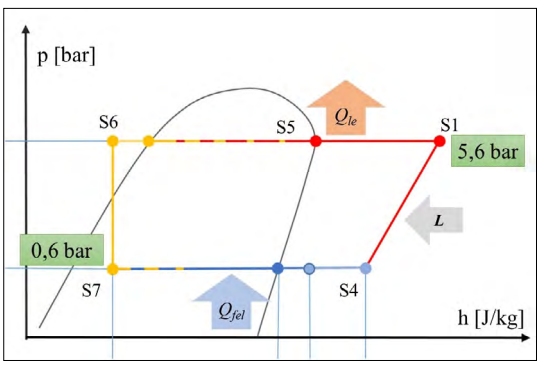

Figure 10. *Illustration of the refrigeration cycle on a p-h diagram.*

3. Conclusions

The demonstration device requires little space, is easy to use, and is safe. It presents the important parts of the refrigerator and gives an opportunity to follow the elementary processes.

With the help of the measuring unit, the temperature changes can be followed in real time. The measurement locations can be presented on the demonstration equipment.

In the refrigeration circuit, the temperature, pressure, and state of the refrigerant change. This is explained by the demonstration equipment and verified and illustrated by the measurements.

The implemented demonstration equipment connects theoretical and practical concepts.

References

[1] Kakucs A.: *Áramlástan*. Scientia Kiadó, Kolozsvár, 2006.

[2] Juhász L., Maiyaleh T., Vadász J., Vasáros Z.: *Gyakorlati hűtéstechnikai ismeretek.* Nemzeti Klímavédelmi Hatóság, Budapest, 2020.

[3] Santa R.: *Investigation of the Thermodynamic Characteristics of the Ester Oil and R152a, R125, R134a and R123 Refrigerant Mixtures.* Acta Universitatis Sapientiae Electrical and Mechanical Engineering, 13 (2021) 14–24. https://doi.org/10.2478/auseme-2021-0002

[4] Sánta R.: P*ressure Drop during Condensation of Refrigerant R134a inside Horizontal Tubes.* IEEE 3rd International Symposium on Exploitation of Renewable Energy Sources (EXPRES), (2011) 117–122. https://doi.org/10.1109/EXPRES.2011.5741804

[5] *A kompresszoros hűtőgép kivitelezése*. https://www.netfizika.hu/a-kompresszoros-hutogep-kivitelezese. (letöltve: 2021. május 11.).

[6] Harsányi R., Juhász M. A.: *Fizikai számítástechnika: elektronikai alapok és Ardunio programozás.* Typotex Kiadó, 2014. (letöltve: 2021 május 15.)

[7] Santa R.: *Comparative Analysis of Heat Pump System with IHX Using R1234yf and R134a.* Periodica Polytechnica, Mechanical Engineering, 65/4. (2021) 1–11. https://doi.org/10.3311/PPme.18390

[8] Sánta R.: *Investigations of the Performance of a Heat Pump with Internal Heat Exchanger*. Journal of Thermal Analysis and Calorimetry, 146. (2021) 11130. https://doi.org/10.1007/s10973-021-11130-5

[9] Sánta R., Garbai L.: *Measurement Testing of Heat Transfer Coefficients in the Evaporator and Condenser of Heat Pumps*. Journal of Thermal Analysis and Calorimetry, 119/3. (2015) 2099–2106. https://doi.org/10.1007/s10973-014-4303-4

sciendo

Műszaki Tudományos Közlemények vol. 17. (2022) 60–64.
DOI: Hungarian: https://doi.org/10.33895/mtk-2022.17.13
English: https://doi.org/10.33894/mtk-2022.17.13

EME MTSZ MTK

STUDYING THE COMMUNICATION POSSIBILITIES BETWEEN A COLLABORATIVE ROBOT AND AN INDUSTRIAL COMPUTER

Szabolcs Balázs TÓTH,[1] Timotei István ERDEI,[2] Géza HUSI[3]

University of Debrecen Faculty of Engineering, Debrecen, Hungary

[1] *szabolcs978@gmail.com*

[2] *timoteierdei@eng.unideb.hu*

[3] *husigeza@eng.unideb.hu*

Abstract

This project is based on the study of collaborative robots (hereafter: Cobot) and industrial PCs, including the communication possibilities between them. In the course of the project, a number of possibilities were studied in order to solve the problem and then summarised to select a collaborative robot and an industrial PC. After that, the focus of the project was on the communication options between the two systems: communication via I/O ports and net-work communication (TCP/IP, Modbus/TCP). Finally, the possible solutions were analysed from different points of view (complexity, flexibility, technical aspects, etc.) and communication between the chosen devices was implemented. The implementation was mainly carried out in a simulation environment, but as the project progressed a communication solution was tested on real industrial devices.

Keywords: *KR, Cobot, UR, PLC, IPC, Beckhoff, TCP/IP, Modbus/TCP.*

1. Introduction

Robots are becoming more and more important in industry, so a large part of the work is no longer done by humans. However, there are still tasks where human interaction is required. This is why Cobots have been developed [1].

There are many ways to communicate with a robot. Robots are most often controlled by wired, wireless or autonomous methods [2].

The goal of this research was to implement a communication solution between a Cobot and an industrial controller.

2. Selected industrial controller and robot

After examining the main features of collaborative robots and industrial controllers, one of each was selected. For the controller, the Beckhoff CX5140 Embedded PC was chosen, shown in Figure 1. With the CX series of embedded PCs, Beckhoff combines PC technology with modular I/O level. It also provides a range of communication options such as TCP/IP, which fulfils the requirements set at the beginning of the project.

The Cobot chosen is the UR10 Cobot shown in Figure 2, which has several communication options including support for TCP/IP communica-

Figure 1. *CX5140 Embedded PC.* [3]

Figure 2. *UR10 Cobot.* **[4]**

tion protocol, making it an excellent subject for the task. Its programming is also relatively simple and easy to learn. UR10 is designed for larger tasks where accuracy and reliability are a priority. With the UR10 collaborative robotic arm, we can automate larger processes and tasks with loads up to 10 kg. With a reach radius of up to 1300 mm, the UR10 Cobot is designed to be more efficient for tasks over larger areas **[4]**. The programming of both devices is easy to learn, although the industrial controller requires some prior knowledge.

3. Communication possibilities between the selected systems

Three communication options were studied. TCP (transmission control protocol) is the Internet standard that ensures the successful transfer of data packets between devices over a network. TCP works with the Internet Protocol (IP) to determine how data is exchanged over the Internet. The two protocols are collectively referred to as TCP/IP **[5]**.

Modbus TCP is nothing more than sending a Modbus RTU message wrapped in an Ethernet packet, but instead of a serial connection, the message is transmitted over a network. TCP/IP provides the transmission medium for Modbus TCP messages. Simply put, TCP/IP allows the exchange of binary data blocks between automation devices **[6]**.

I/O modules are the simplest way to communicate. The TCP/IP communication protocol, which is server/client based, is best suited to the flexibility of the task.

4. TCP/IP server and client program

In order to implement communication between the two industrial devices in the server/client system, a wired LAN communication was required. The industrial controller was selected as server and the robot as client. The IP addresses of the devices have the same network segments, the server IP address is 192.168.2.100 and the client IP address is 192.168.2.113. This results in a subnet mask of 255.255.255.0, which is in class C of the IPv4 address class.

The embedded PC program was written in Beckhoff's own development environment in TwinCat 3 in ST. The program for UR10 was written in URSim Offline Simulator in the programming language of URScript.

Figure 3 shows the program part of the server states. State 0 is the listener state, when the server is running and waiting for incoming connections. State 1 is set up when a successful connection is established, and from there it enters state 2, i.e. message exchange. After sending a message, the program enters state 3 and then state 4 after the server is closed.

Figure 4 shows a part of the client program. When writing the client, a 'connection' and a 'server' Boolean variable was selected in the BeforeStart segment. The 'server' variable is set to TRUE as soon as the connection is established with the server. Then after a successful connection, the client sends a message to the server and enters the message send/receive state. Based on predefined messages, the UR client can perform various tasks and due to the peculiarity of TCP/IP, messages are delivered in the order they are sent.

5. Operation of server/client connection

The flowchart in **Figure 5** shows how the connection works.

The server is first set up and started. Then, when the server is waiting for the client to connect, the client program is started and within a few seconds the connection is established (assuming all settings are correct).

Figure 6 shows a TCP/IP connection implemented in a simulation environment. Once the connection is established, the server can send and receive messages from the client. This is true back and forth. **Figure 7** shows the tasks that the robot client can perform based on the instructions from the server.

```
CASE nState OF
0: (* Listening State *)
    bReceive := FALSE;
    IF eState = eSOCKET_SUSPENDED THEN
    sMessage := 'Kapcsolatra vár...';
    MEMSET(ADR(sReceivedData),0,SIZEOF(sReceivedData)); (* Delete Received data *)
    ELSE IF eState = eSOCKET_CONNECTED THEN
        nState := 1;
    END_IF
    END_IF
1: (* Connection State *)
    IF NOT fbServer.bBusy THEN
            IF NOT fbServer.bError THEN
                IF eState = eSOCKET_CONNECTED THEN(* Connected *)
                    sMessage := 'Kapcsolat létrejött!';
                    bReceive := TRUE;
                    nState := 2;
                END_IF
            END_IF
    END_IF
2:(* Exchange data State *)
            (* ---------------------- Receive data ---------------------------------- *)

        IF NOT fbSocketReceive.bBusy AND NOT fbSocketReceive.bError THEN
            IF fbSocketReceive.nRecBytes = 0 THEN
                bDisableSendButton := TRUE; //Disable Send Button
                //IF there's no data received, reset the fbSocketReceive
                bReceive := TRUE;
            ELSE
                bDisableSendButton := FALSE; //Unlock Send Button
            END_IF
        END_IF
        (* ---------------------- Send data ---------------------------------- *)
        IF bSEND THEN
            bReceive := FALSE;
            fbSocketSend.bExecute := TRUE;
                MEMSET(ADR(sReceivedData),0,SIZEOF(sReceivedData)); (* Delete Received data *)
            nstate := 3;
            bSEND := FALSE;
        END_IF
3:(* Send data State *)
            MEMSET(ADR(sSentData),0,SIZEOF(sSentData)); (* Delete Sent data *)
            fbSocketSend.bExecute := FALSE;
            IF NOT fbSocketSend.bBusy AND NOT fbSocketSend.bError THEN
                fbSocketReceive.bExecute := TRUE;
                nstate := 1;
        END_IF
4: (* Disconnect *)
    IF bEnable THEN
```

Figure 3. *Part of the server program.*

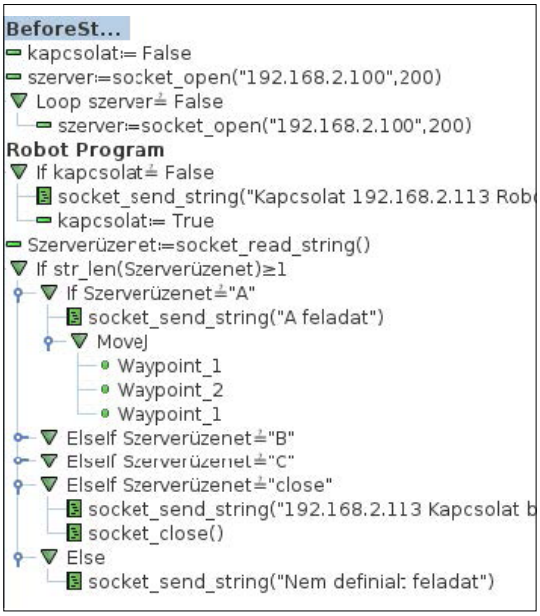

Figure 4. *Part of the client program.*

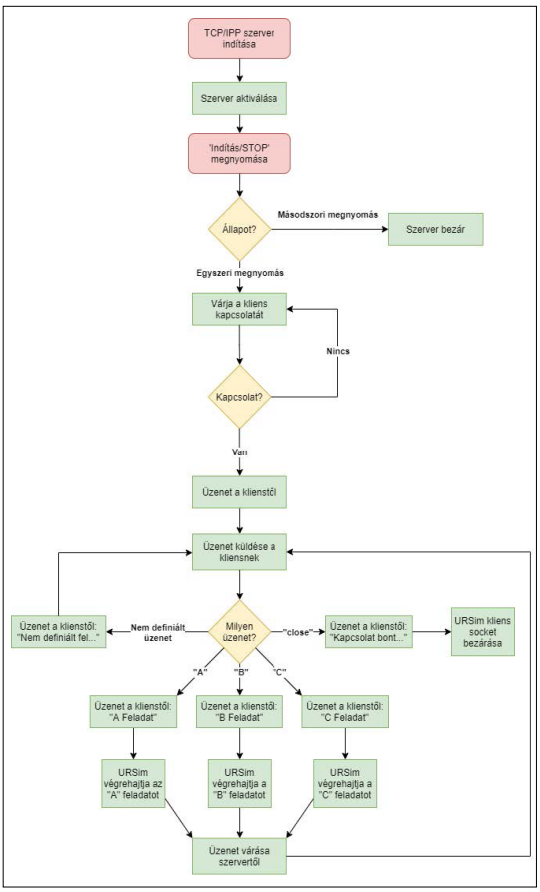

Figure 5. *Server/client connection flowchart.*

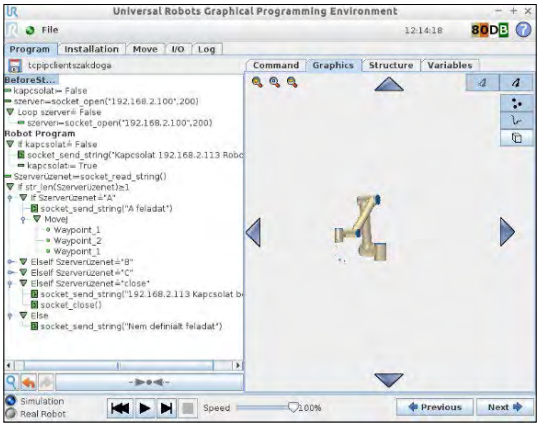

Figure 6. *Connection in simulation environment.*

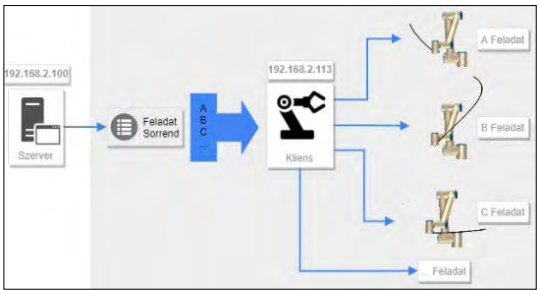

Figure 7. *Robot tasks.*

The client program can now perform 3 different tasks besides closing the socket and sending the "undefined task" message. It can receive an "A", "B" or "C" message and execute the task accordingly.

This configuration is created by directly connecting the two devices. However, in some cases, the communication can be improved by adding a router if connection of multiple clients to the same server is required.

The implemented communication was tested in real life with a UR10 Cobot and a CX5140 industrial controller at Vitesco's Debrecen premises.

6. Related developments

One of the big advantages of TCP/IP communication protocol is that the server program can easily be extended, so it can be written to connect to multiple clients. However, only a two client solution has been developed here for now. This is an important development because it allows 2 robots to work collaboratively in a workspace at the same time on a given workstation. Furthermore, the position of each robot can be read and sent to the other robot. Taking this development further,

a collaboration is created in which not only the human works with the robot, but also the robot works with another robot by enabling the two devices to communicate with each other through an intermediate TCP/IP server. In this way, industrial work can be done more securely.

In the simple Pick and Place task shown in **Figure 8** two Cobots work together with the operator. The TCP/IP communication solution allows a fast exchange of data between the two robots and the operator can track the task via the server HMI..

The HMI of the server shown in **Figure 9** allows the operator to give various instructions to the client.

From the user interface of client 2 shown in **Figure 10** we can retrieve the robot's position with commands and later return the robot to that fixed state. This solution gives room for further possibilities which this research plans to implement in future studies.

7. Conclusion

The goals set for the project have been met and are explained in the project report. The communication solution has been implemented in a simulation environment and tested on real industrial equipment. As a further development, the implementation of a more secure collaborative space was realised.

Acknowledgements

I would like to take this opportunity to thank Ádám Kamrás Beckhoff, software engineer at Beckhoff, for helping me with my work. Ádám Kamrás's professional knowledge was a great help for me to understand how Beckhoff IPCs work.

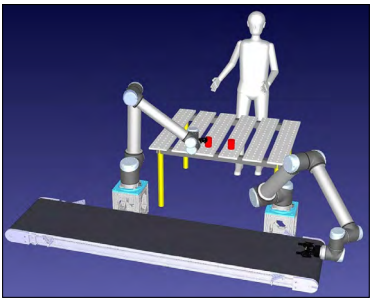

Figure 8. *Collaboration between human and robot.*

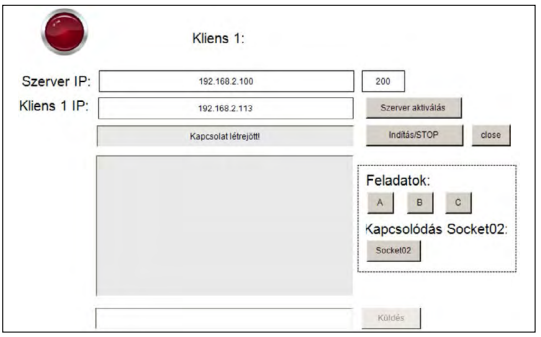

Figure 9. *Server HMI, client 1.*

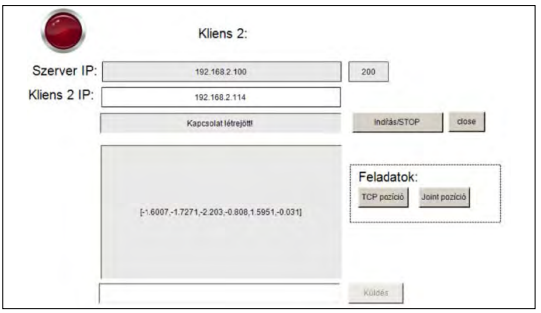

Figure 10. *Server HMI, client 2.*

References

[1] Kollaboratív robotok (2021.09.20) https://www.mmk.hu/informaciok/hirek/kollaborativ-robotok

[2] Kulcsár B.: *Robottechnika*. LSI Oktatóközpont, 1998.

[3] Beckhoff Automation GmbH (2021.09.28) https://www.beckhoff.com/hu-hu/products/ipc/embedded-pcs/cx5100-intel-atom/cx5140.html

[4] Universal Robots (2021.09.28) https://www.universal-robots.com/cb3

[5] Casad J.: *TCP/IP in 24 Hours*. Sams Teach Yourself, Pearson Education (US), 2017.

[6] Real Time Automation (2021.10.04) https://www.rtautomation.com/technologies/modbus-tcpip

SZERZŐK JEGYZÉKE
LIST OF AUTHORS